Genome Engineering to Improve Acetate and Cellulosic Hydrolysate Tolerance in *E. coli* for Improved Cellulosic Biofuel Production

By

Nicholas Richard Sandoval

A thesis submitted to the Faculty of the Graduate School of the

University of Colorado in partial fulfillment

of the requirement for the degree of Doctor of Philosophy

Department of Chemical Engineering 2011

This thesis entitled:

Genome Engineering to Improve Acetate and Cellulosic Hydrolysate Tolerance in *E. coli* for Improved Cellulosic Biofuel Production

written by Nicholas Richard Sandoval

has been approved for the Department of Chemical Engineering

_____

Ryan T. Gill

_____

James W. Medlin

Date _____

The final copy of this thesis has been examined by the signatories, and we find that both the content and the form meet acceptable presentation standards of scholarly work in the above mentioned discipline.

Sandoval, Nicholas Richard (Ph.D., Chemical Engineering)

Genome Engineering To Improve Acetate and Cellulosic Hydrolysate Tolerance in E. coli for Improved Cellulosic Biofuel Production

Thesis directed by Associate Professor Ryan T. Gill

Abstract

Engineering organisms for improved performance using lignocellulose feedstocks is an important step toward a sustainable fuel and chemical industry. Cellulosic feedstocks contain carbon and energy in the form of cellulosic and hemicellulosic sugars. Pretreatment processes that hydrolyze lignocellulose into its component sugars often also result in the accumulation of growth inhibitory compounds, such as acetate and furfural among others. Engineering tolerance to these inhibitors is a necessary step for the efficient production of biofuels and biochemicals. For this end we use multiple genome-wide and targeted tools to alter the genetic makeup of *E. coli* so we can obtain the desired trait of growth on lignocellulosic hydrolysate and tolerance to inhibitory concentrations of acetate. Each of these tools used introduces mutations within a population. These populations are placed in a selection environment where the fittest survive. The change in population genotypes is then analyzed. We applied a recently reported strategy for engineering tolerance towards the goal of increasing *Escherichia coli* growth in elevated acetate concentrations (Lynch, Warnecke et al. 2007). We performed selections upon an *E. coli* genome library using a moderate selection

pressure. These studies identified a range of high-fitness genes that are normally involved in membrane and extracellular processes, are key regulated steps in pathways, and are involved in pathways that yield specific amino acids and nucleotides. Supplementation of the products and metabolically-related metabolites of these pathways increased growth rate in acetate.

Directed evolution has been used successfully to increase tolerance to a variety of inhibitors on a variety of microorganisms. However, the number of unique and non-neutral mutations searched has been limited. With recent advances in DNA synthesis and recombination technologies, new advanced tools can be used. We report a two step strategy that can search a very large number of mutations that are more likely to improve the tolerance of the organism. First, the trackable multiplex recombineering (TRMR) tool searches a genome-wide library for single mutations which have a mutation which either turns up or down gene expression. Based on microarray analysis, a small number of targets are selected for recursive multiplex recombineering. We constructed and searched a library of mutations in the ribosomal binding site of targeted genes, including clones which have multiple mutations. We conducted this strategy in two inhibitory environments (acetate and lignocellulosic hydrolysate). For both cases, we successfully found single mutants from the first step, but in the second step, we found no tolerant mutants for acetate and multiple tolerant single mutants for the hydrolysate. A model was applied to predict the outcome of these selections with varying epistatic effects. This strategy is capable of searching a very large mutational space, but without prior knowledge of epistatic interaction, successful multiple mutants are not guaranteed.

Dedication

This thesis is dedicated to JMJ.

Acknowledgements

I am blessed to have so many people help me with the work here presented. First, I thank my advisor, Prof. Ryan Gill, for all the help and encouragement over the years I have known him. I would also like to thank the rest of my thesis committee for their time and advice: Prof. Bryant, Prof. Demmig-Adams, Prof. Kaar, Prof. Medlin, and Dr. Zhang.

Tirzah Y. Glebes (formerly Mills) contributed to chapters two, three, and four both experimentally and in help producing the written products. She has been the most dependable lab mate and friend one could ask for.

Dr. Joe Warner contributed to chapter four with help doing TRMR selections and analyzing TRMR data. Dr. Phillipa Reeder is thanked her contributions to chapter four based on her previous work with hydrolysate.

I would like to thank Paul Handke, Lauren Woodruff, Eileen Spindler, Joost Groot, Mike Lynch, Tanya Lipscomb, Sean Lynch, Jamie Prior, Julie Struble, Pernilla Turner and all other current and former members of the Gill research group that helped my thought process, gave me good feedback, and taught me so much.

Contents

Tables

Figures

Chapter 1

Introduction

This thesis will discuss in general, two goals. The first is of immediate practical consideration: the increased tolerance of *E. coli* to acetate stress and lignocellulosic hydrolysate stress for better fermentation of biofuels and biochemicals. The second concerns the relatively general question of how best to effect positive change on microorganisms via mutation to engineer a desired trait.

The process of generating genetic diversity within a population of organisms with a selective pressure, generating a fitter organism is not a new one. Nature has provided over a very long period of time the basis for all of these tools that will be described here: evolution. We will use the basic principle of survival of the fittest in order to achieve our goals.

Natural evolution is not as single-minded and thoroughly product-oriented as the engineer, so while nature has given us the framework to engineer traits, we must direct the mutations and the selection to yield the desired trait. Mutations occurring in nature occur slowly and not in a manner directed toward changes in phenotype. In the past, it

was common to put a microorganism in selective conditions for a very long period of time, and allow mutations to arise independent of the researcher, yielding a tolerant, but uncharacterized strain. Discovering what mutations were made and which of those made the strain tolerant was often deemed too difficult to do, so it was often left undone. Even when mutations were found, determining a causal link between the mutation and the change in phenotype was difficult since most random mutations are neutral or deleterious.

A better strategy is to build a library with very specific mutations that have a high likelihood of changing the strain's phenotype. This can be best achieved by introducing mutations that affect gene expression. By introducing specific mutations, it is possible to identify these mutations much more easily later on. However, until recently, this has been impossible or difficult to do.

Recent advances in both the introduction of mutations and finding out what those mutations are allow researchers now to explore new areas with great return. Advances in synthetic DNA production allow researchers to order DNA with custom sequences, making possible Trackable Multiplex Recombineering (TRMR) and Multiplex Automated Genome Engineering (MAGE), since both of these methods use synthetic DNA for site-specific recombination. The advent of DNA microarrays has allowed the genotyping of an entire population. This advance allows a quantifiable value to be assigned to the various types of mutations. These recent advances in technology have opened the door to both engineering traits in strains and elucidating how mutations confer tolerance. Both the Scalar Analysis of Library Enrichments (SCALES) and TRMR tools have utilized this technology to make the processes high throughput.

In chapter two, a review of the motivations for pursuing lignocellulosic biofuels is presented along with the technical complications that arise with such a pursuit. A review of the literature shows that lignocellulosic feedstocks for biofuel production are desirable for a variety of reasons. A renewable source of transportation fuel not dependent on foreign production, the effective utilization of agricultural waste, reduction in green house gasses, and government incentives make lignocellulosic feedstocks attractive. However, the pretreatment and saccharification necessary for fermentation give rise to a variety of inhibitory compounds. Organic acids, specifically acetic acid, exist in high quantities and can cause distress via changes in osmolarity and pH. Native mechanisms exist to reduce the effects of weak acid tolerance, but further engineering is needed to restore growth. Chapter two also explores the various ways that have been used to engineer traits and the effectiveness thereof.

Chapter three discusses the use the SCALES tool to engineer tolerance and elucidate mechanisms of toxicity and tolerance in *E. coli*. The SCALES tool ideally has roughly 300,000 distinct clones. These variations in the genotype come in the form an increased copy number library where the phenotype depends on the vector used (*e.g.* copy number, promoter), and the genetic elements contained in clone. We hypothesized that using a SCALES selection method would yield valuable information regarding mechanisms of tolerance. We show a moderate selection pressure is best when attempting to identify a wide variety of genes which may have a moderate fitness. The goal is to enrich a wide range of beneficial clones, which gives us more information compared to a small number of very high fitness clones. The multi-scale analysis allows the microarray data to be transformed into individual clone data. This clone data

is then compiled to yield one fitness value for each gene. These gene fitnesses were compiled in a variety of ways, and the most useful was projection onto metabolic maps. These maps show that some genes which encode for proteins that catalyze key steps in the production of certain metabolites have a high fitness. The supplementation of these and related metabolites increased the growth rate significantly. The difficulty of obtaining a genetic solution to acetate tolerance is also discussed.

Chapter four describes a multi-tool strategy to make genetic changes that will confer a beneficial trait change. In this strategy, two systems are each used on two conditions. Improved growth in both hydrolysate and acetate are desired. The first step is to do a wide, but shallow search over the entire genome using the TRMR tool. It is said to be shallow because it only searches the up and down mutations contained in the library. The TRMR library consists of two mutations for just about every gene in *E. coli* (2 x ~4,000 = ~8,000). Each clone has an integration within the chromosome that has either a construct to encourage gene expression ('up') or discourage gene expression ('down'). An acetate selection in high concentration is employed because only the best clones are desired for the next step. The hydrolysate TRMR data was obtained from the work of Dr. Phillipa Reeder, which was published in the original TRMR article [1]. The second step of the process described in chapter four is to choose as targets those genes which appear with top fitness from the TRMR data analysis for further study. The MAGE process will be used to generate a library of clones that have mutated ribosomal binding sites which will affect the level of expression of the targeted genes. The mutations are either totally degenerate (for those TRMR clones with a high 'down' fitness) or partially degenerate (for those with a high 'up' fitness). Each target has

~65,000 (down) or ~2000 (up) permutations per target. The phenotype will depend on the location and number of mutations and the strength of the mutated ribosomal binding site. This process is done recursively with a mixed pool of ssDNA oligonucleotides for recombination so that a single clone can accumulate multiple mutations.

The TRMR selection yielded a variety of genes with high fitness in either the up or down direction which did not abide by a consistent theme or motif. Reconstruction of the TRMR clones to confirm the effectiveness of the selection proved difficult and only two of the desired eight reconstructions were tested. Of those two reconstructions, one conferred tolerance to acetate stress.

The MAGE libraries which were based on the results from both hydrolysate and acetate TRMR studies underwent selection. The hydrolysate MAGE library yielded multiple clones with increased growth. When sequenced, the clones contained only one mutation in the target regions. To generate multiple mutations, recombination was done again with a limited number of targets using the previously identified single mutants as the base strain. After a second selection, clones were identified that had multiple mutations, but these clones did not grow better in hydrolysate compared to the single mutants. The acetate MAGE library underwent selection as well, but no clones that were selected had increased growth. Those clones that were sequenced showed no mutations.

Chapter 2

Review: Cellulosic hydrolysate toxicity and tolerance mechanisms in *Escherichia coli*

Journal: Biotechnology for Biofuels

Authorship:

Sandoval, N.R.

Mills, T.Y.

Gill, R.T.

2.1 Introduction

World governments are calling for increased production of renewable transportation fuels in light of increases in energy consumption [2-6]. The United States has mandated the production of 36 billion gallons of biofuels by 2022, with even greater increases of up to 60 billion gallons by 2030 proposed by the current administration [2, 7]. However, corn ethanol production, the predominant method of biofuel production currently in U.S., is limited to 10-15 billion gallons per year [8]. Moreover, corn ethanol has come under criticism for its potential to increase greenhouse gas (GHG) emissions when compared to fossil fuels, its negative impact on food markets, and other environmental concerns [9-11]. In light of these facts, new

feedstocks and processes capable of producing 20-50 billion gallons of biofuel per year, while not increasing GHG emissions or otherwise negatively affecting the environment, must be responsibly developed and commercialized within the next two decades. Biofuels derived from lignocellulosic biomass hold promise for making up a significant fraction of this market.

Lignocellulosic feedstocks, such as switchgrass, poplar, and corn stover, are comprised of polymerized sugars, mainly glucose and xylose, which can be used as a carbon source for biofuel production. These feedstocks are attractive because they are often now regarded as waste and no value is being produced from them. Use of cellulosic feedstocks have the potential to provide GHG savings of 65-100% in comparison to gasoline [12]. When land-use changes are considered, cellulosic ethanol still has the ability to reduce overall GHG emissions depending on the source of biomass and associated land-use change [9]. Feedstocks that do not require a substantial change in land use include crop and municipal wastes and fall grass harvests[9]. Other potential feedstocks include waste from pulp and paper mills and construction debris [2]. These feedstocks are of great interest because they require no additional land-use conversion [9].

In order to use these feedstocks in fermentation, the sugars contained within the polymer chains must be released. To achieve this, very violent processes (generally referred to as pretreatment) must take place to produce hydrolysate, the sugary liquid product of pretreatment. Many types of processes exist and have been recently reviewed for the pretreatment of lignocellulosic biomass to produce a fermentable

hydrolysate [13-17]. The overall goal of pretreatment is to produce glucose from cellulose, convert hemicellulose to pentoses, and to remove lignin [14].

The necessarily harsh conditions used in pretreatment create a variety of compounds that inhibit the fermentation performance. Inhibitors have been categorized previously by Olsson and Hahn-Hägerdal [18]. Specifically, acetic acid is released from acetylxylan decomposition, furan derivatives result from sugar dehydration, and phenolic compounds are derived from lignin. Furan derivatives include 2-furaldehyde (furfural) and 5-hydroxymethylfurfural (HMF), which result from pentose and hexose dehydration, respectively [19, 20]. Subsequent degradation of furfural and HMF introduces formic acid and levulinic acid, respectively, into the hydrolysate. Lignin degradation produces phenolic compounds of interest which include acids, alcohols, aldehydes, and ketones [21].

Although many fermentative microorganisms exist, *Escherichia coli*, *Saccharomyces cerevisiae*, and *Zymomonas mobilis* are the most promising for industrial biofuel production [22]. Each microorganism has limitations in native substrate utilization, production capacity, and tolerance. Unlike *S. cerevisiae* or *Z. mobilis*, *E. coli* natively ferments both hexose and pentose sugars (the others can only natively ferment hexoses). *E. coli* on the other hand, has no native ethanol production pathway, so heterogeneous genes must be supplemented to produce the biofuel [23]. Ethanologenic *E. coli* also has higher tolerance to lignocellulosic inhibitors than its fermentative counterparts [24-26]. In 2007, Jarboe *et al.*, compared ethanol production between these three microorganisms, determining that *E. coli* is comparable with or surpasses other reported production levels, despite its low membrane tolerance to

ethanol [27]. These qualities along with advanced knowledge about the *E. coli* genome and regulation make this bacterium a good candidate for further development.

As depicted in Figure 2.1, generally accepted categories of antimicrobial activity for inhibitors in lignocellulosic hydrolysate include: (a) compromising the cell membrane, (b) inhibiting essential enzymes, or (c) negative interaction with DNA or RNA [28-33]. These compounds often act by inhibiting multiple targets. Although efforts are underway to limit the amount and types of inhibitors created during pretreatment, at the present time, economically viable processes still fall short. Regardless of pretreatment optimization, inhibitors such as acetic acid, released directly from hemicellulose decomposition, will remain in the hydrolysate. Thus, the need to engineer more tolerant fermentative microorganisms exists. In this work, known modes of acetate toxicity and tolerance pertaining to *E. coli* will be reviewed, in addition to new technologies that are aimed at engineering the bacterium for various traits.

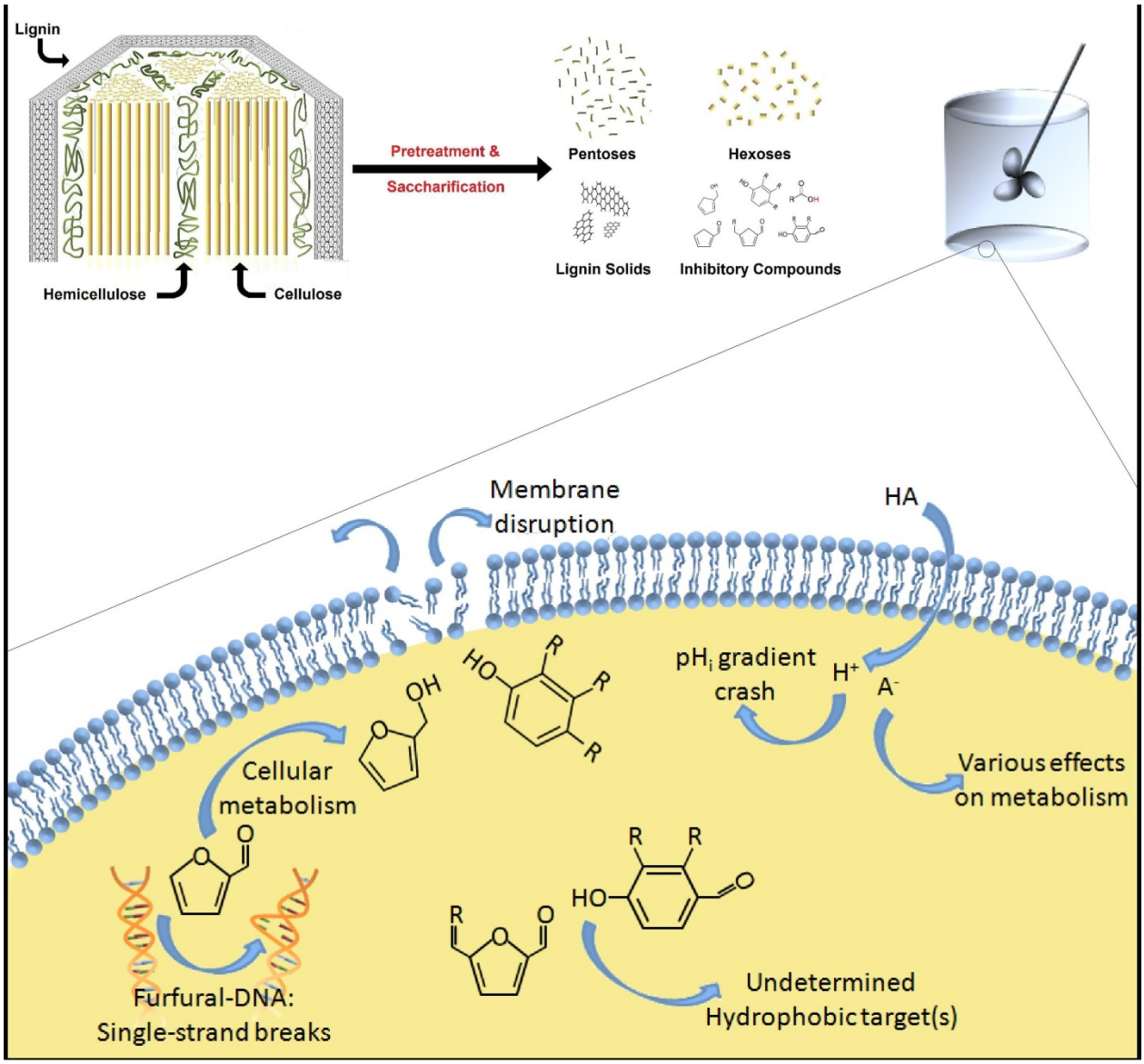

Figure 2.1 - Hydrolysate inhibitors

Lignocellulosic biomass is processed into component sugars, lignin solids, and inhibitory compounds. These inhibitors can affect microbial growth in various ways including DNA mutation, membrane disruption, intracellular pH drop, and other cellular targets.

2.2 Organic Acids

Organic acids derived from lignocellulosic biomass pretreatment and subsequent saccharification inhibit the growth and metabolism of *E. coli* (Figure 2.1). This, in turn, reduces the yield, titer, and productivity of biofuel fermentation. Various organic acids are created in pretreatment steps: acetic acid is derived from the hydrolysis of acetylxylan, a main component of hemicellulose; others (formic, levulinic, etc.) are a result from degraded sugars [34].

Acetic acid is usually found at the highest concentration in the hydrolysate [35-41]. Levels of acetate depend on the type of cellulosic biomass and the pretreatment method. Concentrations typically range from 1 to >10 g/L in the hydrolysate. Formic acid, while more toxic to *E. coli* than acetic acid, is typically present at much lower concentrations than acetic acid (commonly a tenth of acetic acid concentrations) [24, 36, 37]. Other toxic weak acids, whose hydrolysate concentrations are rarely reported, are present at an even lower concentration than formic acid [36, 38, 39, 42].

2.2.1 Modes of Toxicity

Weak organic acids have been shown to primarily inhibit the production of cell mass, but not the fermentation itself [24]. Acetate is the most studied organic acid inhibitor in *E. coli*. Acetate is a natural fermentation product that is known to accumulate due to “overflow metabolism” and inhibit cell growth. Acetate concentrations as low as 0.5 g/L have been shown to inhibit cell growth by 50% in minimal media [43, 44]. However, in *E. coli* KO11, concentrations of acetate up to 12 g/L did not significantly affect ethanol yield, although ethanol titer decreased with high levels of acetate [45]. Attempts have been made to mathematically describe the

relationship between growth rate and acetate concentration, with varying results. Koh *et al.* (1992) proposed the following equation for specific growths (μ) in a batch reactor:

$$\frac{\mu}{\mu_{\max}} = \frac{1}{1 + k \cdot [Ac]} \quad \text{Eq. 2.1.}$$

The value of the constant, *k*, ranged from 0.125 L/g to 0.366 L/g depending on the strain and media [46]. Luli and Strohl (1990) reported an exponential decay model of inhibition [47]:

$$\frac{\mu}{\mu_{\max}} = e^{-k \cdot [Ac]} \quad \text{Eq. 2.2.}$$

The value of the constant was calculated as 0.06 L/g of acetate. In both shake flasks and a fermentor, Nakano *et al.* (1997) report a linear inhibition trend. Specific growth rates in shake flasks were four times as low for any given concentration of acetate as compared to the fermentor. This difference in toxicity was attributed to the controlled dissolved oxygen in the fermentor [48]. The IC_{50}, the concentration of acetate that inhibits growth by 50%, ranges from 2.75 to 8 g/L depending on the strain and media [24, 46, 47].

Weak acids, in the undissociated form can permeate the cell membrane, and once inside, dissociate to release the anion and the proton. These “uncoupling agents” disrupt the transmembrane pH potential (or, proton motive force) since, effectively, a proton is allowed to cross the membrane without the generation of ATP [49]. This dissociation of the weak acid in the cytoplasm is due to the fact the intracellular pH, pH_i, is naturally at a pH of ~7.8, which is much higher than the weak acid’s pK_a [43]. As

these acids dissociate inside the cell, the pH_i decreases, which can inhibit growth [43]. External pH has a large affect on the toxicity of the weak acids. *E. coli* KO11 in LB media with 5.0 g/L acetate reached an ethanol titer twice as fast at an initial pH of 7.0 compared to an initial pH of 6.0, and thrice as fast compared to an initial pH of 5.5 [45]. When *E. coli* LY01 was subjected, at a starting pH of 6.0, to acetic, formic, or levulinic acid at the IC_{50} observed at a neutral pH, the growth rate decreased to 0, 35, and 10 percent, respectively, that of control growth [24]. Formic acid may be more toxic due to the fact it has an extraordinarily high membrane permeability [50]. This external pH effect is, in part, due to the fact that the acid exists in its undissociated form at higher concentrations, allowing for higher permeation of the cell membrane.

The anion also has an inhibitory effect. The anion accumulates inside the cell, which can affect the cell turgor pressure [43]. Inhibition has been shown to be anion specific [24, 43, 44]. When *E. coli* inhibition from acetate was compared to that of benzoate, the same growth rate was observed for differing pH_i (7.26 for benzoate and 7.48 for acetate) [43]. Zaldivar and Ingram (1999) reported that the toxicity of weak acids depended highly on the hydrophobicity of the acid [24]. The more hydrophobic the acid, the more toxic it is.

The modes of toxicity of weak acids are not easily elucidated. Formic and propionic acid have been shown to inhibit the synthesis of macromolecules, as the cells stop growing after addition of the acids [51]. More so than other macromolecules, DNA synthesis was slowed [51]. DNA repair-deficient strains were shown to be more sensitive to weak acids when tested in stationary phase [52]. However, repair deficient strains were not overly sensitive to organic acids in growth phase [53]. This plus the

lack of an observed SOS response suggests that the DNA was not damaged by these acids [53]. The hypothesis of membrane disruption has also been investigated. Leakage of cell contents in the presence of weak organic acids was small when compared to the leakage associated with a membrane disrupting antibiotic (polymyxin B) or even ethanol, and thus is not likely to be the primary cause of weak acid inhibition [24, 54]. Weak acids have been shown to reduce the intracellular pools of some amino acids. Glutamate and aspartate, precursors to many other amino acids, were shown to be at a significantly lower concentration in the cytoplasm when *E. coli* was grown in the presence of weak acid [43]. Glutamate has been shown to be important during growth as a protective osmolyte [55, 56]. Lysine, arginine, glutamine, and methionine were also found at lower concentrations when *E. coli* was incubated with weak acid [43, 44]. The addition of methionine to the incubation mixture has been shown to alleviate much of the toxicity associated with acetate [44].

2.2.2 Modes of Tolerance

E. coli acid resistance mechanisms are thought to increase *E. coli* survival when passing through the low pH environment in the stomach. It has long been known that cells can sense and regulate intracellular pH [57]. Also, it has been shown that treatment of bacteria to moderately low levels of pH (5.0) before exposure to very low pH (3.0-3.5) increases the tolerance more than 50-fold [58].

E. coli naturally has several known mechanisms to combat acid stress. One mechanism for acid tolerance requires the presence of an amino acid decarboxylase coupled with an antiporter that exports the decarboxylated product and imports the amino acid used [59-61]. It is widely thought that tolerance is due to the fact that the

decarboxylation and antiporter reactions consume and export one intracellular proton across the cell membrane. This raises the pH_i of the cell, which is beneficial for survival and growth [59-63]. The transmembrane potential is also affected by these acid resistance mechanisms. *E. coli*, which normally has a negative transmembrane potential, had a positive potential during acid stress when either the arginine- or glutamine-dependent systems were activated. This mimics what is seen in acidophiles [62]. These mechanisms of tolerance have also been reviewed and depicted by Warnecke *et al*. (2004) [64].

All acid resistance mechanisms, however, are not equally effective. The glutamate-dependent acid resistance mechanism is the most studied and the most robust, the arginine-dependent mechanism provides a moderate level of resistance, and the lysine-dependent mechanism confers a minimal level of tolerance [60-63, 65, 66]. The levels of tolerance are highly dependent on the strain, treatment before shock, the media used, growth phase, and the strength and length of acid stress [59-63, 65, 66]. The differences in efficacy among the mechanisms may lie in the optimal pH for the amino acid decarboxylase. The optimum pH for the glutamate, arginine, and lysine decarboxylases is 4, 5, and 5.7, respectively [62]. The lower the optimal pH of the enzyme, the more efficient it is during times of acid stress.

These acid resistance mechanisms exhibit complex regulation. Low pH can induce heat and oxidative shock regulons, genes coding for membrane-proteins, and acid consumption [67]. It is known that the *rpoS* regulon is induced by exposure to weak acids [65, 68, 69]. Once induced, the *rpoS* response leads to higher survival rates at low pH, oxidative stress, and heat stress [69]. However, the *rpoS* response alone is

not sufficient for acid tolerance. Cultures exposed to NaCl, which also induces the *rpoS* response, failed to increase acid survival [69]. *RpoS* has also been implicated in glutamine-dependent acid resistance [63]. This system has been shown to involve at least two sigma factors (σ^S and σ^{70}) and at least five regulatory proteins (coded by *crp*, *ydeO*, *gadE*, *gadX*, and *gadW*) in the expression of the decarboxylases (*gadA* and *B*) and the antiporter (*gadC*) [70-72].

Other modes of tolerance to weak acids are also known. DNA stabilization via *dps* protein interactions has been shown to be beneficial at low pH [73]. Acetate treatment was shown to increase expression of many other genes; these genes were mostly involved in general metabolism of the cell as well as outer membrane protein production [69]. In a genomic library selection with 3-hydroxyproionic acid, genes coding for inner membrane proteins and certain genes involved in cell metabolism were found to be most enriched [74, 75].

2.3 Engineering Tolerance

Engineering tolerance to hydrolysate byproducts is an attractive method for improving lignocellulosic biomass based biofuel production in *E. coli*. Several methodologies have been used for this purpose. The conventional approach is to perform long-course adaptation studies. This method has been used to generate the ethanologenic *E. coli* LY01 strain. Over a three month period, *E. coli* KO11 was grown recursively in ethanol-containing media and plated on chloramphenicol-containing solid media (on which large colonies indicated good ethanol production) [76]. The LY01 strain showed 50% relative growth rate (μ) at 30 g/L ethanol, whereas the parent KO11

showed 50% relative growth rate (μ) in 20 g/L [25]. The resultant *E. coli* LY01 strain was not only more tolerant to ethanol than KO11, but showed a decreased sensitivity to toxic aldehydes as well [25]. Gonzalez *et al.* (2003) showed that expression levels of genes involved in producing protective osmolytes, antibiotic resistance proteins, and cell envelope components were significantly different in LY01 and KO11 [77]. Using chemical mutagens can, over a short period of time, achieve similar results as long-course adaptation. Randomly mutating *E. coli* using NTG mutagenesis has been used to increase the complete inhibition concentration of vanillin from 3 to 4 g/L [78].

Genomic library selection is a powerful tool that can discover genes or operons that, with increased copy number, confer a desired phenotype. The advent of DNA microarrays has made it easier to identify these beneficial genes. SCALEs (Scalar Analysis of Library Enrichments), and its predecessor PGTM (Parallel Gene Trait Mapping), have used *E. coli* genomic library selection and microarrays to engineer tolerance to Pine-Sol antibiotic, antimetabolites, 3-hydroxypropionic acid, and naphthol [74, 79-82]. Genomic selections employing libraries of heterologous genes have also been used to engineer tolerance. A genomic library of *Sphingomonas* sp. 14DN61 was used in *E. coli* to find the PhnN enzyme, which converts aromatic aldehydes, such as vanillin, to their milder corresponding carboxylic acid [83]. Other methods of creating tolerant strains include engineering sigma factors, which alter the transcription of the cell. Global transcription machinery engineering (GTME) utilizes random mutagenesis of sigma factor genes to create libraries of mutated sigma factors. These mutants are then selected for improved tolerance. As a proof of concept, a 40% increase in growth rate at 40 g/L ethanol tolerance was reported [84]. Furthermore, mutants identified via

GTME selection using high levels of acetate (30 g/L) exhibited increased growth rate (μ) by a factor of five [85].

Rational design (*i.e.* mutation for tolerance based on *a priori* knowledge) of *E. coli* to better cope with toxins in hydrolysate has yielded mixed results. After determining methionine biosynthesis was inhibited in the presence of acetate, Roe *et al.* (2002) overexpressed the *metE* gene, which converts homocysteine to methionine, and the *glyA* gene, which is necessary for ^{5}N-methyltetrahydrofolate regeneration (a part of methionine synthesis). However, no decrease in acetate sensitivity was found with either clone [44]. Heterologous cloning of potentially beneficial genes has also been attempted. Aldehyde oxidoreductase from a *Nocardia* species reduces aromatic carboxylic acids to the corresponding aldehydes that are subsequently natively converted to the milder corresponding alcohol. This gene was cloned into *E. coli*, but a 50-fold lower specific activity was seen [86]. When incubated with a cofactor and the *Nocardia* sp. post-translation enzyme, heterologous expression produced a specific activity 20-fold higher than before [86]. In another effort, *Pseudomonas putida* benzaldehyde dehydrogenase was cloned into *E. coli*. Coupled with a NahR reporter system, catalytically active enzyme was selected for using a tet-based host [87]. The fungus *Coniochaeta ligniaria* was found by selection of various microorganisms sampled from soil in media containing furfural and HMF. It was later shown to degrade both furfural and HMF [88]. The genes responsible for such degradation may be attractive metabolic engineering targets. In a novel fermentation strategy, Eiteman *et al.* (2008) propose using *E. coli* strains designed to only be able to use a single substrate as a carbon source [89]. In a two part fermentation, a strain designed to only consume

acetate acts first, then, the detoxified hydrolysate would undergo simultaneous fermentation by a glucose-consuming strain and a xylose-consuming strain [89, 90].

2.4 Perspectives

Biofuels production must find cost effective and sustainable feedstocks. The commercial potential of biofuels largely depends on the abundance and cost of the feedstock. From 2000 to 2007, global biofuel production tripled, but is still only 3% of the global transportation energy [91]. As this number grows, commercial processes will necessarily rely more heavily upon lignocellulosic biomass. Much work is still required to improve the efficiency of fermentations of biomass hydrolysate to levels that are cost competitive with fermentation of pure sugar streams. Emphasis should be placed upon not only further reducing the cost of enzymatic hydrolysis step but also upon better understanding of hydrolysate toxicity mechanisms and methods for engineering tolerance. More specifically, elucidating the modes of action of specific compounds present in hydrolysate will prove critical since the levels of inhibition of various aldehydes and weak acids can vary greatly. It is for this reason that new technologies must emerge in order to more rapidly decipher toxicity and tolerance phenotypes. Once such understanding is generated, processes involving fermentation of lignocelluosic hydrolysates that meet and surpass the productivity of sugar-based bioprocesses will be enabled.

Chapter 3:

Elucidating Acetate Tolerance in *E. coli* Using a Genome-Wide Approach

Journal: Metabolic Engineering

Authorship:
Sandoval, N.R.
Mills, T.Y.
Zhang, M.
Gill, R.T.

3.1 Introduction

Cellulosic biofuel production is a key priority in the effort to reduce fossil fuel consumption and convert to a sustainable transportation fuel economy. Ethanol produced from sugar (dextrose), a first generation biofuel, has the capacity to produce 10 to 15 billion gallons of fuel per annum [Department of Energy, 8]. However, the United States consumes 140 billion gallons of fuel in the same period, leaving a large gap to fill [Energy Information Administration, 92]. Moreover, the Energy Independence and Security Act of 2007 mandates the production of 36 billion gallons of biofuels by

2022. In order to meet that demand, cellulosic ethanol and other next-generation biofuels are required.

Various feedstocks like corn stover, switchgrass, wood, municipal waste, or any number of plant products contain carbon and energy in the form of cellulosic and hemicellulosic sugars. Benefits from using such feedstocks include a reduction in greenhouse gas emissions, reduced land-use change, and a smaller effect on food markets when compared to corn ethanol [9, 12]. However, there are significant barriers associated with commercial use of cellulosic feedstock.

A key obstacle involves the pretreatment of cellulose and hemicellulose polymers in order to generate mono- and disaccharide sugars for consumption by microbial catalysts. Several of the most attractive pre-treatment processes, however, result in the accumulation of compounds that inhibit downstream conversion processes (see review of Sun and Cheng) [14]. To address these problems, common industrial strains are being engineered with increasingly sophisticated technologies to be tolerant to the offending toxins and more alternative production strains with native tolerance are being considered [93-95].

In particular, acetic acid is produced from acetylxylan decomposition; furfural and hydroxymethylfurfural are dehydration products of five and six-carbon sugars [18]. Other toxins such as formic acid, levulinic acid, and phenolic compounds are formed from further degradation of feedstock components [96]. Acetic acid is typically the inhibitory compound present at the highest concentration after pretreatment with concentrations from 1 to 10 g/L [35-41]. Acetate concentrations of 0.5 g/L have been

shown to significantly retard growth of *E. coli* [43, 44]. In order for use of lignocellulosic biomass as biofuel feedstocks to become economically viable, the fermenting microorganism must be able to tolerate higher concentrations of acetic acid and other toxins [96]. The goal of this research was to identify genetic elements and pathways that play an important role for acetate tolerance in *E. coli*.

Conventional methods for engineering tolerance involve recursive iterations of mutagenesis and selection or phenotypic screening. While these methods have been shown to be effective, the identification of beneficial mutations is difficult. The frequency of total mutations within the genome after such a selection or screen is often low (*e.g.* hundreds of point mutations in a genome millions of base pairs long). Of those, most will be harmful or neutral. Mutations that are beneficial are typically less than one percent [97]. The result is that even with next generation sequencing or resequencing technologies methods for increasing the frequency of mutations within the analyzed DNA pool are required. Another option is transcriptional profiling, but the resultant data suffer from the same frequency problems (changes in the expression of dozens to hundreds of genes), the data is correlative not causative between genotype and phenotype, and many phenotypes are caused by physiological alterations that do not include changes in the expression of relevant genes. Indeed, a cellular response to a toxin, which can be seen by transcriptional profiling, may not lead to protection of the cell from that toxin [98]. Rational engineering of phenotypes is also an attractive option. However, in order for this approach to be effective, the targeted phenotype must be well understood at the genetic level. In the case of acetate, and many other toxic compounds, such knowledge does not exist.

In this study, a genomic library selection method is employed. Specifically, the high-throughput, genome-wide tool Scalar Analysis of Library Enrichements (SCALES) was used to elucidate mechanisms of tolerance to acetic acid in *E. coli* [81]. SCALES is not the only advanced method to engineer beneficial phenotypes; transcription machinery engineering, directed and accelerated evolution using recombination, genome shuffling are all methods that can rapidly generate large varieties in phenotype via genotypic alterations [84, 99-101]. SCALES was used here since we have previously successfully applied this method to identify genes promoting growth in a variety of contexts [79, 102-105]. The SCALES method uses plasmid-based genomic libraries with four different insert sizes, with each library covering the entire genome at 125 NT resolution. The libraries were mixed together, subjected to growth selection, and tracked using DNA microarray technology on plasmid-library DNA.

The particular advantage to the SCALES approach is that it enables the genome-scale mapping of causal relationships between genes and desired phenotypes. Here, we applied this method to identify genes conferring acetate tolerance to *E. coli*. Based on the function of such genes, we hypothesized that acetate tolerance could be further increased through supplementation of specific amino acids and/or pyrimidine ribonucleotides to the minimal growth medium. Testing of this hypothesis revealed a significant increase in growth rate and even a restoration of the growth rate in the absence of acetate stress.

3.2 Materials and Methods

3.2.1 Bacteria, plasmids, and media

E. coli K12 (ATCC #29425) was used to obtain genomic DNA. Genomic library selection used pBTL-1 vector [106]. Clones that were based on SCALES data were constructed in pEZseq HC-Amp (Lucigen, Middleton, WI). Overnight cultures used Luria-Bertani (LB) medium. Sampling was done with solid LB medium with agar. Selections and growth testing was done with MOPS minimal medium [107]. All cultures were incubated at 37°C and used 100 µg/mL carbenicillin.

3.2.2 Genomic library, transformation, and selection

Genomic libraries were prepared in the Gill laboratory previous to this study. Genomic libraries were prepared in the same method as described in Warnecke *et al.* (2008) with the use of pBTL-1 vector for the genomic library [104]. Genomic library insert sizes of 1, 2, 4, and 8 kb were used in this study. Purified genomic library plasmid DNA from each of the four libraries was transformed via electroporation into *E. coli* BW25113 Δ*recA*::Kan obtained from the Keio collection [108]. The electrocompetent cells were made such via glycerol wash method [109]. A sample of each transformation reaction was plated on solid media to ensure each library had greater than 10^6 transformants, ensuring complete genomic representation at 125 NT resolution.

After transformation and recovery in TB media, library transformation cultures were mixed together and inoculated into a 50 mL MOPS minimal medium culture in a shake flask. When this starter culture reached an optical density at 600 nm (OD_{600}) of

0.2, a 0.5 mL aliquot was inoculated into the selection environment. The selection environment was a shake flask with 50 mL of MOPS minimal medium with carbenicillin supplemented with 1.75 g/L acetate titrated to neutral pH with 10 M KOH. The OD_{600} was monitored throughout the selection period. In order to maintain the culture in exponential phase, serial transfers were done at 24, 48, and 60 hours after the start of the selection. Each selection culture medium was identical to the previous batch.

3.2.3 Sampling and microarray analysis

After 72 hours of selection, samples of individual clones were obtained by taking an aliquot from the selection culture and plating a 1/10,000 dilution onto LB plus carbenicillin solid media. Ten clones were isolated for sequencing and growth rate testing. In order to obtain sample DNA for use with microarrays, a total aliquot of 1 mL from each of two time points, t=0 and 72 hours, was plated onto 20 LB plus carbenicillin solid media plates. After 24 hours, the colonies were harvested by scraping the plates into LB media and spinning them down to obtain a cell pellet. A portion of the pellet was taken to harvest its plasmid DNA via the Qiagen Hi-Speed Midi Kit per manufacturer's instructions.

The plasmid DNA was prepared for microarray in the same method as described in Warnecke *et al.* (2008) [104]. Data analysis of the resulting .cel file was done with the SCALES software created by Lynch *et al.* in accordance with the authors' instructions [81]. A median filter was used in order to remove fitness spikes under 750 bp. Signals were normalized using the total amount of plasmid DNA applied to the microarray.

3.2.4 Determination of Growth Characteristics

Stock acetic acid solution was prepared by titrating 5 mL of an HPLC-grade 50% acetic acid solution (Fluka) on ice with 10 M KOH to neutral pH. Overnight cultures were prepared from freezer stocks using 5 mL LB plus carbenicillin media in a 15 mL centrifuge tubes. Stationary phase overnight cultures were used for a 2.5% inoculation of 5 mL MOPS minimal medium plus carbenicillin in a 15 mL centrifuge tube. The OD_{600} was monitored until the culture reached an OD_{600} = 0.200 ± 0.01. Growth curves were constructed by introducing a 5% inoculation into 5 mL MOPS minimal medium plus carbenicillin supplemented with prepared acetic acid solution to a final concentration 1.75 g/L in a 15 mL centrifuge tube or with 50 mL of media in a 250 mL shake flask. All cultures were incubated at 37°C and were shaken at 225 rpm. OD_{600} was monitored over the course of exponential growth and final measurements were taken after 24 hours. Specific growth rate was calculated by linear regression on the natural logarithm of the exponential phase OD_{600} over time. Amino acid and nucleotide base supplementation studies were done by preparing stock solutions of amino acids and bases and supplementing the media to a final concentration of 10 mM and 0.4 mM, respectively.

3.2.5 Determination of Individual Gene Fitness

Individual gene fitnesses were determined by analyzing the clones found in the SCALES data. Multiple clones may contain the same gene or part of a gene. To calculate the gene fitness per clone, the clone fitness (W) was multiplied by the fraction of the gene contained in the clone; this was then divided by the length of the gene. Once this was done for all clones that contained the gene, these were summed to yield

the total gene fitness. This process was repeated for every gene in the ecocyc.org database for *E. coli* K12 MG1655.

$$Total\ Gene\ Fitness = \sum_{Clones\ with\ Gene} (Clone\ Fitness \times Fraction\ of\ Gene\ Contained\ in\ Clone)$$

3.3 Results

The overarching goal of this study was to identify strategies for increasing tolerance to acetate in *E. coli*. For this effort, a genomic library selection using microarray analysis in the method of SCALES was performed. We identified a number of regions in the genome that conferred high fitness to *E. coli* in the presence of elevated acetate concentrations. We then analyzed this data by summarizing individual gene data at the level of metabolic pathways [105]. Based on this analysis, we developed hypotheses regarding metabolites that could be used to improve growth in the presence of acetate.

3.3.1 Application of SCALES method and moderate selection pressure to identify acetate tolerance regions

The SCALES method was employed here in order to look at the acetate anion specific mechanisms of tolerance (Figure 3.1). Organic acids, such as acetate, are known to inhibit as a result of pH- and anion-related effects. Acids enter the cell and dissociate to form a proton and an anion. This lowers the intracellular pH and allows protons to enter the cell without the production of ATP [96]. Mechanisms of tolerance related strictly to low pH have been well studied [96]. The inhibition caused by the

anion, which is specific to the type of anion, is not well understood. Thus, selections were performed at neutral pH to emphasize anion-related inhibition over proton based inhibition.

We have previously shown that selection design plays a critical role in dictating enrichment patterns [103, 104]. Here, we designed selections to focus on growth rate, as opposed to increased MIC (minimum inhibitory concentration, the lowest concentration of the toxin that markedly inhibits growth). Our strategy involved repeated batch selections using a sub-MIC level of acetate. We specifically performed selections at 1.75 g/L acetate, where the specific growth (exponential growth rate constant) was 20% of the level in the absence of any added acetate. Our use of a moderate selection pressure is based on a desire to enrich for a broad range of beneficial clones as opposed to the use of a high selection pressure, which would have eliminated all but the most tolerant few clones (which can lead to loss of useful information).

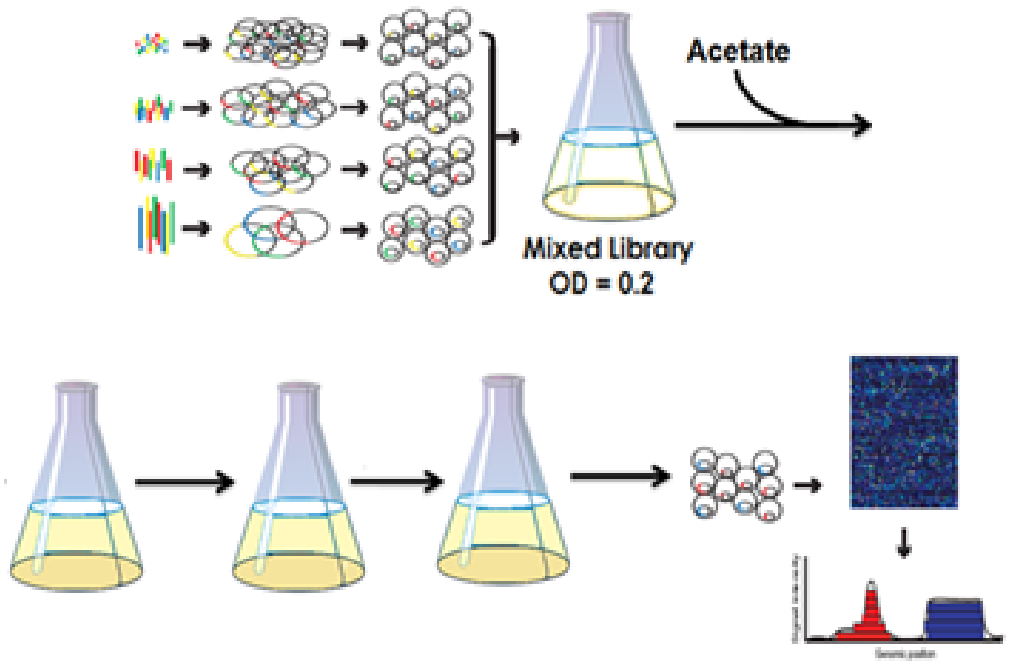

Figure 3.1 - Overview of selection strategy and SCALES analysis

Plasmid-based genomic libraries of different and defined insert size were transformed into *E. coli* BW25113 *ΔrecA*, mixed, introduced to a starter culture with minimal media. After the mixed library starter culture reached an OD_{600} of 0.20, an aliquot was taken and introduced into the selection culture. Sample plasmid DNA was isolated from beginning and end time points and applied to an *E. coli* Affymetrix gene chip for analysis with the SCALES programs.

The SCALES method utilizes multiple genomic libraries of varying sizes so that the precise genetic element conferring tolerance might be identified. To this end, each library fully represented the *E. coli* K12 genome. The selection was performed in a defined minimal medium to eliminate unknown factors. We chose to do a serial transfer of batches method to avoid selection of biofilm phenotype that has been seen in continuous batch cultures [104]. A total of four batches were used over the course of the 72 hour selection. Samples were taken for microarray use at the beginning and end of selection.

The relative concentration of each of the *ca.* 400,000 clones in our mixed libraries was determined before and after selection (Figure 3.2a). Fitness, defined as the ratio of relative concentrations of clones between two time points, was then calculated at a resolution of 125 bp across the entire genome. This data was then decomposed to produce individual clone fitness values (top clones with associated genes, gene products, and important pathways associated with gene products are listed in Table 1). Over 30,000 distinct clones were identified. Only a small fraction of these clones (<10%) have a fitness greater than 1 (Figure 3.2b). This still leads to a relatively large number of clones that have either a moderate or high fitness. Although many of these clones contain overlapping genetic regions, it appears as though there are many mechanisms to confer a moderate amount of tolerance to acetate (at least at the moderate level of selection pressure we employed). It is interesting to note that the distribution of fitness approximates a normal distribution, which is unusual compared to the results of selections we have previously reported, yet understandable given the

moderate selection pressure employed and the fact that the stressor is an *E. coli* metabolite [103].

	Genomic Position		Size	Fitness	Genes in Clone	Gene Product	Pathway
	Start	Stop					
1	100625	101875	1250	22.8	*murC‡, murG*	UDP-N-acetylmuramate-alanine ligase	peptidoglycan biosynthesis III
2	4353125	4354625	1500	15.2	*yjdL‡, cadA*	dipeptide transporter	-
3	4352875	4354625	1750	12.3	*yjdL*, cadA*	dipeptide transporter	-
4	2947500	2948750	1250	11.4	*argA*, recD*	N-acetylglutamate synthase	arginine biosynthesis
5	4051625	4053375	1750	9.75	*glnG*, glnL*	NtrC transcriptional dual regulator	-
6	4283500	4285500	2000	9.47	*acs**	acetyl-CoA synthetase	acetate conversion to acetyl-CoA
7	269000	271500	2500	9.40	*insI-1*, insN-1*, insO-1*, perR*	transposase of IS30, CP4-6 prophage (insN-1 and insO-1)	-
8	483000	485000	2000	9.14	*acrA*, acrB, acrR*	membrane fusion protein	AcrA(B or D)-TolC multidrug efflux transport system
9	1679000	1680250	1250	8.91	*folM*, ydgC*, rstA*	dihydrofolate reductase, hypothetical protein	tetrahydrofolate biosynthesis
10	4344000	4345750	1750	8.29	*fumB*, dcuB*	fumarase B	TCA cycle

***Gene fully contained within the clone. ‡Gene most prevalent in clone. Function and Pathway columns are referring to either fully contained or most prevalent genes.**

Table 3.1 – Top clones in SCALES selection

Top clones identified in the SCALES acetate selection and analysis with associated genes, gene products, and important pathways associated with gene products.

a

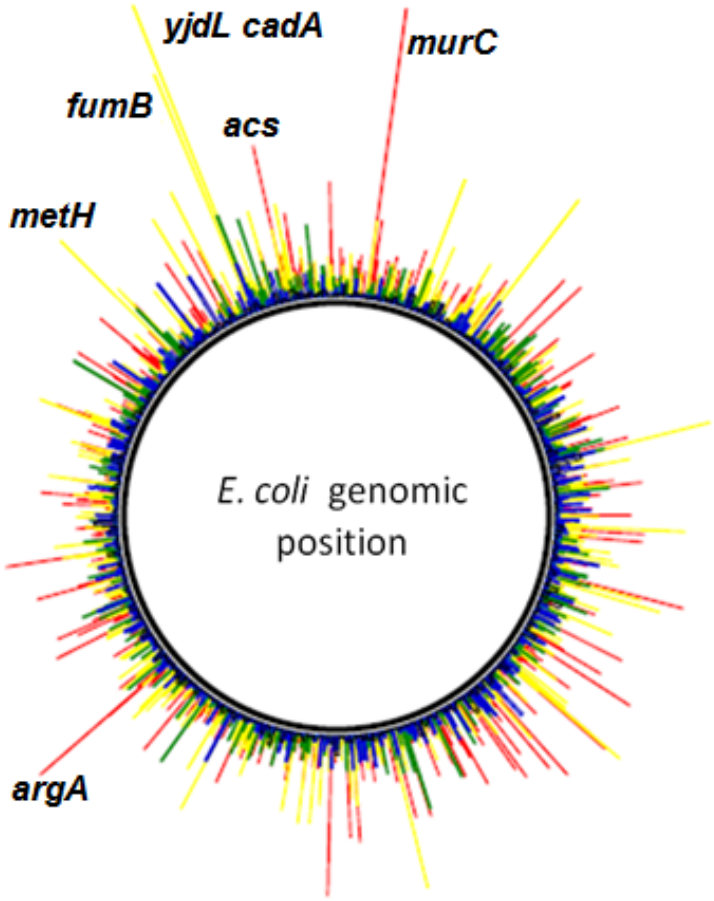

b

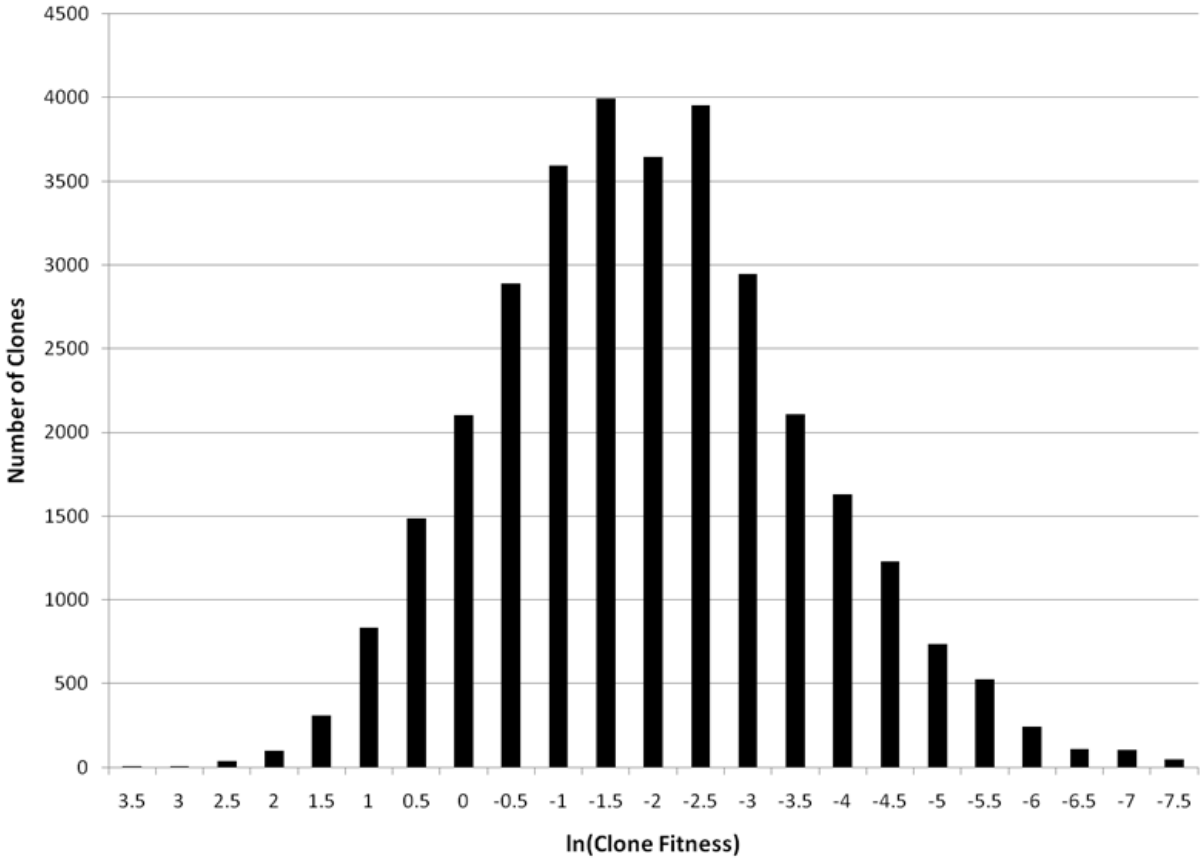

Figure 3.2 - Fitness of clones

a) Circle plot showing the result of SCALES analysis of acetate selection. Clone fitness is mapped over *E. coli* genome. Peak location represents location of clone in E. coli genome; peak size is relative to fitness. Colors denote the size of the clones: Red 1kb, Yellow 2kb, Green 4kb, and Blue 8kb. Labeled peaks show over what genes the high-fitness peaks lie. b) Histogram depicts the number of clones against the natural log of fitness in bins of 0.5. The natural log was used due to the very large range in fitness values. Over 90% of clones have a fitness less than 1 (ln(fitness)<0).

3.3.2 Examination of individual clones and genes

The SCALEs method provides a list of clones that appear to have increased fitness in a particular environment. In our acetate selections, the fittest clone (*W*=22.8) corresponds to increased copy number of the majority of the coding region for the gene *murC* (see Figure 3.3a). The MurC protein (UDP-N-acetylmuramate-alanine ligase) is an essential enzyme in the production of peptidoglycan and thus has been the target of antimicrobial research [110]. In *E. coli*, it catalyzes the ligation of the first amino acid in the peptide moiety in peptidoglycan.

The next fittest clone contains the gene *yjdL*. In fact, multiple clones contained this gene (the best clones had fitness *W*=15.2, 12.3, 8.1, 7.2, 5.4 *et al.*). In total, *yjdL* was found with the highest fitness in the selection. The gene encodes a dipeptide transporter [111]. It is located adjacent in the genome to the gene *cadA*, which with *yjdL*, is included in a clone with high fitness (see green box in Figure 3.3b). The CadA protein (lysine decarboxylase) has been shown to be a part of the lysine-dependent acid resistance system. In this system, the product of the CadA-catalyzed reaction, cadaverine, is pumped out of the cell at the same time lysine is pumped into the cell by the CadB protein. This process effectively pumps one proton out of the cell in order to maintain a proper pH gradient. It is of note that a transcriptional activator of *cadA*, CadC, is also contained in a clone with a moderately high fitness (*W*=2.9, data not shown).

The clone with the next highest fitness primarily contains the gene *argA* (*W*=11.4) (see Figure 3.3c). The *argA* gene codes for the protein N-acetylglutamate synthase. Of

note, the sixth fittest clone contains the gene *acs* (*W*=9.5), which codes for acetyl-CoA synthetase.

As can be seen in each of these cases, a single gene can be contained in multiple clones. The sum of the fitness of these clones may be large, but if the individual clones do not have a very large fitness, the gene may not appear in the list of top clones. In order to consider such genes, we converted the clone fitness into gene fitness. If a gene was fully contained within a clone, that gene was credited with that clone's fitness. If a gene was contained partially in a clone, that gene was ascribed with a fraction of the clone's fitness corresponding to the fraction of the gene that was contained within the clone. These values were then summed over every clone that included that gene, yielding gene fitness for every gene in the genome.

3.3a

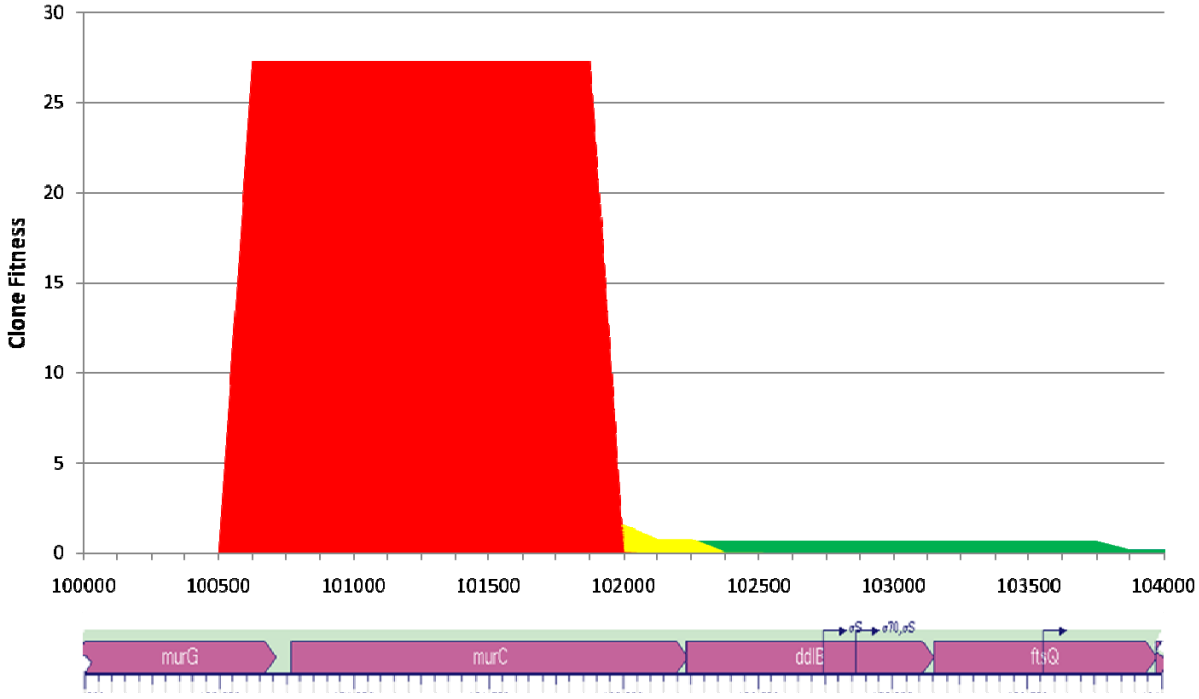
Clone Fitness
30
25
20
15
10
5
0
100000
100500
101000
101500
102000
102500
103000
103500
104000
murG
murC
ddlB
ftsQ

3.3b

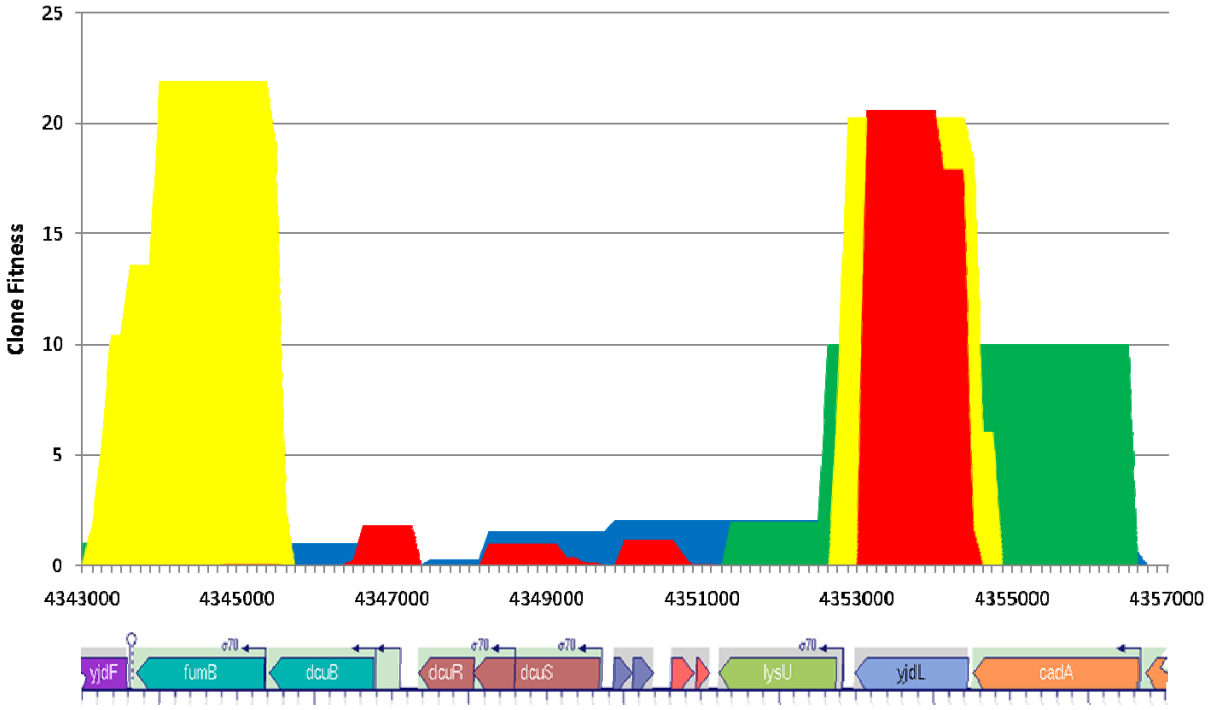
Clone Fitness
25
20
15
10
5
0
4343000
4345000
4347000
4349000
4351000
4353000
4355000
4357000
yjdF
fumB
dcuB
dcuR
dcuS
lysU
yjdL
cadA

3.3c

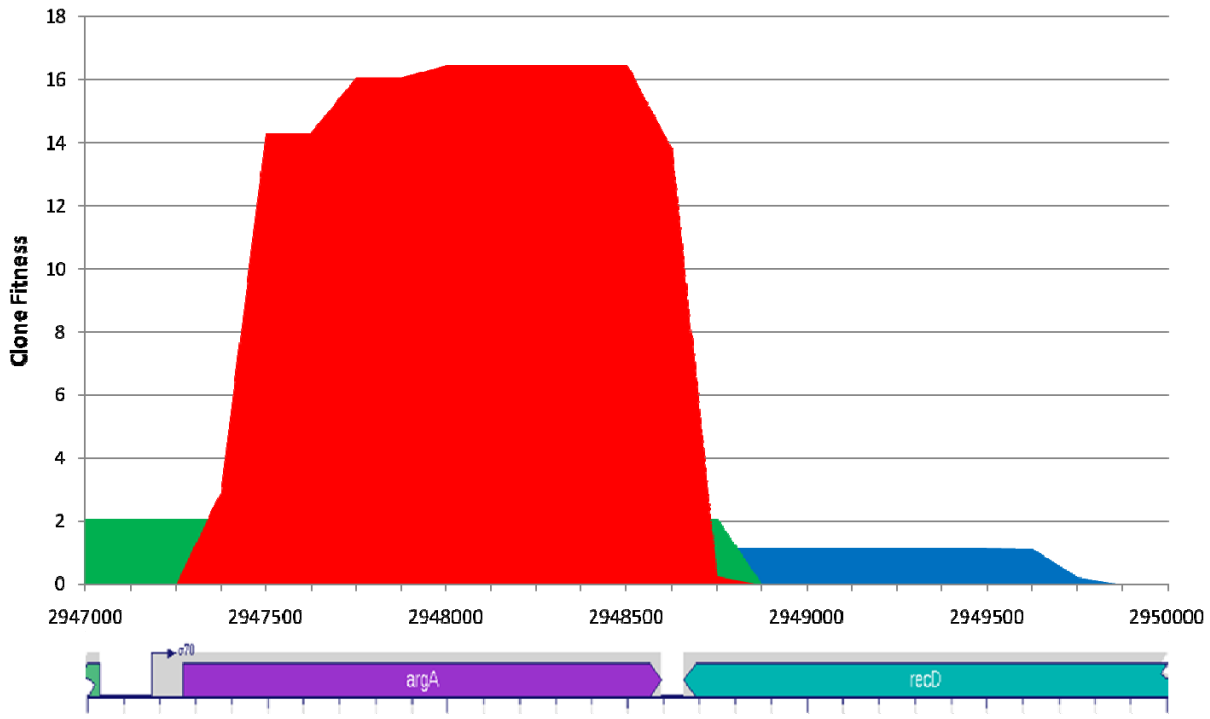

Figure 3.3 - Regions of circle plot in detail.

Shown are the top three clones found in SCALES: a) *murC* region, b) *fumB* with *yjdL* and *cadA* region, and c) *argA* region. On the y-axis is the fitness of the clones with 125 bp resolution. On the x-axis is the position on the *E. coli* genome. Shown below the genomic position is the cartoon of genetic elements in that region taken from ecocyc.org.

3.3.3 Projection of gene fitness onto metabolic maps

In many cases, genes with the highest fitness have products with closely related functions. While these genes are not close to each other in terms of genomic position in the *E. coli*, they may be closely related metabolically. In order to investigate these interactions, we have constructed metabolic maps with the gene fitness overlaid on each of the enzymatic steps of a pathway. We were then able to summarize gene fitness at the level of individual metabolic pathways as well as individual metabolites (building off the strategy reported previously in Warnecke *et al.*) [105].

This summary analysis indicated that many of the top genes conferring high fitness are involved in amino acids biosynthesis (see Figure 3.4a). This is of note in that acetate addition has been shown to reduce the intracellular pools of the amino acids glutamate, aspartate, lysine, arginine, and glutamine [43]. Moreover, methionine has previously been shown to partially restore growth in acetate [44].

A pathway linked to methionine synthesis, the tetrahydrofolate (THF) biosynthetic process, was also found to have multiple genes conferring high fitness. THF is a cofactor in many reactions where a single carbon is donated. These reactions are often times involved in the production of amino acids, such as methionine and glycine, as well as pyrimidine deoxyribonucleotides. The genes *folM*, *metH*, *metF*, and *glyA* were all found to have high fitness values.

Another pathway of interest, the pyrimidine ribonucleotides *de novo* biosynthesis, is shown in Figure 3.4c. The first committed step of the pathway, the coupling of aspartate and carbamoylphosphate, is catalyzed by L-aspartate carbamoyltransferase,

is made up of the products of the *pyrB* and *pyrI* genes. The *pyrL* gene codes for the leader peptide sequence and is normally necessary for the expression of the *pyrB* and *pyrI* genes [112]. The *pyrL*, *pyrB*, and *pyrI* genes were all found with high fitness.

These areas of interest have overlapping metabolites. The biosynthesis of arginine requires glutamate while the pathways forming lysine, threonine, methionine, UTP, and CTP all require aspartate; as previously mentioned acetate severely lowers the intracellular pools of these two amino acids. The synthesis of methionine also requires the use of the THF pathway. The THF pathway meets the pyrimidine deoxyribonucleotides *de novo* biosynthesis pathway (to produce dTMP from dUMP), for which the precursors are produced via the pyrimidine ribonucleotides *de novo* biosynthesis pathway. As can be seen, these pathways that have many genes with high fitness are interconnected.

3.3.4 Media supplement strategies to increase acetate tolerance

Genes involved in the production of arginine, methionine, and lysine were found to have high fitness. We hypothesized supplementation of these amino acids in the growth medium would improve the growth characteristics of the wild type strain in the presence of acetic acid. To assess this, we tested the growth of the control strain in the presence of acetate supplemented with 10 mM concentrations of various amino acids. In addition to those associated with genes exhibiting a high fitness, we chose glutamate and aspartate because their intracellular pools had previously been shown to decrease [43]. Threonine was also included because it had been shown to increase growth rate in a similar weak acid stress condition (3-hydroxypropionic acid) [105]. Also included

was a negative control, alanine, which was not expected to be beneficial based on SCALES fitness data and not found in previous weak acid stress work. As can be seen in Figure 3.4b, the two amino acids associated with the genes exhibiting the highest fitness, arginine and methionine, restored 71% and 62% of the growth rate, respectively. Threonine and lysine restored 29% and 26% of growth, respectively.

Figure 3.4c shows that the first committed step in pyrimidine ribonucleotides *de novo* biosynthesis is catalyzed by the product of genes (*pyrI*, *pyrB*, *pyrL*) with high fitness. Thus, we hypothesized that supplementation of pyrimidines would result in improved growth characteristics. To assess this, we tested the growth rate of the control strain in minimal media with 2.5 g/L acetate, supplemented 0.4 mM of each of the following nucleotide bases: cytosine, guanine, adenine, thymine and uracil. As seen in Figure 3.4d, two pyrimidines, cytosine and uracil lead to ~30% and ~70% restoration of specific growth, respectively. The purines and thymine did not significantly increase growth rate.

We next attempted to find combinations of supplements that would further increase growth. We combined three amino acids (arginine, methionine, and lysine) and two pyrimidines (uracil and cytosine) predicted by the data and shown in Figures 3.4b and 3.4d to benefit growth. All ten combinations of two different supplements were tested. We found that the best combination of supplements was what would be expected from the individual supplement data (Figure 3.5). The increased specific growths were 60%-90% of what would be expected if the increase in growth rate of the combinations were purely additive.

a

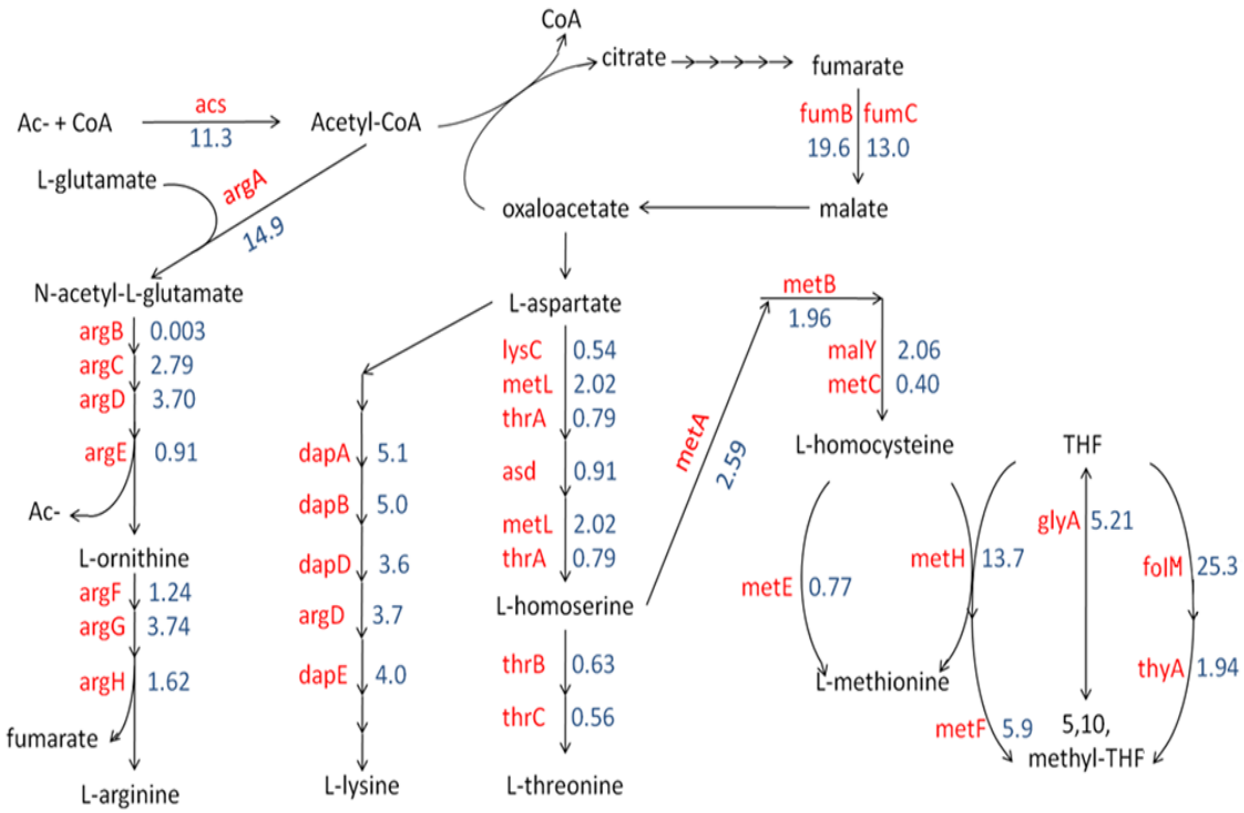
CoA
citrate
fumarate
fumB 19.6
fumC 13.0
Ac- + CoA
acs 11.3
Acetyl-CoA
L-glutamate
argA 14.9
oxaloacetate
malate
N-acetyl-L-glutamate
L-aspartate
metB 1.96
argB 0.003
argC 2.79
argD 3.70
argE 0.91
Ac-
lysC 0.54
metL 2.02
thrA 0.79
asd 0.91
metL 2.02
thrA 0.79
malY 2.06
metC 0.40
metA 2.59
L-homocysteine
THF
dapA 5.1
dapB 5.0
dapD 3.6
argD 3.7
dapE 4.0
L-ornithine
argF 1.24
argG 3.74
argH 1.62
fumarate
L-homoserine
thrB 0.63
thrC 0.56
metE 0.77
metH 13.7
glyA 5.21
folM 25.3
thyA 1.94
L-methionine
metF 5.9
5,10, methyl-THF
L-arginine
L-lysine
L-threonine

b

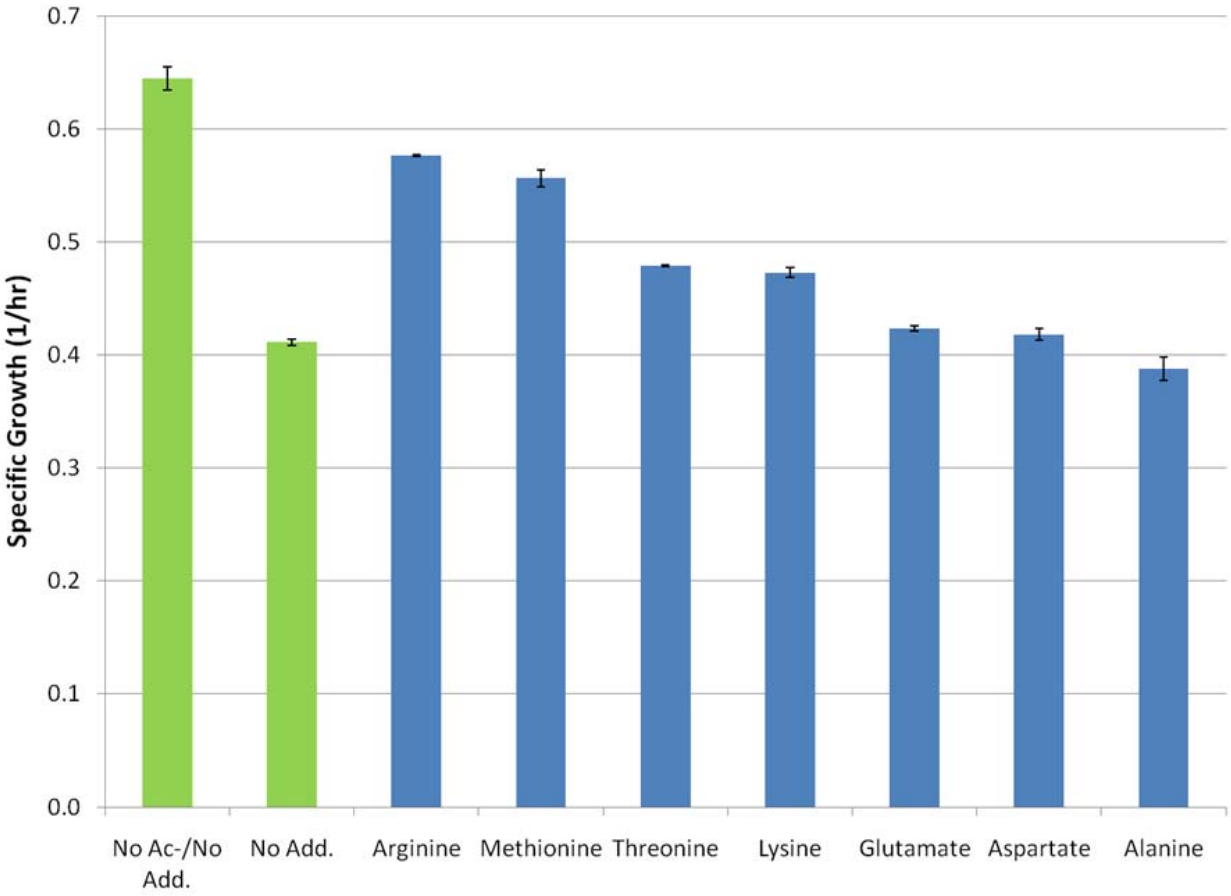
Specific Growth (1/hr)
0.7
0.6
0.5
0.4
0.3
0.2
0.1
0.0
No Ac-/No Add.
No Add.
Arginine
Methionine
Threonine
Lysine
Glutamate
Aspartate
Alanine

3.4c

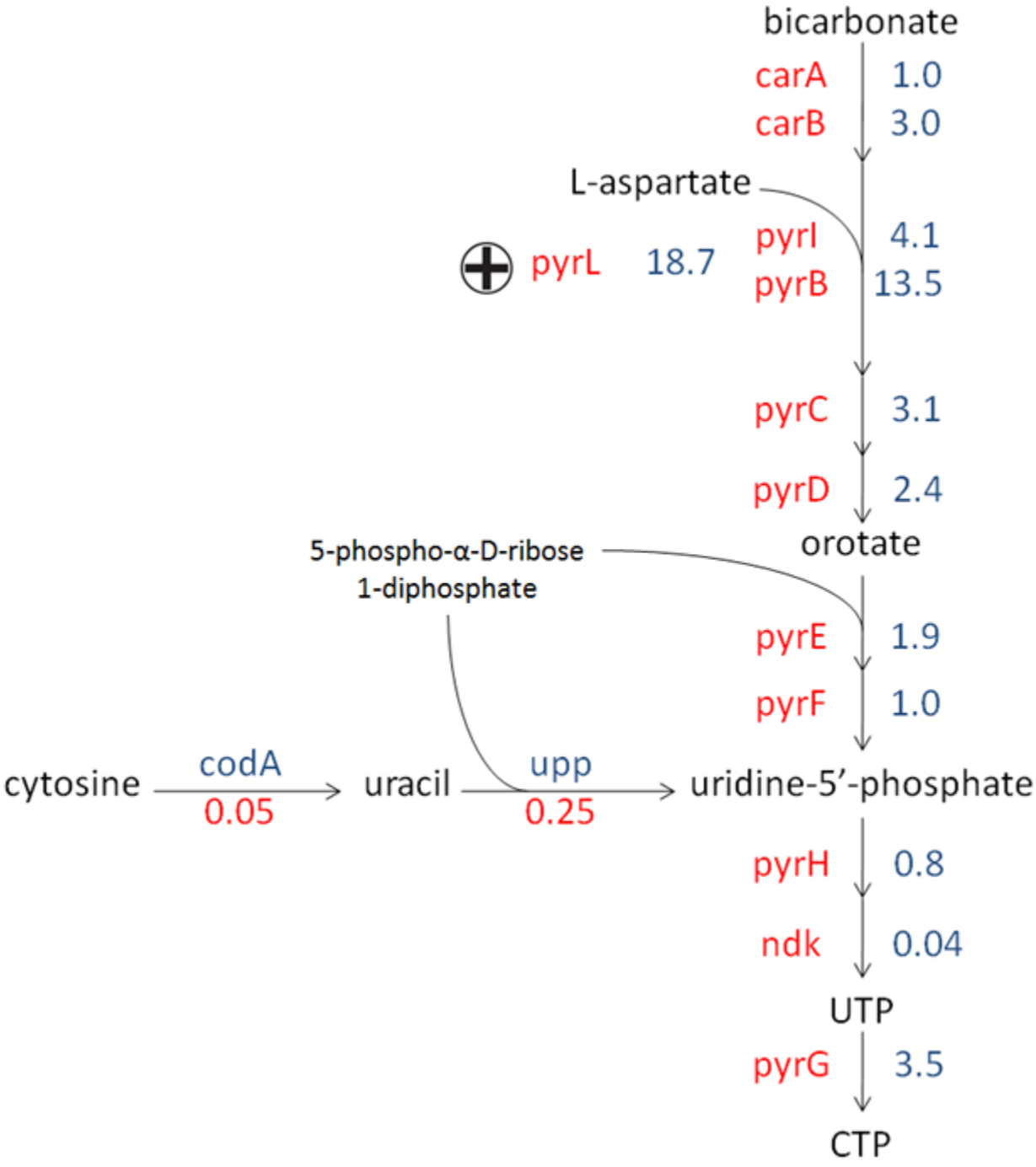
bicarbonate
carA 1.0
carB 3.0
L-aspartate
pyrI 4.1
pyrL 18.7
pyrB 13.5
pyrC 3.1
pyrD 2.4
orotate
5-phospho-α-D-ribose
1-diphosphate
pyrE 1.9
pyrF 1.0
cytosine
codA
0.05
uracil
upp
0.25
uridine-5'-phosphate
pyrH 0.8
ndk 0.04
UTP
pyrG 3.5
CTP

3.4d

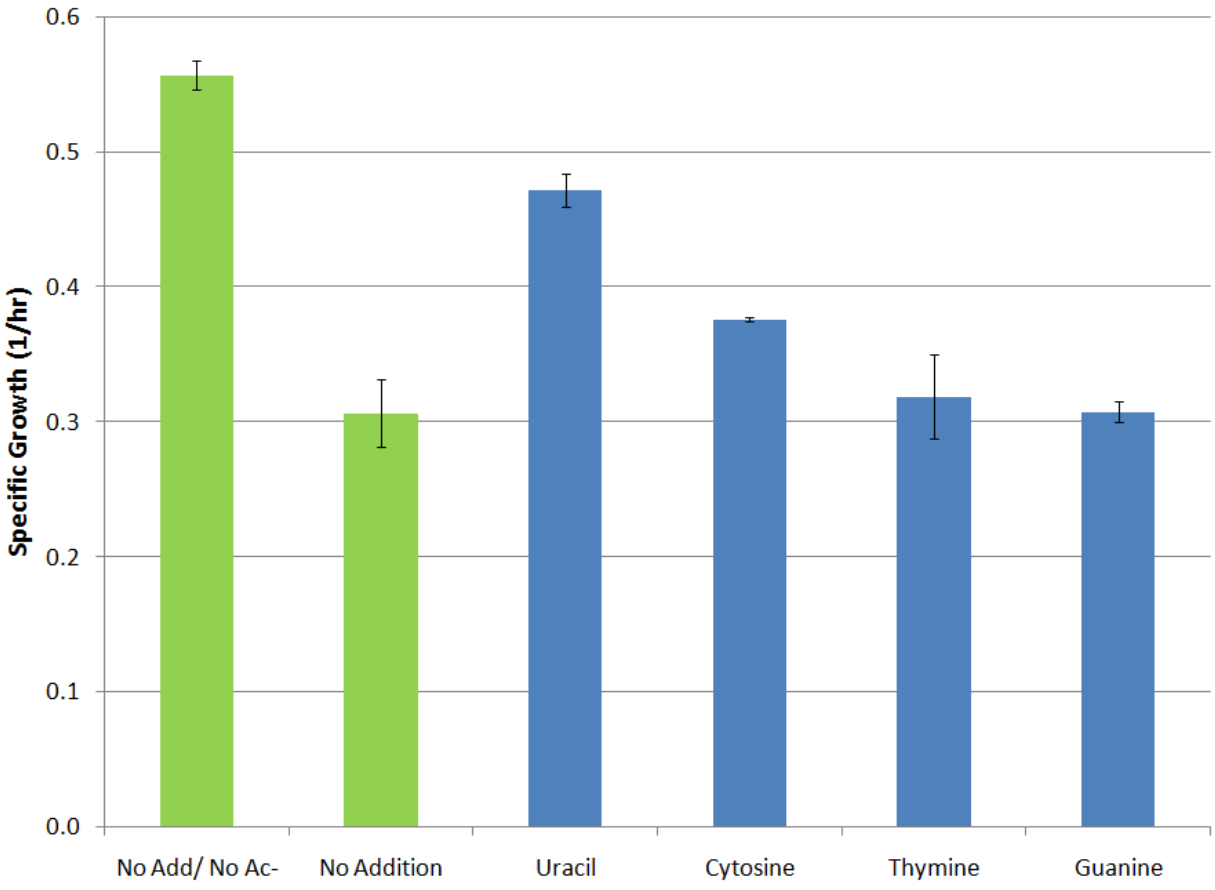

Figure 3.4 - Supplementation growth studies

a) Metabolic pathways of selected amino acid and related pathways. This metabolic map shows the pathway flow of a part of the E. coli metabolism. Each reaction is represented by an arrow, the gene(s) that code for the enzyme that catalyzes that step is shown alongside its gene fitness. b) Confirmation of findings from metabolic maps. Certain amino acids were supplemented at 10 mM to *E. coli* cultures under an acetate stress of 2.5 g/L. c) Metabolic pathway of pyrimidine ribonucleotide *de novo* biosynthesis. Also shown is the side pathway for cytosine and uracil to entire the pathway. Each reaction is represented by an arrow, the gene(s) that code for the enzyme that catalyzes that step is shown alongside its gene fitness. d) Confirmation of findings from metabolic maps. Nucleotide bases were supplemented at 0.4 mM to E. coli cultures under an acetate stress of 2.5 g/L.

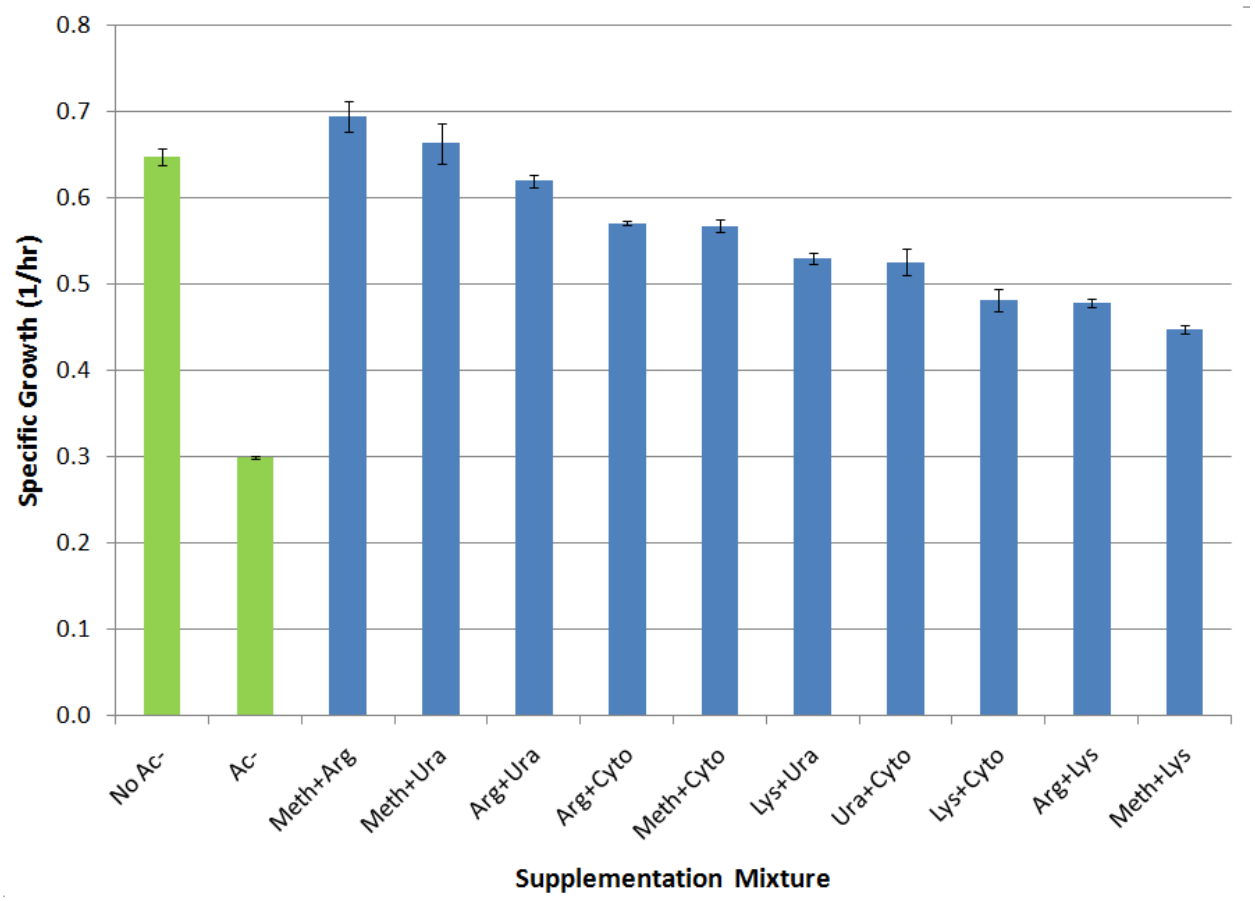

Figure 3.5 - Combination of supplements

The top five tolerance-conferring supplements were combined in twos. The amino acids were supplemented at 10 mM and the nucleotides were supplemented at 0.4 mM. Meth = methionine, Arg = arginine, Lys = lysine, Ura = uracil, and Cyto = cytosine.

3.3.5 Genetic strategies to increase acetate tolerance

In addition to supplement strategies, we constructed 10 clones overexpressing individual genes assigned high fitness by our summarization procedure described above. We then tested these clones for an increased growth rate in the presence of acetate. Interestingly, we found that individual overexpression of any of the genes produced highly variable increases in growth rate. In fact, while we did observe average increases in growth rate on the order of 5-15%, the variation was high enough that we could not conclude that any of the growth rates were significantly different than that of the control. These clones constructed after SCALEs analysis were tested under conditions similar to the selection. However, slight variations in initial pH has a large effect on whether the weak acid is in the associated or dissociated state, so intracellular concentrations of acetate may vary greatly from test to test. Also, it is important to note that these reconstructions were made in a different vector than the library (pEZseq for reconstruction, pBTL-1 for the library). While the features of the vector are similar (both have a pLac promoter), it is thought that this change may also have had an effect on the growth rate of these clones in acetate.

In addition to reconstructing the top fitness clones, ten clones were picked directly from sample plates at the end of the selection. The plasmids in each clone were sequenced (Table 3.2) and growth was studied under selection conditions (Figure 3.6). Each tolerant clone taken from the selection contained the *lpcA* gene. While all these clones contained the same gene, they were not the same clone. Each insert in the plasmid was a different size.

Clone	Insert Start on Genome	Insert Stop on Genome	Insert Size	Gene in insert
A	2819954	2822492	2538	*recA*
B	2369713	2372768	3055	*pmrD*
C	2818903	2822432	3529	*recA*
D	N/A	N/A	N/A	Blank vector
E	243415	244229	814	*lpcA*
F	3766534	980620	?	Multiple insert Clone
G	243413	244325	912	*lpcA*
H	243429	244951	1522	*lpcA*
I	2857854	3336956	?	Multiple insert Clone
J	243418	245587	2169	*lpcA*

Table 3.2 – Identification of Inserts from Picked Colonies

Post-selection clones were picked and sequenced. Inserts of clones are identified through sequencing. Multiple insert clones are those that contained more than one ligation inserts, so the true insert size could not be determined. N/A = not applicable. ? = unknown.

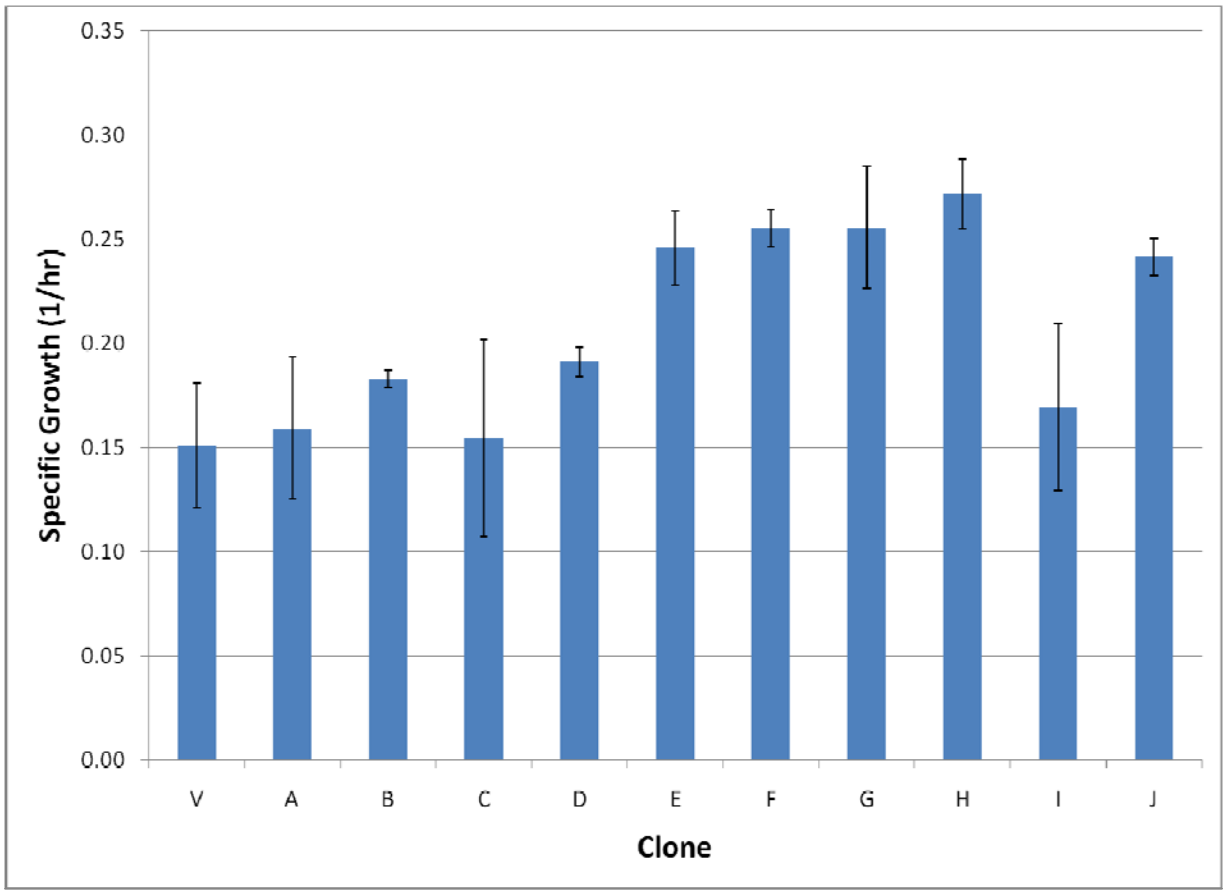

Figure 3.6 – Growth Rate of Selected Picked Clones

Growth rates of selected clones in 1.75 g/L acetate and MOPS minimal media. n=3.

3.4. Discussion

Acetate has long been a challenge in the biotechnological processes requiring fast growth, such as recombinant protein production or chemical production [113]. Initial efforts focused on reducing the amount of acetate produced by the cell, and were generally accomplished by deleting genes in acetate producing pathways. The lignocellulose hydrolysate problem is fundamentally different. The microbe is not producing the inhibitor, but subjected to it extracellularly at the outset. Thus, in order to achieve a more efficient process, mechanisms of tolerance must be elucidated and then engineered into a host organism.

The SCALES method has been used multiple times previously in *E. coli* in order to find a variety of desirable phenotypes (*e.g.* high growth rate, anti-metabolite tolerance, naphthol tolerance, 3-HP tolerance) [79, 81, 103, 104]. The method has proved effective in finding clones with improved growth rate properties. The selection employed here was designed to examine the detrimental effects of the acetate anion specifically as opposed to low pH in general, which is already reasonably well-studied [114]. The anions of weak acids are known to inhibit growth, with different anions of weak acids exhibiting different levels of toxicity [96]. The mechanisms of inhibition by such anions are not well understood.

This is not the first time that acetic acid stress response has been studied with microarray technology. In previous studies, transcriptional profiling was performed. Both studies showed a general stress response, with one showing increased motility transcripts and decreased carbon uptake transcripts [69, 115]. The method presented

here differs fundamentally from these by monitoring plasmid amounts, rather than RNA transcripts.

3.4.1 Transcriptionally regulated steps key

Our SCALES studies yielded genome-wide, multi-scale data, which can be used to identify genes, operons, genetic elements, or combinations thereof beneficial to growth in a particular environment. The clones conferring the highest acetate-relevant fitness, while containing varied genetic elements, shared a few key patterns. First, the genes that conferred the highest fitness often corresponded to a key transcriptionally regulated step within a specific metabolic pathway. In the case of *murC*, the addition of L-alanine is the first transcriptionally regulated step in the peptidoglycan biosynthesis III pathway (according to ecocyc.org). Another example is *argA*, the first committed step in the arginine biosynthesis pathway. A third example involves the conversion of malate to fumarate, which is the most regulated step in the TCA cycle. There are three genes that code for an enzyme which performs this reaction. Two of those, *fumB* and *fumC* had a very high fitness value. Fourth, the first committed step of pyrimidine ribonucleotides *de novo* biosynthesis is catalyzed by L-aspartate carbamoyltransferase. This enzyme is coded for by the *pyrLBI* operon, where *pyrL* is a leader peptide, *pyrB* is the catalytic subunit of the enzyme and *pyrI* is the regulatory unit. Each of these genes conferred high fitness. In cases where the end product of a pathway is important, one might expect to see that all of the genes in that pathway have a moderately high fitness (as was observed in Warnecke *et al.*) [105]. While we did observe this phenomenon in a few cases (such as the L-lysine biosynthetic pathway), we most often observed enrichment for genes corresponding to the key regulatory step in pathways relevant to

acetate stress. One explanation is that acetate is a natural *E. coli* metabolite, which is different from the non-natural metabolite (3-hydroxypropionic acid) studied by Warnecke *et al* (2008) [104]. Given the combination of increased copy number libraries with a leaky promoter (one that constitutively expresses genes at a low level) upstream of cloned library insert regions, it is reasonable to speculate we selected for clones that were deregulated in key pathways for acetate tolerance.

3.4.2 Products of pathways with high fitness genes confer tolerance

It is well known that *E. coli* is more tolerant to chemical inhibitors when grown in complex and rich media. The present study shows the components of complex media may not all aid in toxin tolerance, and those that do aid tolerance do not aid equally. Genes that consume acetate and are involved in certain metabolite biosyntheses were found to possess high fitness. First, the product of the gene *acs* encodes an enzymatic function that could increase acetate catabolism in *E.* coli. That is, Acs converts free acetate into acetyl-CoA, a central metabolite that feeds into various pathways involved in amino acid biosynthesis, among many others. For example, acetyl-CoA feeds into the arginine pathway through the activity of another high fitness gene (*argA*). Similarly, acetyl-CoA can enter the TCA cycle, which connects pathways for biosynthesis of lysine, threonine, and methionine. These pathways all also contain high-fitness genes. Based on the latter findings, we devised supplementation strategies using amino acids as well as pyrimidines.

We observed that addition of arginine, methionine, threonine, lysine, uracil or cytosine was sufficient to offset the growth inhibition resulting from acetate addition to minimal medium. Based on prior efforts [105], and the SCALES studies described

above, this result was expected. A previous study examining the proteomic response demonstrated increased expression levels of amino acid transporters including ArtI, which imports arginine [116]. However, it was unexpected that genes associated with threonine biosynthesis were not found to have high fitness after selection, even though threonine addition did improve growth. Furthermore, it was surprising that neither glutamate or aspartate addition significantly increased growth rate, even though both are key reactants in the synthesis of arginine, threonine, lysine, cytidine-triphosphate, and uridine-triphosphate and were previously shown to exhibit depleted intracellular pools [43]. This may occur since these amino acids are metabolically before the key regulated step in the pathways that produce the tolerance-conferring metabolites. Supplementation of glutamate and aspartate would thus not alleviate the need for the tolerance-conferring metabolites if they cannot get past these important, regulated steps. The THF cycle is of particular interest. It has been seen as an area affected by weak acids in previous selections [105]. The THF cycle is an important area for further analysis since it is a part of a large number of metabolic pathways.

The pyrimidine ribonucleotide *de novo* biosynthesis pathway (PRdnBP) produces UTP and CTP. The pathway does not directly use a pyrimidine base, but cytosine and uracil can be converted to uridine-5'-phosphate via the salvage pathways of pyrimidine ribonucleotides. Supplementation of cytosine and uracil would bypass the aspartate carbamoyltransferase-catalyzed step, which is regulated. Initially, we were surprised that addition of thymine to the media did not increase the growth rate similar to cytosine and uracil, since thymine is also a pyrimidine. However, thymine, unlike the other two, is not a part of the pyrimidine salvage pathway and thus cannot be incorporated into the

PRdnBP. Uracil increases the growth rate much more than cytosine. This may be due to the extra step necessary for cytosine to enter the PRdnBP, since cytosine must first be converted to uracil.

3.4.3 Extracellular functions important

The third general area where top-ranked genes were found is membrane functions. Genes such as *yjdL*, *murC*, other membrane-bound proteins, and genes involved in the production of outer-membrane structures may prove crucial in the protection of the cell from acetate stress. Another gene of interest that did not appear in SCALEs data with high fitness, but was isolated from dilution plates at the end of the selection was *lpcA*. This gene codes for the enzyme sedoheptulose 7-phosphate isomerase, which catalyzes the first committed step in ADP-L-*glycero*-β-D-*manno*-heptose biosynthesis, a core component of lipopolysaccharide. This gene is the subject of further study in the laboratory.

3.4.4 Acetate a complex target

Acetate is a central and highly regulated compound, which functions not only as a metabolite but also as a regulatory molecule. This complex role complicates our studies, as well as those of others attempting to identify acetate modes of action. Our results suggest that acetate inhibition does not happen through a single inhibited target, rather we observe a broad range of genes capable of mediating at least some of the acetate based growth defect. These observations were confirmed via our supplementation studies, where addition of various amino acids and nucleotide bases into the media led to better growth characteristics. Collectively, these observations promote the future use of new methods for searching for combinations of genes that

further enhance tolerance [99, 100]. The identification of strains that can tolerate high levels of acetate would be useful not only in cellulosic biofuels production but also in any biotechnology application where overflow metabolism is a significant challenge.

Chapter 4:

Using genome-wide and targeted tools to engineer acetate tolerance in *E. coli* for improved cellulosic biofuel production

Authorship:

Sandoval, N.R.

Kim, J.Y.H

Glebes, T.Y.

Reeder, P.

Aucoin, H.A.

Warner, J.R.

Gill, R.T.

4.1 Introduction

Beneficial phenotypic traits in microorganisms arise from changes in the microorganisms' genotype. In nature, random mutations occur over time. When the change in genotype is detrimental (which is more often than not), the mutant is eliminated from the population; when the mutation is neutral, the mutant is maintained in the population. In some rare circumstances, the mutation may be beneficial, whereby

the mutant increases its proportion in the population [117]. In directed evolution, the goal is to direct this natural occurrence of trial and error to a beneficial end.

The mutational search space of the *E. coli* organism (*i.e.* the entirety of possible mutations in *E. coli*) is far too large to effectively search all possible permutations of the genome ($\sim 4^{4,600,000}$). Laboratory methods are limited to searching roughly $\sim 10^{9}$ unique mutants. Strategies for defining and producing a relevant set of mutations and then exhaustively searching that reduced set are required at the genome scale. These approaches require high-throughput methods for introducing directed mutations and then afterwards quantifying the effect of these mutations on the desired trait. New multiplex synthesis and recombination technologies are enabling the construction of such methods.

Microarray technology has allowed for fast and inexpensive population-wide genotyping. Scalar Analysis of Library Enrichment (SCALEs) and a related predecessor Parallel Gene-Trait Mapping (PGTM) use microarrays to analyze whole genomic library selection populations [81, 118]. Recent advances in multiplex synthesis of DNA *in vitro* and recombination have made recombination with synthetic DNA a viable option for genome engineering [119-125].

The Multiplex Automated Genome Engineering (MAGE) method does recombination with pooled single-stranded DNA oligonucleotides (or simply ‘oligos’; 70-90 nucleotide long ssDNA) with fully or partially degenerate sequences [99]. These degenerate oligos specifically target the ribosomal binding site (RBS) of previously-chosen genes, resulting in altered gene expression. The recombination, which can be

done with very high efficiency (>20% at times with ssDNA), takes place recursively so that within the population there exist mutants that have multiple mutations [120, 121, 124]. This automated process allows for the generation of billions of unique combinations of RBS mutants.

While MAGE is appropriate for a pre-determined set of targets, it is limited in scope to up to 30 genes. Trackable Multiplex Recombineering (TRMR) was developed to speedily identify specific genes that have an effect on a certain trait on a genome-wide scale [1]. TRMR uses those same advances in synthetic DNA production and recombination technology, but has unique features. TRMR targets nearly every gene in *E. coli* K12 with both a double-stranded 'UP' or 'DOWN' insertion cassette. This insertion cassette includes a promoter and a strong RBS for the UP cassette and no promoter and weak RBS for the DOWN. Both versions of the insertion have a blasticidin resistance marker and a unique 20 bp barcode tag for use with microarrays. The resistance marker is important due to the fact that recombination efficiency is low for double stranded DNA recombination.

We propose a strategy where these two approaches, a trackable genome-wide binary mutation library (TRMR) tool and a tool that generates multiple mutations over certain targets (MAGE), are combined to effectively search an extremely large mutational search space. First, a selection is performed on the TRMR library and the results are analyzed. The fittest mutants from that selection are chosen as targets for the generation of a MAGE library, thus limiting the scope of further exploration. A selection is performed on the MAGE library, which explores a much deeper search space. We describe here the results of our efforts to utilize such a strategy through two

model systems with practical implications: acetate tolerance and growth on corn stover hydrolysate.

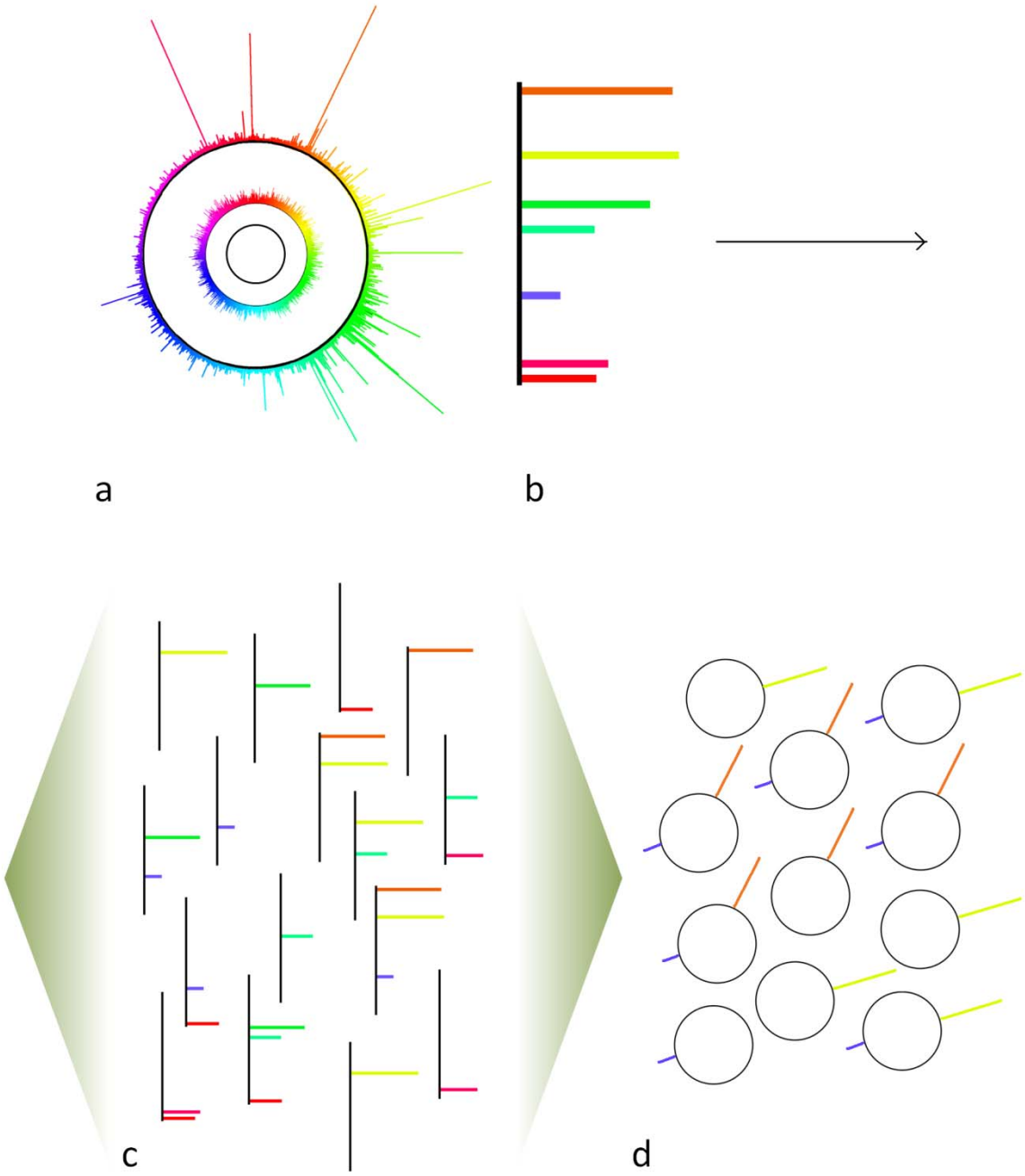

Figure 4.1 - Overview of two step mutation and selection strategy

a) The TRMR library (middle circle) is generated by introducing mutations into wild type *E. coli* (inner circle). A selection is performed yielding data on high-fitness mutants. b) A few mutants are chosen to be targets for further study. c) A MAGE library is constructed where mutations are made via recursive recombination, generating a large diversity of clones with one or more mutations. d) A selection is performed on the MAGE library to yield most tolerant clones

4.2 Materials and methods

4.2.1 Bacteria Plasmids and Media

E. coli K12 (ATCC #29425) was used for double stranded DNA trackable multiplex recombineering (TRMR) clone reconstructions. Plasmid pSIM5 was provided by Donald Court and used for the double stranded DNA recombination [122]. *E. coli* strain SIMD 70, derived from a strain called SIMD 50, was provided by Donald Court and was used for single stranded DNA recombination [126]. Overnight cultures used Luria-Bertani (LB) medium. Samples on solid media were with LB media and agar unless the antibiotic blasticidin was used, in which case a low-salt LB media with agar was used. MOPS minimal media was used as described. Pretreated corn stover cellulosic hydrolysate was provided by the National Renewable Energy Laboratory (Golden, CO). Blasticidin was used at a working concentration of 90 µg/mL. Chloramphenicol was used at a working concentration of 20 µg/mL.

4.2.2 TRMR Library and Selections

The TRMR library had been prepared in the Gill laboratory previous to the present study [1]. Preparation of the TRMR library for all selections and the sample populations for microarray analysis were done according to the instructions of the author [1]. Frozen stocks of the up and down library as well as control strain JWKAN were thawed and recovered separately in LB medium for over three hours until exponential growth was observed. All TRMR selections were performed at 37°C in a shaking incubator rotating at 225 rpm.

Selections in acetate were performed in 200 mL of MOPS minimal medium with 0.2% glucose and 16 g/L acetate. Stock acetic acid solution was prepared by titrating HPLC-grade 50% acetic acid solution (Fluka) on ice with 10 M KOH to neutral pH. Portions of the up and down libraries were mixed for an equal number of cells. The JWKAN strain was introduced into the library mix so that the JWKAN strain started with roughly 20 times the number of the average TRMR mutant present in the library, or in a ratio of 1:400. This final library mixture was introduced into the selection environment at a 2.5% inoculation. The acetate selection was performed for 69 hours.

Selections in hydrolysate were performed as described previously [1]. Briefly, selections were performed in a decreasing concentration of hydrolysate over three batches (20%, 19%, and 18% in that order).

4.2.3 TRMR Sequencing and Microarray Analysis

Final and pre-selection cultures were harvested for microarray analysis and aliquots of final selection cultures were sampled onto solid LB plates for colony picking. One billion cells (10^9) per sample were taken to ensure a representative population. TRMR barcodes were amplified from extracted genomic DNA via PCR as described previously (Promega Wizard Genomic DNA Purification kit or Invitrogen PureLink Genomic DNA Kit) [1]. The barcode DNA was purified after being run on an agarose gel via a gel extraction kit (Qiagen). From each sample, 600 ng of the sample barcode tags were applied to the Geneflex Tag4 16K V2 array (Affymetrix) and the resulting data was analyzed as described previously [1].

Control tags were supplemented in known quantities so that calculations of the

concentration of sample barcode tags might be made from the array signal. The concentration of each allele was divided by the total amount of sample DNA applied to the array to calculate the frequency of each allele. The fitness of each allele (*W*) was calculated by dividing the post-selection frequency of the allele by the pre-selection frequency of the allele.

Individual clones were genotyped by amplifying the barcode region of the insert via PCR and then subsequently sequenced conventionally.

4.2.4 TRMR Clone Reconstruction

TRMR clones were reconstructed in *E. coli* K12 via recombination using the pSIM5 plasmid. TRMR up and down inserts were amplified from genomic DNA extracted from the library population. Fifty base pairs of homology were added to each end of the insert specific to the desired location of insertion. The homology regions chosen were identical to those in the original TRMR library. Recombination was performed at 30°C as previously described [123]. Recombination recovery cultures were plated onto low-salt LB with agar solid medium with blasticidin. To ensure the TRMR insert was located in the proper location and orientation in the genome, the surrounding region was amplified via PCR, purified, and sequenced.

4.2.5 Growth Studies

Stationary phase overnight cultures were used for a 2.5% inoculation of 5 mL MOPS minimal medium in a 15 mL centrifuge tube. These cultures were monitored until the optical density at 600 nm (OD_{600}) reached 0.200 ± 0.01. A 4% inoculation was introduced into the growth test medium. The optical density (OD) was subsequently

monitored. For growth studies involving hydrolysate, 1 mL of culture was centrifuged, decanted, and resuspended in water or minimal media before the OD was observed.

4.2.6 Library Construction of Mutated Ribosomal Binding Site

The mutated ribosomal binding site (RBS) libraries were constructed via λ-red recombination. The previously-mentioned SIMD 70 was used as the base strain for the recursive multiplex recombineering.

Single stranded DNA oligonucleotides were designed to replace the RBS of the previously selected gene target with either a partially or completely degenerate sequence according to the allele found in the TRMR selection. The oligo pools had an eight-base degenerate sequence five bases upstream of the target's start codon. The up allele oligo pools were designed with the sequence 5'-DDDRDRRD-3' (where D = A, G, or T and R = A or G). The down allele oligo pools were designed with the completely degenerate of sequence 5'-NNNNNNNN-3' [99]. On either side of the degenerate sequence a 41-base homology region specific to the target [124]. The first four 5' bases are linked with phosphorothioate bonds in order to reduce single stranded exonuclease activity [124]. The oligonucleotide was designed so that the sequence was that of the lagging strand, which has been shown to increase recombination efficiency [119-121].

The SIMD 70 strain has a $galK_{tyr145UAG}$ mutation that disables the strain from metabolizing galactose. An oligonucleotide that corrects this mutation to code for a functioning *galK* gene (mutated region 5'-…CAACTATATCACCTA…-3', corresponding with oligo 478 in [124]) was used in conjunction with MacConkey agar plates with 1% galactose to test for recombination efficiency.

Multiple rounds of recombination were performed on SIMD 70 with the various mixed oligo pools. Recombination was performed at 30°C as previously described [123]. After each round of recombination, the recombined cultures were allowed to recover for 1-2 hours in adequately prepared Terrific Broth. The recovery culture was then used to inoculate a Luria Broth culture for the next round of recombination. If the cells were not immediately recultured, the recovery culture was pelleted and chilled at 4°C until further use. The *galK*$^{+}$ oligo was spiked in at a rate of 1:20 so that the recombination frequency of the final library could be tested on MacKonkey agar with 1% galactose.

4.3 Results

In order to find solutions to the problem of inhibition due to various conditions, a proper search must be done. The search space of mutations in the *E. coli* genome (~$4^{4,600,000}$) is too large for laboratory methods and time scales. Traditional methods of directed evolution involve long time course adaptation, where the microorganisms are grown over many generations for months or years [76, 127]. This process can be quickened by artificial means of random mutation, but the problem remains that after screening or selection, a mutant with the desired phenotype may have relatively few point mutations in various places across the genome, and of those, very few will be beneficial [97]. This complicates the identification of beneficial mutations [128]. Random mutagenesis and long time course adaptation methods, while producing successful results, do not have the power to effectively explore a large relevant search space and allow for large population genotyping.

Now, with the advent of genome engineering tools such as TRMR and MAGE, we are able to search an immense number of relevantly mutated clones. First, a TRMR selection is performed. A broad (genome-wide) search of relevant mutations (those which are likely to cause changes in gene expression) over a limited depth ('UP' or 'DOWN' mutations) is done to limit the number of unique clones (~8,000). Secondly, those genes with the highest fitness according to TRMR are selected as targets for MAGE library construction. Lastly, the MAGE library is subjected to a focused (<30 genes) search of relevant mutations (modified RBS to alter gene expression) over a deep range of sequences (*i.e.* multiple mutations per clone and degenerate sequences in the oligo pool).

The present study uses two growth conditions to show this search strategy. Acetate and corn stover hydrolysate were chosen to demonstrate how the method works under various metabolic conditions. Acetate is a metabolite that is well known to the cell, can enter into the central metabolism to be used as a carbon source, and can affect regulation within the cell. Corn stover lignocellulosic hydrolysate (provided by the U.S. National Renewable Energy Laboratory) is a complicated mixture of various hexose and pentose sugars, acids (acetic, formic, *etc.*), phenolic compounds from lignin, and aldehydes (furfural, HMF) derived from sugar degradation. Hydrolysate is a mixture containing a wide variety of sugars and toxins, thus making accurate predictions of what changes in the genotype might yield better growth very difficult.

4.3.1 TRMR Selections and Microarray Analysis

As previously shown, the TRMR tool can be used to identify mutations that effect tolerance to a variety of environmental stresses. Here, we applied the TRMR strategy to the previously mentioned three conditions.

The TRMR selection on acetate took place in MOPS minimal media with 0.2% glucose and 16 g/L acetate over the course of 69 hours. Samples were taken before the selection and after for microarray analysis (Figure 4.2). It is through barcode microarray technology that whole population genotyping is possible. Each allele's fitness was calculated by dividing its post-selection concentration by its initial concentration, which was calculated by comparison of control DNA added to the microarray with known concentrations. The fitness reflects the change in population over the course of the selection, rather than the end population only. Table 4.1 reports the top fitness mutants.

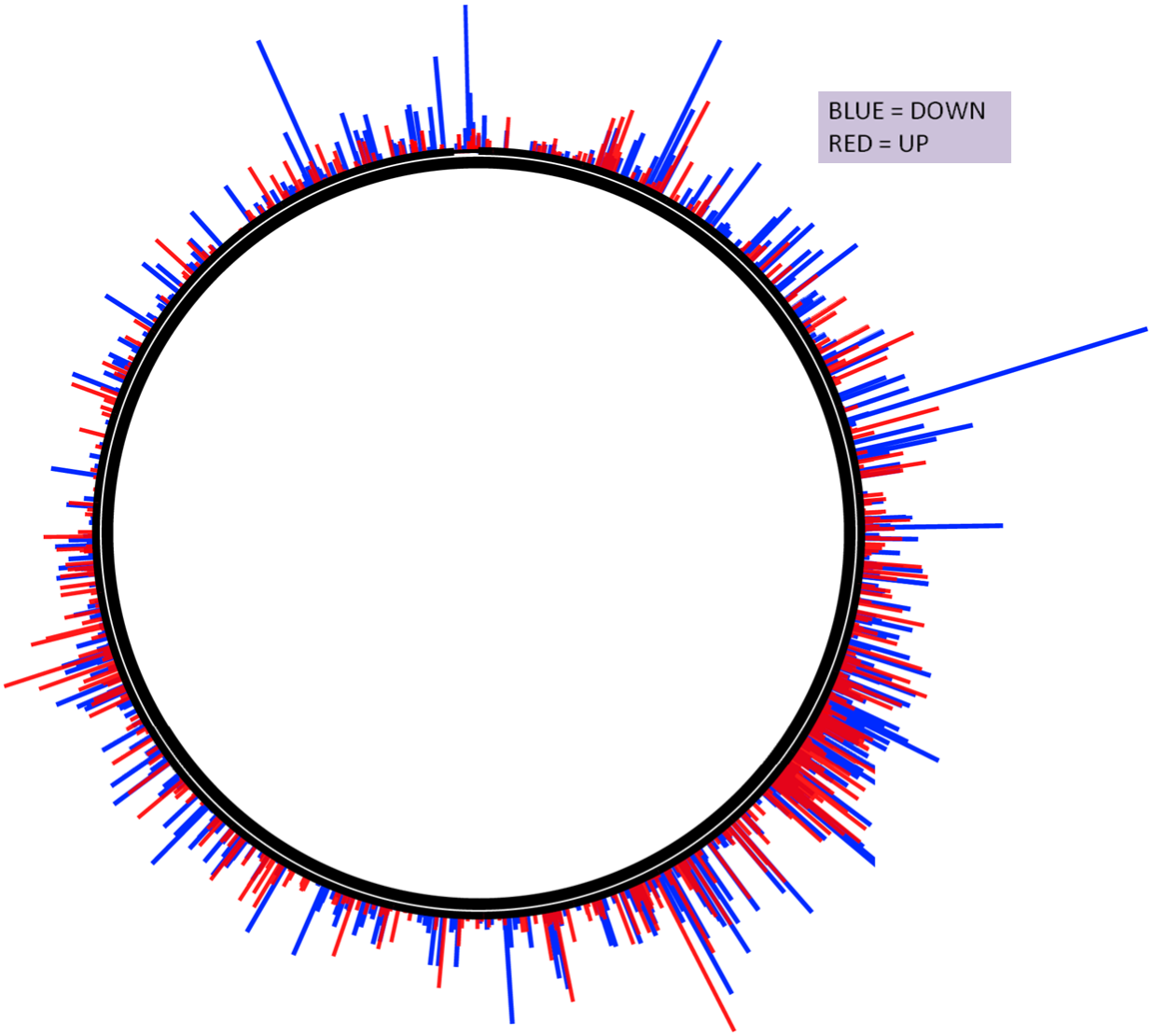

Figure 4.2 - Fitness of Mutants

Circle plot showing the result of TRMR analysis of acetate selection. Natural log of allele fitness is mapped over *E. coli* genome. Peak location represents location of clone in *E. coli* genome; peak size is relative to fitness. Colors denote the type of mutation in the clones: red spikes indicate an 'up' mutation, blue spikes represent 'down' mutations.

Rank	Fitness	genE:insert	Function
1	3980.3	serS:downtag	seryl-tRNA synthetase
2	102.7	tap:uptag	methyl-accepting chemotaxis protein IV
3	78.5	yahF:downtag	predicted acyl-CoA synthetase
4	61.2	yjdM:downtag	conserved protein
5	45.9	deoA:downtag	Thymidine phosphorylase in pyrimidine salvage pathway
6	42.0	aspS:downtag	aspartyl-tRNA synthetase
7	40.8	fabH:downtag	β-ketoacyl-acyl carrier protein synthase III
8	31.3	ynfM:downtag	member of the major facilitator superfamily (MFS) of transporters
9	30.3	rimL:downtag	ribosomal-protein-L12-serine acetyltransferase
10	25.1	ycbS:downtag	predicted outer membrane usher protein
11	24.5	ydiA:downtag	PEP synthetase regulatory protein (PSRP)
12	24.1	tqsA:downtag	quorum signal AI-2 exporter
13	20.9	sdaA:downtag	L-serine deaminase I
14	20.8	exuR:uptag	DNA-binding transcriptional repressor

Table 4.1 – Top Fitness Mutants from TRMR 16 g/L Acetate Selection

The top 14 mutants ($W > 20$) from TRMR 16 g/L acetate selection are listed with the type of mutation and function described.

In calculating fitness, a few issues may arise that will affect the accuracy of the fitness value. These mainly stem from the limited range of the signal from the array. When analyzing the microarray data, a single allele's signal may fall into three distinct categories of signal quantity. The signal may be (i) at or below the baseline signal indicating not enough DNA to quantify, (ii) within the range of the control probe signals, which allows for a reasonably accurate calculation of concentration, or (iii) above the maximum control probe signal, which results in an inaccurate calculation of concentration, usually erring by overestimation. Since this calculation must happen twice to compute fitness (both final and initial allele concentrations are needed), there are nine possible outcomes of the fitness calculation, with only one providing an accurate reading.

Accurate fitness values are obtained when both the final and initial allele concentration falls within the range of the signal of the control probes. If the final allele concentration of DNA is too low to read, we assigned a fitness of zero regardless of the initial value. Since usually only high fitness mutations are imporant, this is no great loss. In fact, this is to be expected, as a selection surely will reduce the diversity of the population to the point where detrimental mutations will be eradicated.

When the final allele signal is within an appropriate range, and the initial allele signal is below the threshold of detectable signals or above the range of control probes, a fitness calculation cannot be accurately done. In the case where the initial signal is below threshold, the initial concentration effectively zero, thus preventing division. Fortunately, in the over 8,000 alleles possible, and over 2,000 alleles with a final population signal over threshold, this occurs seven times in this acetate selection (<

0.4%). In the opposite case (final within range, initial above range), the initial concentration is set to a maximum value corresponding to half the amount of DNA added to the microarray. In these cases (20/2078, ~1% of the acetate selection) the fitness is less than one and these alleles are not considered further.

Now we will consider the case where the final allele concentration is above the range of the control probes. It is unlikely that there is a case where an allele is below threshold in the initial population, yet over the course of selection it grows so well that it is above the upper bounds of the final array. If this were to happen, the fitness could not be accurately calculated, but the allele would be of great interest. This did not occur in the acetate selection. It is much more common that when the final population has alleles that exceed the upper bound, those same alleles were either within or above the bounds in the initial array. In the case that the initial concentration can be accurately calculated, the overly high final allele's concentration is set to a maximum value corresponding to half the amount of DNA that was added to the microarray. This upper limit can lead to a fitness value that is lower than what would be calculated had the limit not been in place (this happened 14 of 2078 times). This particular situation yields alleles that are often of great interest since these are clearly a large portion of the population at the end of the selection. In the case where both final and initial allele concentrations are above the upper limit, an accurate fitness cannot be calculated. In the acetate selection, this was the case 34 times out of 2078.

In all cases but the ideal scenario, the fitness value is not accurate. Fortunately, when the final allele concentration is above the lower threshold (2078 times), the initial allele population is within the proper range 2015 times (97%). In most of the other small

number of cases, we are still able to calculate a fitness value that has reduced accuracy, but can still yield beneficial information.

The TRMR mutants with a high fitness do not fall into a single category of genes, metabolic functions, or related substrates. Some do, however, group into a few general categories of interest. To analyze this data, GOEAST (Gene Ontology Enrichment Analysis Software Toolkit) was used [129]. Gene names of those mutants with a z-score above 1.0 (log fitness one standard deviation above the mean, 164 gene names) were input into the GOEAST program. The program was instructed to yield gene ontology terms that were statistically significantly overrepresented among the top mutants (p-value < 0.10).

GOEAST yielded only three gene ontology terms that contained more than two genes in the term and were statistically significantly overrepresented. While it yielded four additional GO terms that were statistically significant, the latter had only two genes, which is not desired since the purpose was to try to broadly characterize the function of the top fitness genes. The broadest category found was simply ‘gene expression’ which contained seventeen genes (p = 0.071). These genes contained four genes related to tRNA (three of which had the down allele) and five genes coding for ribosomal proteins (two down, 3 up). Three other genes which were contained in this GO term were a part of another GO term, N-methyltransferase activity (p = 0.058). These genes code for proteins that methylate ribosomal subunits. Each of these was found with the down mutation in the TRMR selection. The GO term with the smallest p-value (p = 0.008) was receptor activity. This general term contains all genes that code for proteins that accept a chemical messenger that affects cell activity.

It seems that while GOEAST may be useful to describe genes which are related in a selection, it may not be the best for the acetate selection described here. Individual mutants may yield more information on how mutations may have conferred tolerance. It is interesting to note how thirteen of the top fifteen mutants in terms of fitness contain the down mutation. The top mutation found was *serS* down (W = 3098), which encodes seryl-tRNA synthetase. Its fitness is so high because of a very small starting concentration and a very high ending concentration taken from the microarray data. Another mutation within the top ten in fitness (sixth) is related to the *serS* mutant: *aspS* down (W = 42.0, encoding for aspartyl-tRNA synthetase). It is interesting to note that these two mutations just mentioned would seem to reduce the amount of available amino acids for protein production by reducing the amount associated with tRNA. Another top fitness mutation has a relationship to serine: *sdaA* down (W = 20.9). SdaA degrades serine into pyruvate and ammonia, such that the down mutation would presumingly slow this process.

It is interesting to note that the results from this TRMR selection do not correlate well to the results of a SCALEs selection done to elucidate acetate tolerance [130]. Whereas the SCALEs selection rendered genes with high fitness that contained metabolically active enzymes related to amino acid and nucleotide base production, the TRMR selection rendered genes with high fitness that contained genes related to amino acids (e.g. *serS*, *aspS*) and nucleotides (e.g. *deoA*), but not in their biosynthesis. This is to be expected when comparing the results of these two tools. Since in the two different selections we are not searching within the same space, we cannot expect that

the same results will be produced. This confirms the idea that search space and selections are complicated functions requiring further study.

4.3.2 TRMR Clone Genotyping, Reconstruction, and Testing

To evaluate whether the selection, individual clones must be tested for growth under selection conditions. This was done in two ways. The first was to directly take clones from the final selection population by picking colonies from sample plates. This method is facile since it involves little work to obtain the clone. In order to determine which mutation the clone has, a PCR reaction is performed to amplify the barcode tag within the insert which is subsequently sequenced. While this method is simple, it may not result in obtaining the top fitness clones from the selection. Since fitness is based on the change in proportion of the population (final divided by the initial), and not on the absolute values, often times the highest fitness mutants are not found picking colonies. In the acetate selection ten colonies were isolated and sequenced. With the exception of the prolific *elaD* up clone (*elaD* up is found in almost all TRMR selections), all those sequenced have a fitness value greater than one, meaning they take up a greater proportion of the population after the selection than before it (Table 4.2). These clones should be more resistant to acetate stress when compared to the control (a strain with no effective mutation) and other mutants with a fitness value less than one. While these clones do have a fitness greater than one, these are not the top fitness clones from the selection. When tested for growth, no significant increase in growth was observed (data not shown). Their fitness ranges from 2.2 to 8.3 (putting them between 309th and 53rd in rank among all clones). Another method must be employed to observe the growth characteristics of the top performing mutants.

Clone	Gene	ON/OFF	Fitness	Rank
MOPS 69 A	elaD	ON	1.00	1167
MOPS 69 B	yiaW	OFF	4.06	144
MOPS 69 C	yfbK	ON	6.91	65
MOPS 69 D	dacB	OFF	2.21	309
MOPS 69 E	htpX	OFF	5.37	92
MOPS 69 F	ycjU	ON	8.30	53
MOPS 69 G	yfbO	OFF	3.92	150
MOPS 69 H	yciS	OFF	3.77	163
MOPS 69 I	rplI	OFF	1.68	443

Table 4.2 – Identification of Picked Clones

Identification of particular clones picked from end point sample plates. The fitness of the particular mutant is shown alongside the rank of that fitness against all other clones.

The second method to test selection efficacy is to reconstruct some of the highest fitness mutants. To do so, the double stranded DNA containing the desired insert (up or down) and homology regions on either side must first be constructed. The up or down insert sequence was isolated from the TRMR library via PCR. To generate the specific insert DNA to be used in recombination, primers were designed to anneal with the ends of the insert DNA and have ~50 base overhangs on either side that were specific to the desired insertion site. These insertion sites were chosen to be the same sites used in the construction of the TRMR library.

Eight clones were chosen to be reconstructed from the acetate TRMR selection results. The *serS* down mutant was the clone with the highest fitness from the microarray data (estimated ln(*W*) = 8.3). It, along with the *yahF* down (ln(*W*) = 4.4), *tqsA* down (ln(*W*) = 3.2) and *clcB* down (ln(*W*) = 1.1) mutants, had a chip signal that exceeded the control probes, so an accurate fitness value cannot be calculated, although an estimate was made. The *deoA* down (ln(*W*) = 3.8) clone rounds out the mutants chosen with the down version of the mutation. The *tap* up (ln(*W*) = 4.6) mutant had the highest fitness in the acetate selection and was second overall only to the *serS* down mutant. Two other up mutants were chosen for reconstruction: *ddpA* up (ln(*W*) = 2.7) and *znuC* up (ln(*W*) = 2.6). The oligonucleotides that were used to reconstruct these clones are shown in Table 4.3.

Unfortunately, the TRMR reconstruction was problematic. After a considerable amount of time, only six of the eight have been constructed: *tap*, *ddpA*, and *znuC* up and *deoA*, *tqsA*, and *clcB* down.

As shown in Figure 4.3, four of the six reconstructed clones tested had statistically significantly higher growth in 16 g/L acetate after 24 hours, while two of the nine picked clones had a statistically significantly higher growth. The constructed clone *tap* up performed the best, 46% higher growth compared to the control. The *tqsA* and *clcB* down clones grew 31% more than the control. The *ddpA* up clone grew 21% more than the control. Disappointingly, the other two tested reconstructed clones performed no better than the control, especially the *deoA* down clone, which was in the top five clones within the selection in terms of fitness. This leads us to conclude that the selection may have a moderately high false positive rate, meaning there is a significant portion of the clones listed with a high fitness in the selection that do not increase resistance to acetate.

The *rplI* and *yiaW* down clones, picked from plates after selection, also had a higher growth, but only 11% and 9% better than the control, respectively. The remaining picked clones did not significantly increase growth. This shows that fitness is a better indicator of which clones will grow better under stress conditions compared to simply picking clones at the end of the selection.

Primer	Sequence
serS DOWN FOR	GTCGCAGGCTGTGGCCACATCTCCCATTTAATTCGATAAGCA CAGGATAAGC*GTAGCACACGAGGTCTCT*
serS DOWN REV	TTTTTCAGCGACTGCGTCTGGCTCATTACGCAGCAGATTGGG ATCGAG*CATGGAGGAGATAACGG*
yahF DOWN FOR	CTGTATGGCATGGCCGATGGTTGTGCGCTGAGCCAAACCTAC GGAGGGAATT*GTAGCACACGAGGTCTCT*
yahF DOWN REV	CGAGACAGAATCAAAATAGGTATTCGGTTTAATGACTATTTTAA CTGA*CATGGAGGAGATAACGG*
tqsA DOWN FOR	CGGAGCGAAAAAGACATTATTATTAGCAAAGGAAGAAAAAACG GGGACAAGC*GTAGCACACGAGGTCTCT*
tqsA DOWN REV	CAACATAATGACGATTTTTAGGCCATTGAGCGTGATGATCGGC TTTGC*CATGGAGGAGATAACGG*
deoA DOWN FOR	GTAGACGCATCCGGCAAAAGCCGCCTCATACTCTTTTCCTCG GGAGGTTACC*GTAGCACACGAGGTCTCT*
deoA DOWN REV	CAGCGCATGACCATCACGTTTTTTACGAATAATTTCTTGTGCG AGAAA*CATGGAGGAGATAACGG*
clcB DOWN FOR	TTGCCCATTTCTGCTCATGCATCATCTACACATCTATCCGGAT CTGCGCACT*GTAGCACACGAGGTCTCT*
clcB DOWN REV	AAAGGCCGCGAGAATACCGACGACTGTTGCGATAAGCAGACG GTGGAA*CATGGAGGAGATAACGG*
tap UP FOR	ATTTTGACGAGTATTTACTAACGCGGTCATTGCCGCCTGATGG GGAGCGTTG*GTAGCACACGAGGTCTCT*
tap UP REV	GAGAATCAAAATTAAAAACAGCGTGGTCGAAATTCGAATACGA TTAAA*CATTTATCACCTCCTTACG*
ddpA UP FOR	TCTTGTTTTATATCCCCTGGCACACAGCACGTCAGTTAATCAG GAAACTGTC*GTAGCACACGAGGTCTCT*
ddpA UP REV	GGCAAGGACGAGCGCGAGCAATGTGGGACGAAACGATATCG ATCTCTT*CATTTATCACCTCCTTACG*
znuC UP FOR	TGAGAAGTGTGATATTATAACATTTCATGACTACTGCAAGACT AAAATTAAC*GTAGCACACGAGGTCTCT*
znuC UP REV	GCGTTGGCCAAAAGAAACCGAGACATTTTCCAGGGAAACCAG ACTTGT*CATTTATCACCTCCTTACG*

Table 4.3 – TRMR Clone Reconstruction Primers

The ssDNA primers used to generate the dsDNA insert to reconstruct TRMR clones found with high fitness in the acetate selection are shown. The italicized portions of the sequence are those common regions that anneal to the TRMR insert. The non-italicized region constitutes the homology region for specific insertion.

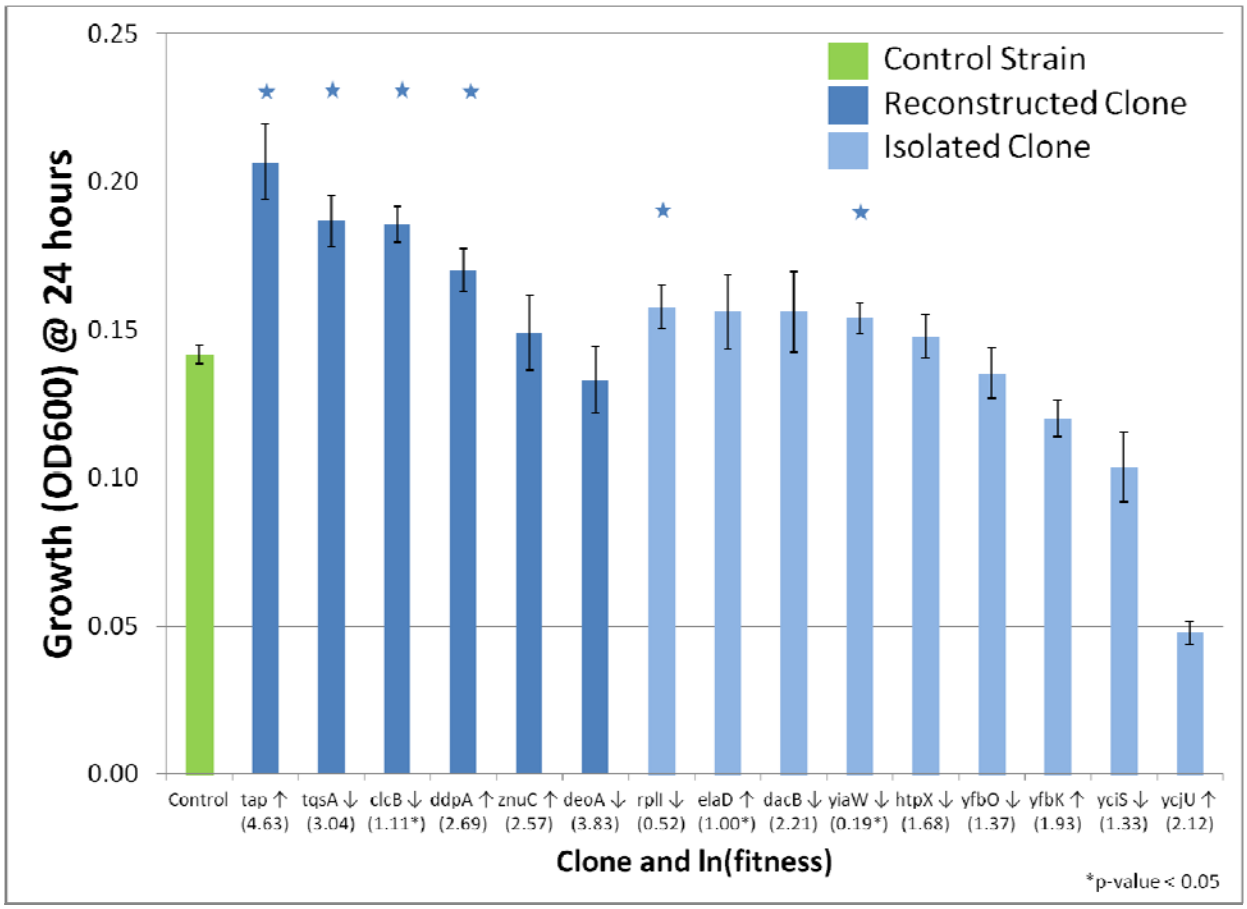

Figure 4.3 – TRMR Clone confirmation

Growth study of selected clones. TRMR mutants were tested for growth over 24 hours in 16 g/L acetate. The gene name and arrow refer to the location and type of mutation for each clone. The number beneath the mutant name is the natural log of the fitness for that clone.

4.3.3 Consideration of Practicalities for Engineering Strains with Multiple Mutations

With the goal of engineering a strain containing multiple mutations which each positively affect the growth characteristics, genes which had mutants with high fitness in TRMR selections were chosen for further study. It is in this section that the practicalities and mathematics of such a goal must be addressed before moving on to the laboratory results on the matter. In the grand scheme employed here, this is the middle stage transitioning from a broad (genome-wide) space in a high-throughput (via microarray) manner to a deep, but narrow space (multiple mutations, with combinations thereof) requiring more labor intensive genotyping**.**

The method employed here to generate multiple mutations is very much like a previously described method, Multiplex Automated Genome Engineering (MAGE) [99]. It is said to be like MAGE, but not MAGE, in that there is no automated portion of our method. For convenience, in referring to the method in this work, the term MAGE will be used with the understanding that we have no automated device. MAGE uses multiple rounds of single stranded DNA (ssDNA) recombination to replace the native ribosomal binding sites (RBS) of target genes with degenerate sequences from synthetic ssDNA.

Like TRMR, MAGE uses recombination to make mutations that are very specific in location and nature so that these mutations effectively alter the expression of the targeted gene. There are differences as well. TRMR employs a library of single-mutation clones that encompasses 97% of the genes in the *E. coli* genome, while

MAGE is limited to a relatively small number of genes (up to ~30). This recusive multiplex recombineering method (*i.e.* MAGE) has the ability to generate multiple mutations per clone.

TRMR clones have a blasticidin resistance cassette, ensuring every clone in the population has a TRMR mutation. This, however, makes the generation of multiple mutations difficult since inserting a large cassette that includes an antibiotic resistance marker requires double stranded DNA (dsDNA) recombination and either the removal of the antibiotic resistance marker before making multiple mutations or the use of a different resistance cassette. Single stranded DNA recombination, which is used in MAGE, has a much higher efficiency of successful recombination when compared to dsDNA insertions [119, 120, 124]. The much higher efficiency allows for the generation of multiple mutations if done recursively (*i.e.* recombination upon an already recombined population). However, an antibiotic resistance cassette is too large to be inserted with ssDNA, so MAGE is limited in what mutations it can make since there is no selective marker. MAGE can be done recursively many times and still a portion of the population will have no mutations at all.

Determining the genotype of the population is different between TRMR and MAGE as well. Since TRMR uses microarrays, an entire population can be characterized at once. Individual clones can be identified via PCR amplification and sequencing of the insert's barcode tag. Currently, there is no way to genotype an entire population of MAGE clones. It requires a PCR reaction for every target chosen, limiting the number of target genes that are practical to engineer.

The type of mutation conferred is also different between the two tools. The TRMR mutations are binary: an 'up' cassette containing a strong promoter and RBS and a 'down' cassette which has no promoter and a weak RBS [1]. Because there are only two mutations possible and ~4,000 *E. coli* genes, there are only ~8,000 unique mutations. MAGE, in comparison, is much more complex. Using degenerate ribosomal binding site replacement sequences, thousands of unique mutations are possible for each target chosen. Since multiple mutations are possible and desired, the number of unique possible mutants gets very large.

The TRMR targets from the hydrolysate and acetate targets were chosen from the top fitness alleles found in the TRMR selections. It is here we transition from searching a broad space in a high-throughput manner to a very deep, but narrow space. In order to search individual clones that contain a significant portion of the population with multiple mutations in the targeted regions, many rounds of MAGE must be run.

Efficiency of recombination is of paramount importance. A greater efficiency of recombination means fewer cycles of MAGE are required to achieve the same number of mutants. More importantly, greater recombination efficiency means more multiple mutants within single clones. Others have shown recombination efficiency under similar conditions consistently around 20% [124]. Wang *et al.* (2011) have generated empirical formulae predicting the recombination frequency of ssDNA recombination based on their experience and the type and size of the mutation [99, 131]. Based on their formula, the recombination work presented here should have a per-round efficiency of 10.1%. Our efficiency, as quantified by using an oligo that restores the operational sequence of the *galK* gene in the SIMD70 strain (oligo 478 in Sawitzke *et al.* 2011), was

4.4% in the acetate MAGE recombination library and 5.0% in the hydrolysate library [124]. While this efficiency is lower than the expected efficiency, it is within an acceptable range.

Since the efficiencies are relatively low, many rounds of MAGE must be performed so a significant number of mutations, especially multiple mutations, arise in the population. To estimate the number of mutations per clone and the number of total mutants, we base our estimates on the galK+ efficiencies obtained during recombination. We assume that only one mutation can occur per round of MAGE per clone (not necessarily true, but accurate for estimating multiple mutation clones since the efficiency is low and double mutations per round are rare), and that there is no bias in efficiency whether or not a clone already has a mutation. For example, if the recombination efficiency per round is 10%, then if two rounds were performed we would estimate that 1% would be double mutants, 18% would be single mutants, and 81% would have no mutations. The initial estimated population after the acetate MAGE process (eleven rounds at 4.4% efficiency) is that 61% of the population have no mutations, 31% have a single mutation, 7.1% have are double mutants, 1.0% have triple mutations, and the remainder have more than 3 mutations per clone. The initial estimate for the hydrolysate library after thirteen rounds of MAGE with 5.0% efficiency is that 51% of the population has no mutation, 35% are single mutants, 11% have double mutations, 2.1% are triple mutants, and the rest of the population has more than 3 mutations per clone. While in both these populations there is a large portion of unmutated clones, we are introducing mutations shown to highly affect fitness under the selection conditions. Under these same selection conditions the control strain did not

grow well (control strain fitness = 0.024 in the acetate selection). It is not unreasonable that we should be able to apply a selection pressure such that tolerant clones will be enriched amidst the background of the wild type population.

The populations of these double and triple mutants will vary between the two libraries by the number of target RBS that are chosen for mutation. In the hydrolysate library, 27 targets were chosen for recombination by Dr. Reeder. Ignoring for now the variations in the degenerate RBS mutations, there are a total of 702 distinct mutants which have a mutation in two of the target regions; there are 17,550 unique combinations of 3 targets. For the acetate MAGE library, however, a relatively small number of eight targets were chosen. There are a total of 56 two-target and 336 three-target combinations. To put these numbers in perspective, a selection will typically start with over 600,000,000 cells. If 10% of the population are double mutants, then each combination of the double mutants in the hydrolysate selection would occur in over 90,000 clones each for the hydrolysate library and over 750,000 clones for the acetate library. The more mutations per clone, the more combinations of targets there are and a smaller portion of the population that falls into that category. Since the number of unique combinations of targets increases nearly exponentially with multiple mutants (*i.e.* single, double, triple and so on), only the single and double mutant populations can be well-searched.

The previous mathematical analysis is concerned with the initial library of mutations. Let us ask if it is reasonable that even after a proper selection we should expect to find a large portion of double and triple mutants in the final selection population. An assumption of the MAGE process is that mutations of multiple targets in

a single clone can function synergistically to yield a clone which has a higher tolerance to toxin than clones with only the individual mutations within them. This assumption may hold for many combinations but may not be true for all. It is difficult to predict this interaction between mutations.

We can classify double mutants in four general categories: antagonistic, less-than-additive, additive, and synergistic combinations. A synergistic clone has two mutations, where the increase in the growth compared to the wild type exceeds the sum of the increase in fitness of the single mutants from which it is comprised. For example, if two single mutant clones each yield an increase in growth of 25% when compared to the wild type, a synergistic clone would have a greater than 50% increase in growth. An additive clone would be similar, but the increase in growth compared to wild type would be the sum of the individual growth rate increases. A less-than-additive clone is one where the double mutant's growth is superior to the single mutant clones, but less than additive. Incompatible combinations are those where two individual mutations increase the fitness compared to the wild type strain, but having both mutations present in one clone decreases the fitness when compared to the original clones. The type of double mutants that are actually produced in the process will determine what clones are found at the end of the selections.

Through a simple model, we can see how some of these scenarios would work in the context of a selection (Figure 4.4). There are four cases of how multiple mutations could affect the growth rate. We model a selection based on our recombination efficiencies. The wild type specific growth rate was set to a value typical for a 90% growth inhibition (0.05 1/hr). An assumption is made that most mutations will be neutral

and a small portion (10%) of mutations will be beneficial (increase in growth rate of 35%, as observed). When multiple beneficial mutations are present in a clone, the mutations' benefits may be independent of one another (benefits of single mutations are compounded additively), or the mutations may interact. Interactions may be synergistic (benefits are 10% higher than additive), less than additive (10% lower than additive), or antagonistic (growth 15% less than the single beneficial mutation for every additional mutation). As can be seen in Figure 4.4, after 200 hours of selection, double and triple mutants quickly become a significant portion of the population in the synergistic model, more slowly in the additive model, and then even more so in the less-than-additive model. In the antagonistic interaction model, the double and triple mutants are depleted in the population. The model is described mathematically in equation 4.1.

$$P_{tot} = \sum_{n=1}^{5} P_{n0}\left[\sum_{r=1}^{n}\binom{n}{r}\alpha^{r}\left(1-\alpha\right)^{n-r} e^{\left(\mu_r \cdot f_{antag}^{r} \cdot t\right)}\right] \quad \text{Eq. 4.1}$$

Where P_{tot} = total population, P_{n0} = initial population of those with *n* mutations (based on laboratory efficiencies), n = number of mutations in a clone, r = number of beneficial mutations in a clone, α = fraction of mutations that are beneficial, μ_r = growth rate with *r* beneficial mutations, f_{antag} = antagonistic factor, and t = time. The Calculation of μ_r is shown in equation 4.2.

$$\mu_r = \mu_{WT}\left(f_{increase} \cdot f_{synergy} \cdot r + 1\right) \quad \text{Eq. 4.2}$$

Where μ_{WT} = wild type growth rate (set to 0.05 1/hr), $f_{increase}$ = fractional increase in growth rate of one beneficial mutation (set to 0.35), $f_{synergy}$ = synergy factor, and r =

number of beneficial mutations in a clone. The values for the synergy and antagonistic factors are as follows. For each condition besides antagonistic, the antagonistic factor was set to one, effectively eliminating it from the equation. For the antagonistic condition, the antagonistic factor was set to 0.85. The synergy factor was set to 1.1, 1.0, and 0.9 for the synergistic, additive and the less than additive conditions, respectively. The antagonistic condition also had a synergistic factor of 0.9.

Using these growth rates, a model selection calculated what clones would be in the final population after some amount of time. As can be seen in Figure 4, after 200 hours of selection, double and triple mutants quickly become a significant portion of the population in the synergistic model, more slowly in the additive model, and then even more so in the less-than-additive model. In the antagonistic interaction model, the double and triple mutants are depleted in the population. The model points to the idea that if the selection population starts with a relatively small number of double and triple mutants and the individual mutations are not at least additive in their increase of growth rate, it should not be surprising to find at the end of a selection a large number of clones which have only one or even no mutations.

a.

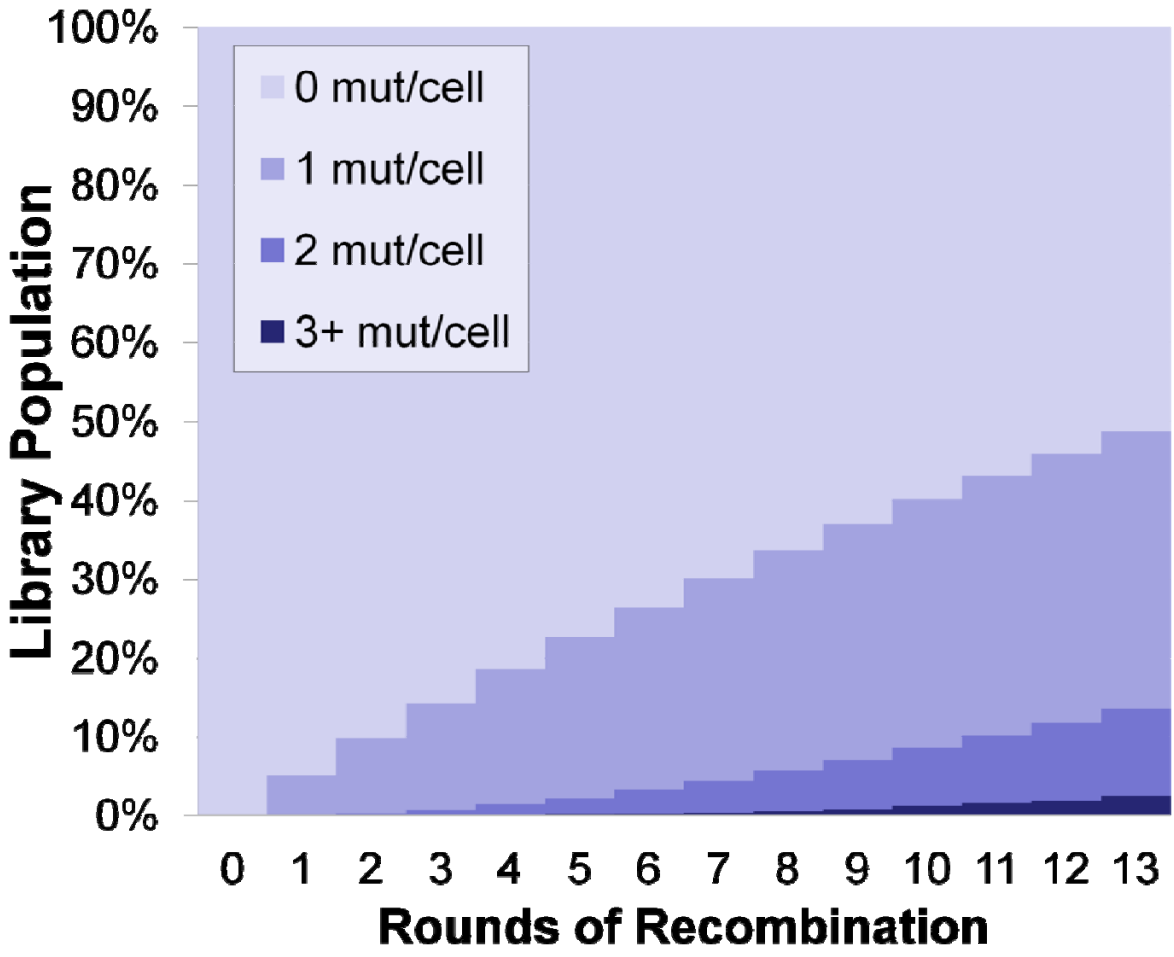
100%
90%
80%
70%
60%
50%
40%
30%
20%
10%
0%
Library Population
0 mut/cell
1 mut/cell
2 mut/cell
3+ mut/cell
0 1 2 3 4 5 6 7 8 9 10 11 12 13
Rounds of Recombination

b.

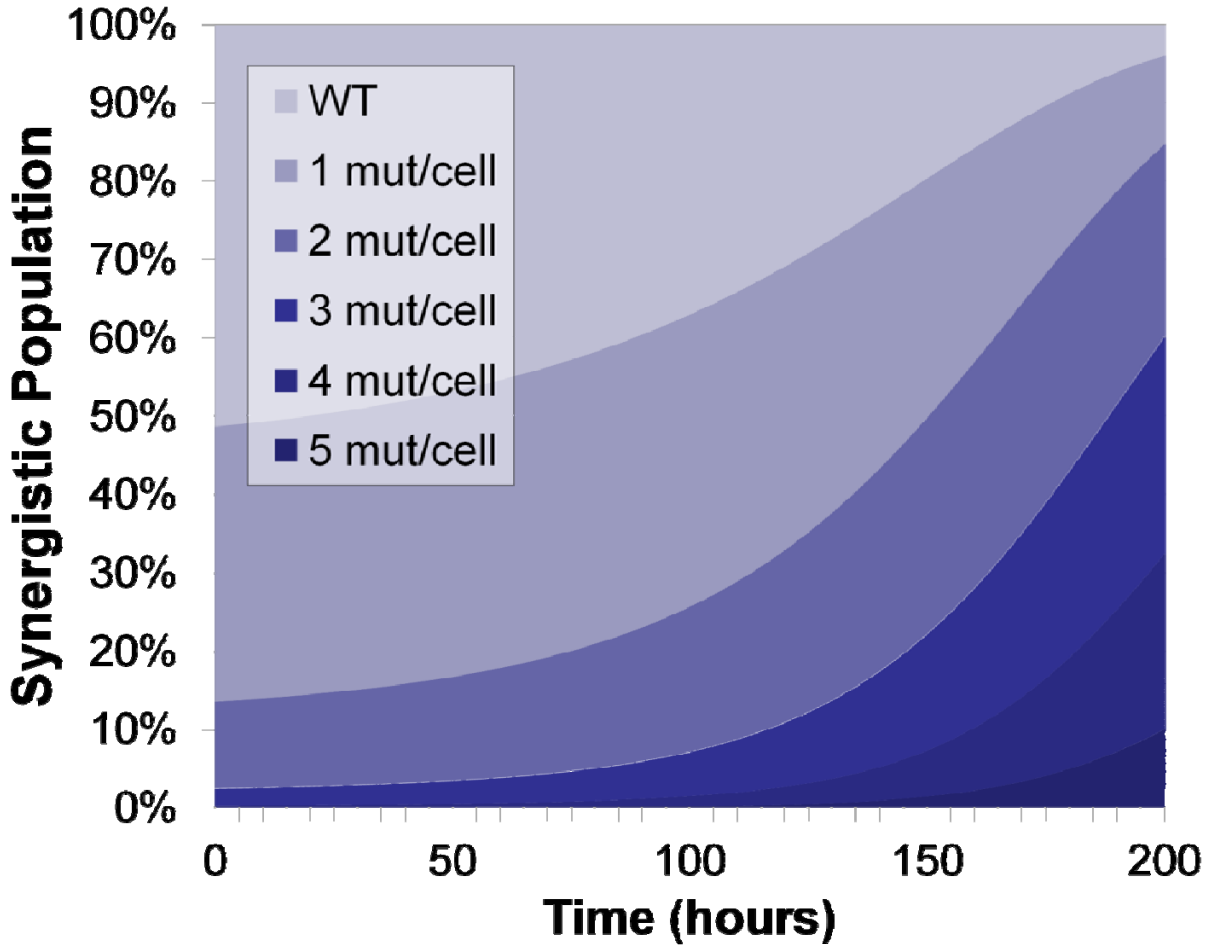
100%
90%
80%
70%
60%
50%
40%
30%
20%
10%
0%
Synergistic Population
WT
1 mut/cell
2 mut/cell
3 mut/cell
4 mut/cell
5 mut/cell
0
50
100
150
200
Time (hours)

c.

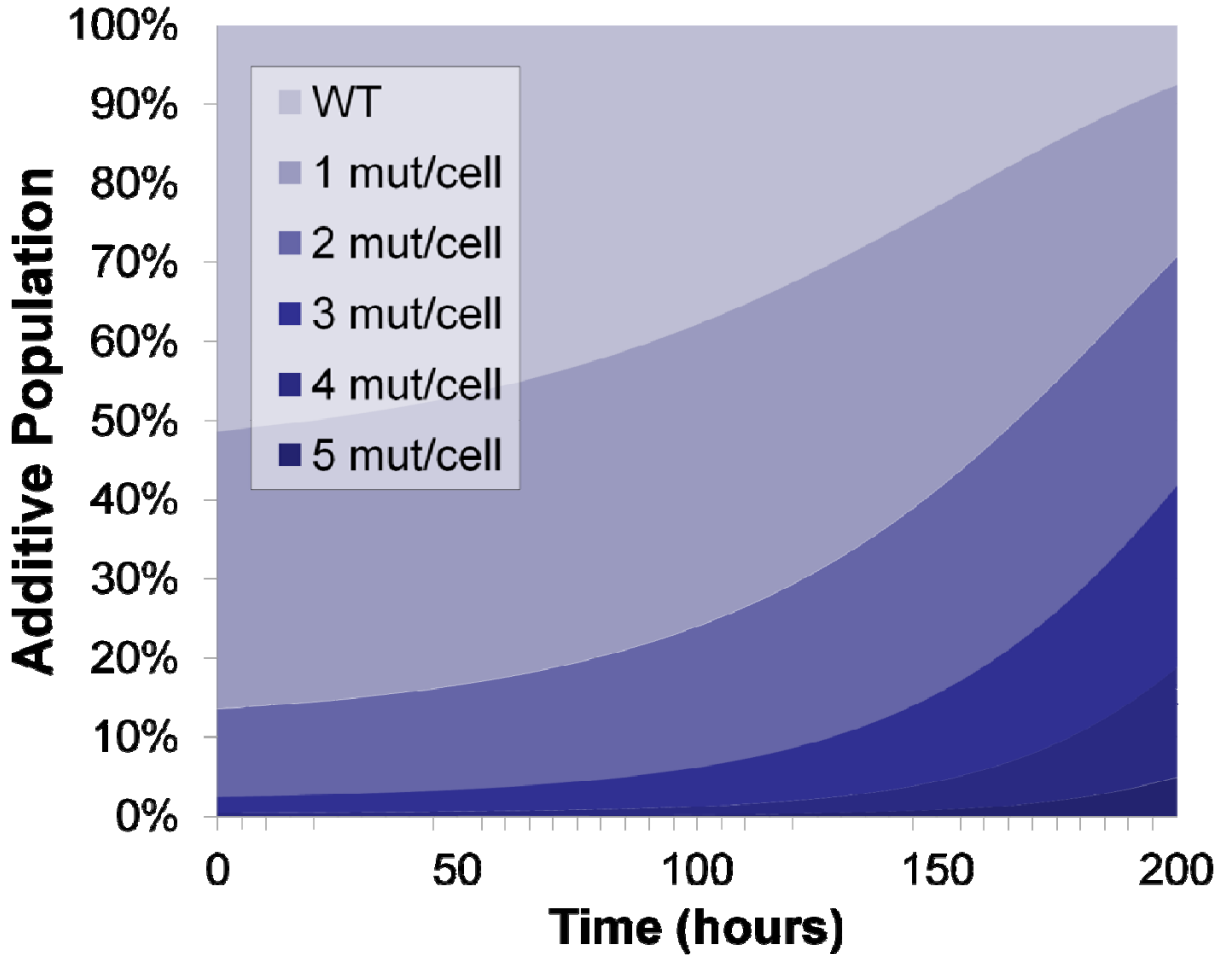
100%
90%
80%
70%
60%
50%
40%
30%
20%
10%
0%
Additive Population
WT
1 mut/cell
2 mut/cell
3 mut/cell
4 mut/cell
5 mut/cell
0
50
100
150
200
Time (hours)

d.

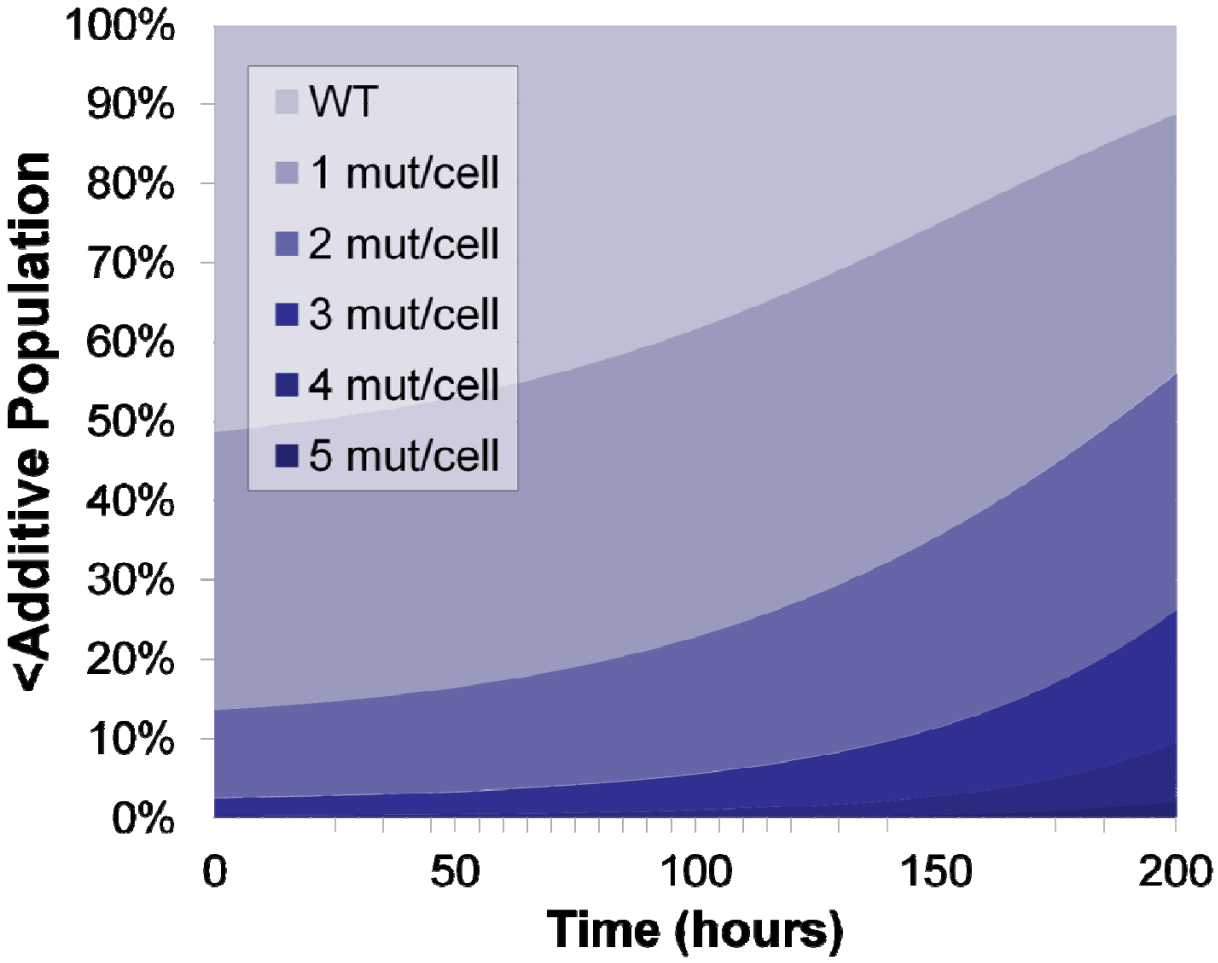
100%
90%
80%
70%
60%
50%
40%
30%
20%
10%
0%
<Additive Population
WT
1 mut/cell
2 mut/cell
3 mut/cell
4 mut/cell
5 mut/cell
0
50
100
150
200
Time (hours)

e.

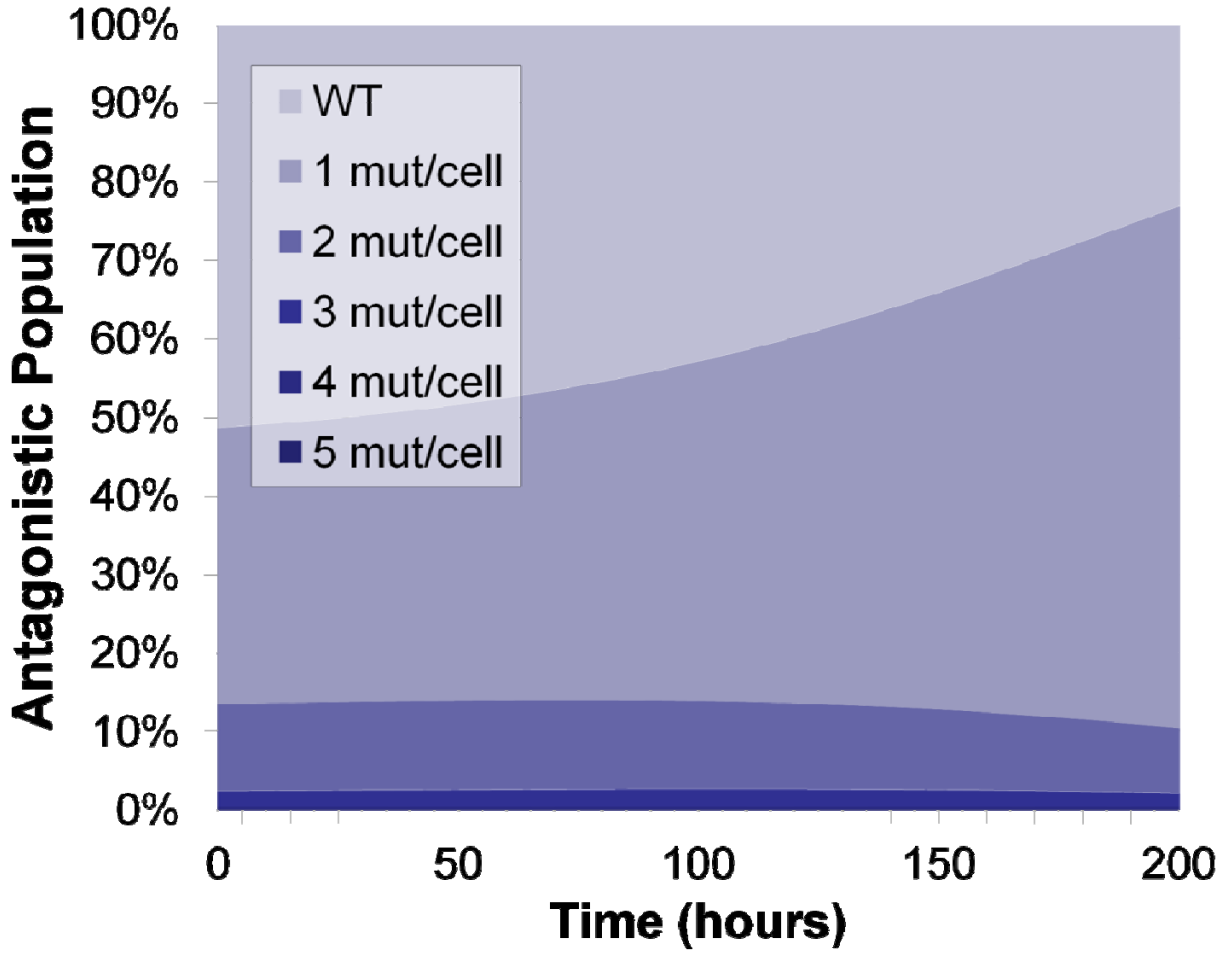

Figure 4.4 – Model Describing MAGE Selections

a) Construction of a MAGE library. Shown is the theoretical population distribution of a MAGE library if the recombination efficiency is 5.0%. Each round generates more mutations and the construction of multiple mutations over the 13 rounds. b) Synergistic selection: A theoretical selection where 10% of single mutants are beneficial and the combinations thereof are synergistic (increase in growth rate is more than additive). c) Additive selection: Same as (b) but combinations are additive. d) Less-than-additive selection: Same as (b) but combinations are less than additive. e) Antagonistic selection: more than one mutation causes a decrease in growth rate. Time for (b) – (d) is 200 hours, increase in growth rate for beneficial single mutations is 35%.

4.3.4 Construction and Selection of MAGE Libraries

Acetate and hydrolysate MAGE libraries were constructed via the MAGE recombination method. As previously mentioned, these two libraries vary greatly in their scope. For the hydrolysate library, 27 targets were chosen from the highest fitness TRMR alleles. Chosen from top alleles in the up direction were *ahpC*, *ptsI*, *ygaZ*, *lpcA*, *eutL*, *ygjQ*, *ydjG*, *talA*, *motA*, *moeA*, *ilvM*, *lolC*, *agaS*, *ybaB*, *tonB*, *nanC*, and *yedQ*. From top down alleles were *puuE*, *ugpE*, *ptsI*, *lpp*, *yciV*, *cyaA*, *ydjG*, *rseP*, *lacZ*, *ybjN*, *ybaB*, *talB*, and *ydaG* (Table 4.4). As mentioned previously, thirteen rounds of recombination were done with the mixed pool of oligonucleotides including a portion of galK+ to track replacement efficiency. Replacement efficiency was estimated to be 5.0% per round, so after all the MAGE rounds we estimate the population to be 35% single mutants, 11% double mutants, 2.1% triple mutants, 0.3% quadruple mutants and the rest parent strain SIMD 70.

The hydrolysate library population was subjected to the stress of selection in 40% corn stover hydrolysate in otherwise MOPS minimal medium [107]. The selection occurred for almost 10 days (232 hours). The culture was serially transferred from one batch to the next to prevent the culture entering stationary phase. There were eleven batches total, allowing 59 generations. The growth rate was monitored throughout the selection and after 11 serial transfers the growth rate doubled compared to the initial batch growth rate (Figure 4.5). After this time, samples were taken and culture was plated to obtain individual colonies.

MAGE Oligo	Sequence
ahpC up	T*T*A*A*AAGGTTTAATTTTGGTGTTAATCAAGGACATCTATAGYYHYYHHH TGTTTTCGATGAGATGTAAGGTAACCAATTTTTGCCGATT
ptsI up	A*C*T*C*GAGTAATTTCCCGGGTTCTTTTAAAAATCAGTCACADDDRRCRR DGGGTTATGATTTCAGGCATTTTAGCATCCCCGGGTATCGC
ygaZ up	T*A*A*G*ATATTCATTCAGTCTATTTATAATATTAACAATCGTDDDRRCRRD ACTCTATGGAAAGCCCTACTCCACAGCCTGCTCCTGGTTC
lpcA up	T*C*G*T*TCAGTTCGTTACGAATAAGATCCTGGTACATGAGGAHYYHYYHG HGCATAAATGTAATAGACAAAATGCAGTGTACCGGATACCG
eutL up	G*T*G*A*CAGACGGTCGAATCAAATCTAAAGCTGGCATGATGCHYYGYYH HHGGGTCATGTTGATGCCGGATGCTTTCTGCTCCAGCATACG
ygjQ up	T*T*C*T*TTCTTTAGCGCCTAAAATCGACCTCCCCCCTTTCGTDDDRCDRR DCGACCATGCTGCGCGCATTTGCCCGCCTTCTTCTCCGTAT
ydjG up	G*T*A*A*TATCCGTTGTGCCTAAAGGTATCTTTTTCATTTGCCHYYHYYHHG CTTCGTATTCTTCCAGCAATTGTTCGACCAGCTTTCTGTT
talA up	G*A*A*G*TGTGAATTAACGCACTCATCTAACACTTTACTTTTCDDDRRCRR DTTCCTATGAACGAGTTAGACGGCATCAAACAGTTCACCAC
motA up	C*C*G*A*GAACAACCAGGTAACCTAATAAGATAAGCACGACATGYYHYYH HHACTGTTGACCATGACAGGATGTTCAGTCGTCAGGCGTTAA
moeA up	G*C*G*T*TTTTCTGACATAATAGGCAAATTCGATTTTGCCTCCDDDRRDRR CTTTTCATGGAATTTACCACCGGATTGATGTCGCTCGACAC
ilvM up	A*A*G*C*GAGCCGATACATTGACCTGATGTTGCATCATGATAAHYYGYYHH HCATTTCTGAATTACTGGCGCCAGGCGGCACCAGCGGCCAG
lolC up	C*G*C*A*GGCCAATAAATAGAGCGACAGGTTGGTACATGAAATGYYHYYH HHTGCTGTAGCAAAGACACGAGTATATAAGCGAAAGCAAGAT
agaS up	G*C*A*A*GTGAAAGCGACAACGCCCGACGTCAAGTTCATCAGADDDRRCR RDGAGTTATGCCAGAAAATTACACCCCTGCTGCCGCCGCAAC
ybaB up	T*T*C*A*TCAGGTTACCCAGACCGCCTTTACCAAACATAGGTTHYYHYYHG HATCACGTTAAGGATGACGAACGTAAGCTGTGCTTACGATC
tonB up	G*G*C*C*AGGGGAAGCGGCGAGGTAAATCAAGGGTCATTGAAGHYYHYY HGHTTTCAGTAGAAAAACCAGGTCTCGATTTTAAATGCAAATA
nanC up	A*T*T*G*TTTATGCGGGCTTTGTATTGCTTTCTGTATCCTACADDDRRCRR DAATTTATGAAAAAGGCTAAAATACTTTCTGGCGTATTATT
yedQ up	C*A*G*C*TCTGGTTTTCCATTTTTGTCTCGTGCTGCACCCTGAGYYHYYHH HACCTGCTTTTTTATGATTCTGGCATAACCTGGCGATAGCG

puuE down	G*A*A*A*GACGACGCTGATGGAATTCATTGTTGCTCATGTTTCNRRNGRNN NGACTCTTCACGGTTAATCGGAAATTAAACGCCCAGACGAT
ugpE down	C*T*G*A*ATATCGTCAGCCACGGACGGTTCTCAATCATTGGTANRRNRGNN NGCTTTCAACATAGCGGAACTGCACCACCGTCAGCACGATG
lpp down	G*T*G*T*AATACTTGTAACGCTACATGGAGATTAACTCAATCTNNNYCNYYN TAATAATGAAAGCTACTAAACTGGTACTGGGCGCGGTAAT
yciV down	A*G*G*T*CGTAAATCACTGCATAATTCGTGTCGCTCAAGGCGCNRRNGRN NNCTGGATAATGTTTTTTGCGCCGACATCATAACGGTTCTGG
cyaA down	A*G*T*C*TCTGTTTCAGAGTCTCAATATAGAGGTACAAGACGTNRRNGRNN NTTTGCTACCCGTCATGACTGTGATTCCGCCAACATCAACG
rseP down	A*T*G*A*ACGAAGCCAAATCCCAGAGAAAACTCAGCATATTACNRRNGRNN NAAGCGTCCTGAATACCAGTAACAACAAGCAAGCAAAGACC
lacZ down	A*A*A*A*CGACGGCCAGTGAATCCGTAATCATGGTCATAGCTGNRRNGRN NNTGAAATTGTTATCCGCTCACAATTCCACACAACATACGAG
ybjN down	A*G*C*G*TATCCAGACCAGGAACGACCAGCGATGTCATAATTTNRRNGRN NNTCTTTCGATAAAAAGACCGGCACAGCTTACGCAAAAAGCG
talB down	G*T*G*T*ACTGACGAAGGGAGGTCAATTTGTCCGTCATGATAGNRRNRGN NNTTAAACAGCTTGTTAGGGGGATGTAACCGGTCTGCCCTGA
ydaG down	A*A*T*T*TTGCAGTGCAGCAGTTAGTTCCGCCACCCGGCGTTANNNYCNYY NATAAGATGGTGCATTACGAAGTAGTTCAGTATTTGATGGA

Table 4.4 – MAGE Oligos for Hydrolysate Library Construction

The sequences of the MAGE oligos for hydrolysate targets are shown. The "*" symbol represents phosphorothioate bonds which slow the degradation of the oligos within the cell. These oligos were designed by Dr. Reeder. The degenerate region is shown with non-traditional symbols for nucleotide bases: R= A or G, D = A, T, or G, and N = A, T, C, or G.

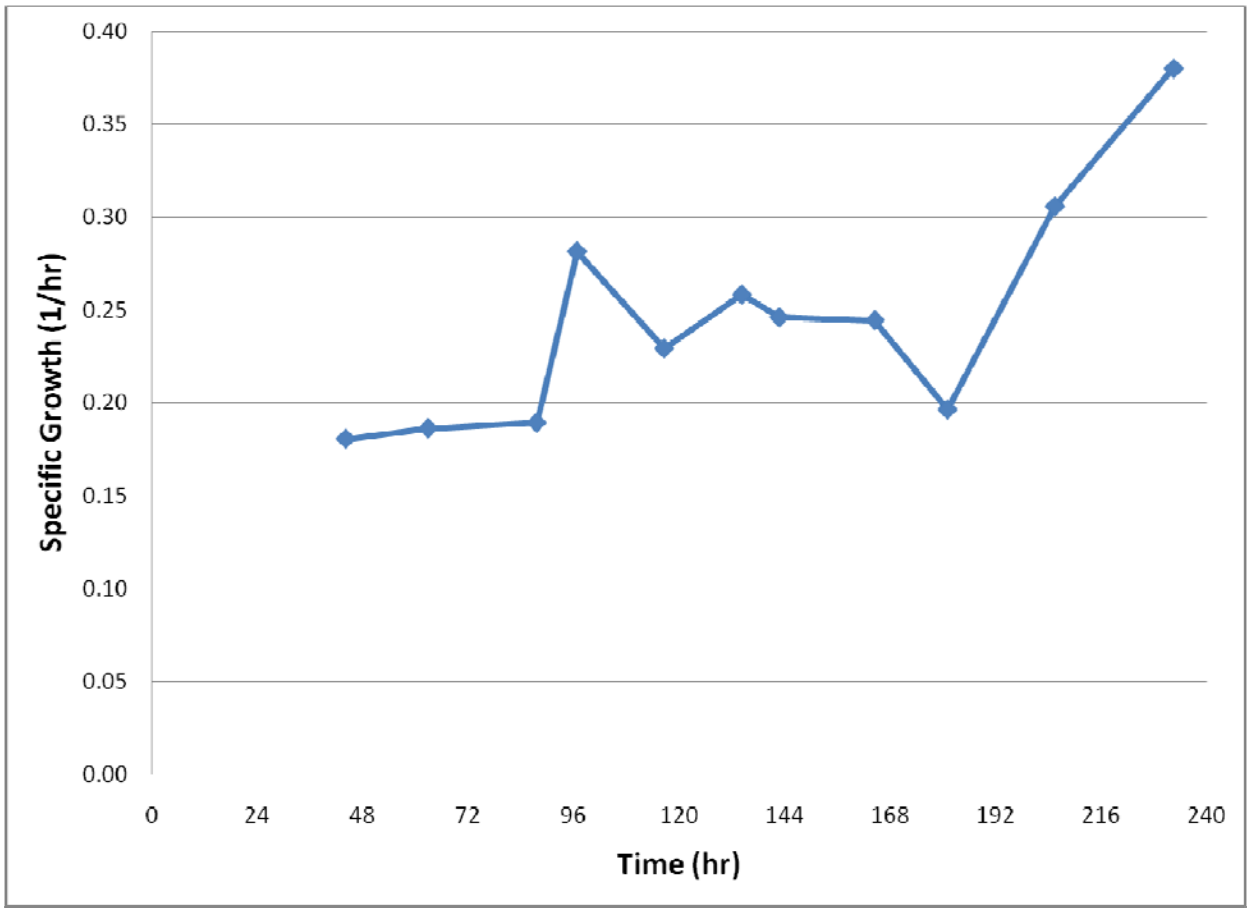

Figure 4.5 – MAGE library 40% hydrolysate selection

Specific growth was monitored for each serial batch of the MAGE library in 40% hydrolysate. Individual serial batches may vary slightly due to random error when preparing the selection media.

Ten individual colonies were selected for examination; these were labeled H40 A through J. As seen in Figure 4.6, after 44 hours of growth in 40% hydrolysate, six of the ten grew statistically significantly higher than the parent SIMD 70 strain (p-value < 0.05). In order to fully genotype a single clone, each target must be sequenced to see if the RBS was mutated. Due to the high cost of sequencing, only two clones were fully characterized. Clones 'H40 G' and 'H40 I' had all 27 target regions amplified via culture PCR and were sent for sequencing. These two clones each had one mutation. The 'H40 G' clone has a modified RBS before the *tonB* gene while the 'H40 I' clone has a mutation in the *ilvM* RBS as seen in Figure 4.7. Each of the remaining clones had these two regions amplified and sequenced, but no further mutations were found. This leads us to believe that the end population was still genotypically diverse, even after a ten day selection. Furthermore, the mixed population from the end of the selection was used as template for amplification of the target regions. One region, the *lpp* RBS, showed diversity in the RBS sequence, as seen in the chromatograph of Figure 4.8. Although the end population showed *lpp* diversity, none of the ten picked colonies had a mutated *lpp* RBS.

In order to evaluate the change in the mutated RBS, we employed the RBS Calculator developed by Salis *et al.* [132]. The RBS calculator is able to estimate the relative strengths of two RBS for a gene. Here we see that the calculator reports an increase in strength for the *tonB* mutation in H40 G (Figure 4.7). This makes sense since the *tonB* TRMR mutant found with high fitness in the hydrolysate

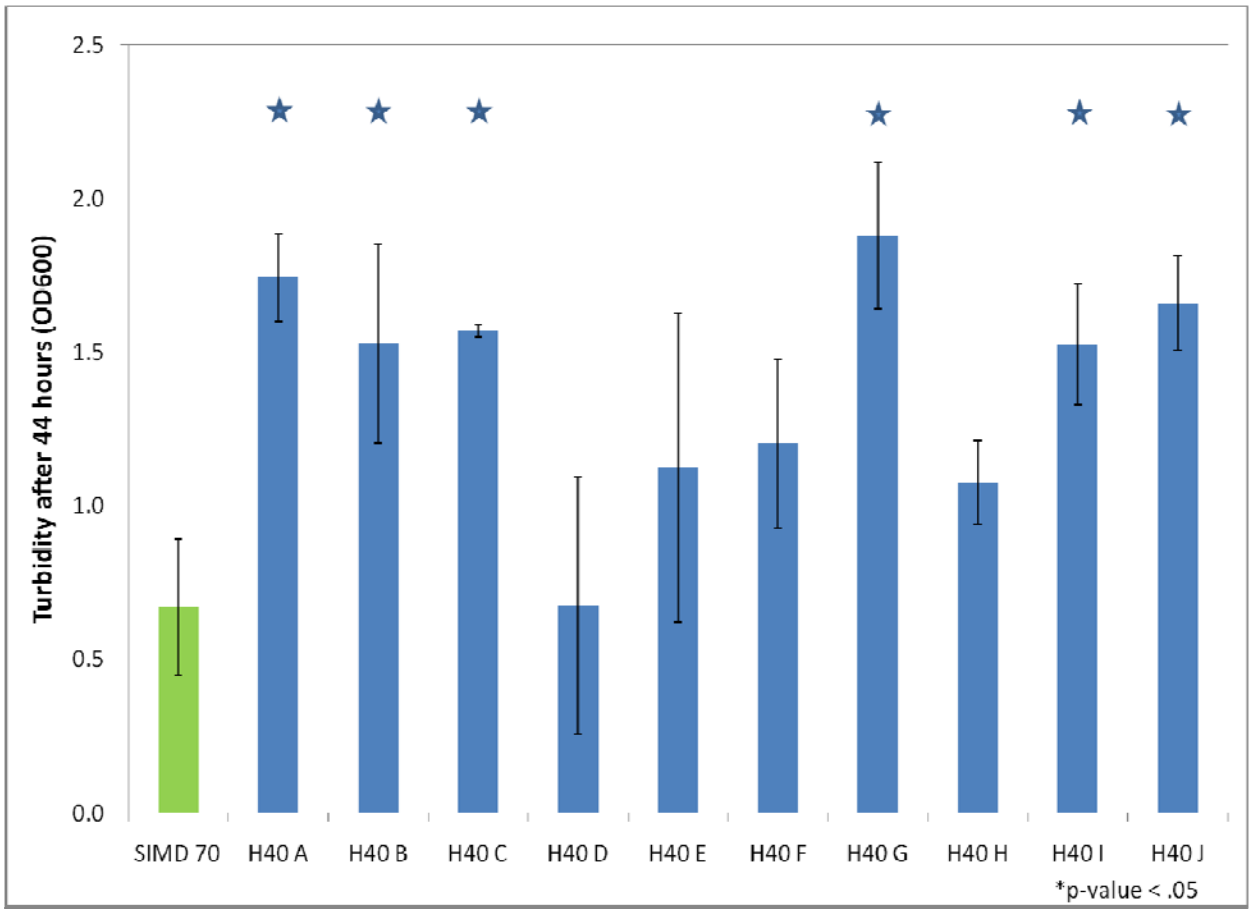

Figure 4.6 - 44 hour growth of post selection isolates in 40% hydrolysate

Growth study of 10 selected clones taken from sample plates after the MAGE selection. After 44 hours of growth in 40% hydrolysate, samples were taken from growth cultures and the turbidity was observed after cells had been washed in water. n=3

a.

H40 G – *tonB* up

```
H40 G          ACTGAAATCAAATAAGCTTCAATG   1572.4
               ||||||||  |       ||||||||
Wild Type      ACTGAAATGATTATGACTTCAATG   535.2
```

b.

H40 I – *ilvM* up

```
H40 I          AGAAATGGAGAGCGGTTTATCATG   194.3
               |||||||   |       ||||||||
Wild Type      AGAAATGTTGGAGAAATTATCATG   717.7
```

Figure 4.7 – Sequence of mutated RBS

The sequences of the mutated regions in clones H40 G (a) and H40 I (b) are shown highlighted in yellow. The start codon for the targeted gene is in blue text. The number to the right of each sequence is the score in arbitrary units from the RBS Calculator.

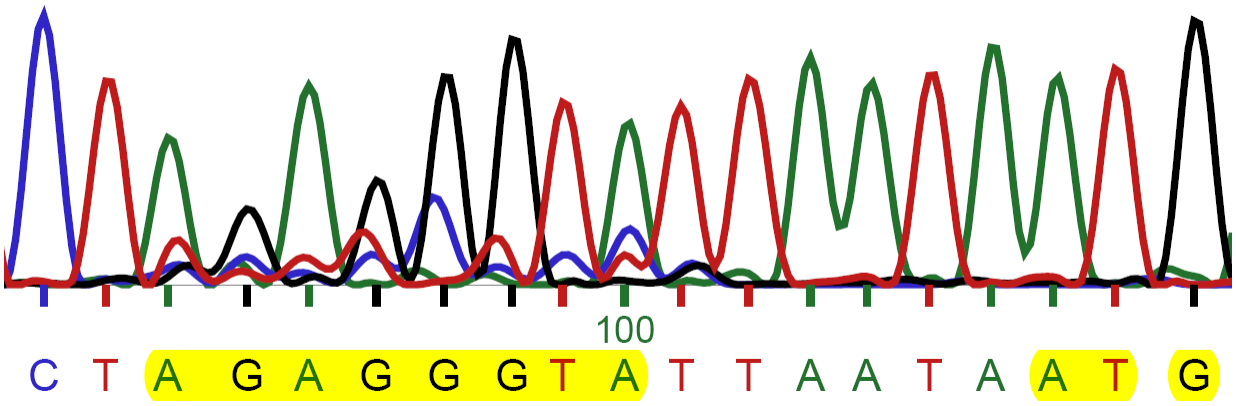

Figure 4.8 – Chromatograph of *lpp* RBS region from end selection population

The final population from the 40% hydrolysate MAGE selection was used as template for PCR and sequencing of the 27 target regions. The *lpp* gene's sequence chromatograph showed diversity in the RBS region. No other target region showed such diversity, including *tonB* and *ilvM*.

For the acetate library, eight targets were chosen from the highest fitness TRMR alleles: *deoA*, *prpR*, *serS*, *tqsA*, *tap*, *ddpA*, *yahF*, and *clcB* (Table 4.5). All but *tap* and *ddpA* were found in the TRMR selection with the down mutation. In this library construction, eleven rounds of recombination were performed with the pool of eight oligonucleotides. The replacement efficiency was estimated to be 4.4% per round, yielding a population that has 31% single mutants, 7.1% double mutants, and 1.0% triple mutants.

This library underwent selection in 10 g/L acetate in minimal media for 110 hours, which comprised 5.25 generations. The culture was serially transferred once to prevent the culture reaching stationary phase. The growth rate was monitored throughout the selection and after 100 hours the growth rate increased by 75%. After this time, samples were taken and culture was plated to obtain individual colonies. Colonies were picked and their growth was examined. None of the 23 colonies selected, surprisingly showed an increase in growth rate. Four colonies were selected and had their target regions genotyped (32 total reactions), but no mutations were found.

MAGE Oligo	Sequence
deoA down	T*T*T*T*TACGAATAATTTCTTGTGCGAGAAAcaaGGTAANNNNNNNNGGA AAAGAGTATGAGGCGGCTTTTGCCGGATGCGTCTACGCCTTA
prpR down	A*A*T*T*ATGAAACAAGACTAAACCCAATATTCGGTTTCTTAACNNNNNN NNGCGCTatgGCACATCCACCACGGCTTAATGACGACAAACCG
serS down	G*T*C*T*GGCTCATTACGCAGCAGATTGGGATCGAGcatGCTTANNNNNN NNTTATCGAATTAAATGGGAGATGTGGCCACAGCCTGCGACCA
tqsA down	G*A*C*G*GAGCGAAAAAGACATTATTATTAGCAAAGGAAGAAAANNNNN NNNCAAGCatgGCAAAGCCGATCATCACGCTCAATGGCCTAAAA
tap up	A*A*A*C*AGCGTGGTCGAAATTCGAATACGATTAAAcatCAACGHYYHYHH HCAGGCGGCAATGACCGCGTTAGTAAATACTCGTCAAAATGT
ddpA up	T*C*T*C*TTGTTTTATATCCCCTGGCACACAGCACGTCAGTTAADDDRDR RDCTGTCatgAAGAGATCGATATCGTTTCGTCCCACATTGCTC
yahF down	A*T*A*G*GTATTCGGTTTAATGACTATTTTAACTGAcatAATTCNNNNNNNN GGTTTGGCTCAGCGCACAACCATCGGCCATGCCATACAGCA
clcB down	C*A*T*T*GCCCATTTCTGCTCATGCATCATCTACACATCTATCCNNNNNN NNGCACTatgTTCCACCGTCTGCTTATCGCAACAGTCGTCGGT

Table 4.5 – MAGE Oligos for Acetate Library Construction

The sequence of the MAGE oligos for acetate targets are shown. The "*" symbol represents phosphorothioate bonds which slow the degradation of the oligos within the cell. The degenerate region is shown with non-traditional symbols for nucleotide bases: R= A or G, D = A, T, or G, and N = A, T, C, or G. Start codons for the target gene are shown in lowercase.

4.3.5 Construction and Selection of Secondary MAGE Libraries

It seems from the hydrolysate selection data that double mutants may be difficult to find. This may be due to an insufficient selection time where synergistic or additive double mutants that have a faster growth rate than single mutants started with such a small initial population size that they would be difficult to find in the final selection population. It also may be due to antagonistic beneficial mutations, where it would be unlikely to find any double mutants after any length of selection. A third reason could be that the double mutants are of the less-than-additive variety, where they may grow slightly better than the single mutants, but start with a smaller population. To gain more insight into which of these situations our selection exemplifies, another, more limited, MAGE experiment was conducted.

Instead of building the library starting with just the SIMD 70 strain, the initial population was an equal mix of the SIMD70 strain, the H40 G clone (with the *tonB* mutation) and the H40 I clone (with the *ilvM* mutation). Starting with these three clones, four targets were chosen for recombination: *lpcA*, *lpp*, *tonB*, and *ilvM*. The *lpcA* target was chosen because it had previously been seen to confer resistance to both acetate and furfural [130]. The *lpp* target was chosen because its RBS was seen to show diversity in the end population. The targets of *tonB* and *ilvM* were chosen because they are the targets where mutations were found in clones H40 G and H40 I. The efficiency reporting galK+ oligo was also added. Six rounds of recombination were performed with the unusually high efficiency of 7.0%. Because two thirds of the initial population already had a mutation, the library after six rounds had a much different composition as the first hydrolysate MAGE library. It is estimated that only 21.5% of the population

have no mutations, 52.9% have a single mutation, 21.3% are double mutants, 3.9% are triple mutants, and the rest have more than three mutations per clone (Figure 4.9a). We can again speculate on what should be found at the end of this selection just as we did before based on synergistic, additive, less-than additive, or antagonistic multiple mutation interactions (Figure 4.9b-e, based on the model as described above and a different starting population). It is clear that it is more likely to find multiple mutations after this selection, but if the double mutations are less than additive, it should not come as a surprise that many of the original mutants (H40 G, H40 I) still persist.

a.

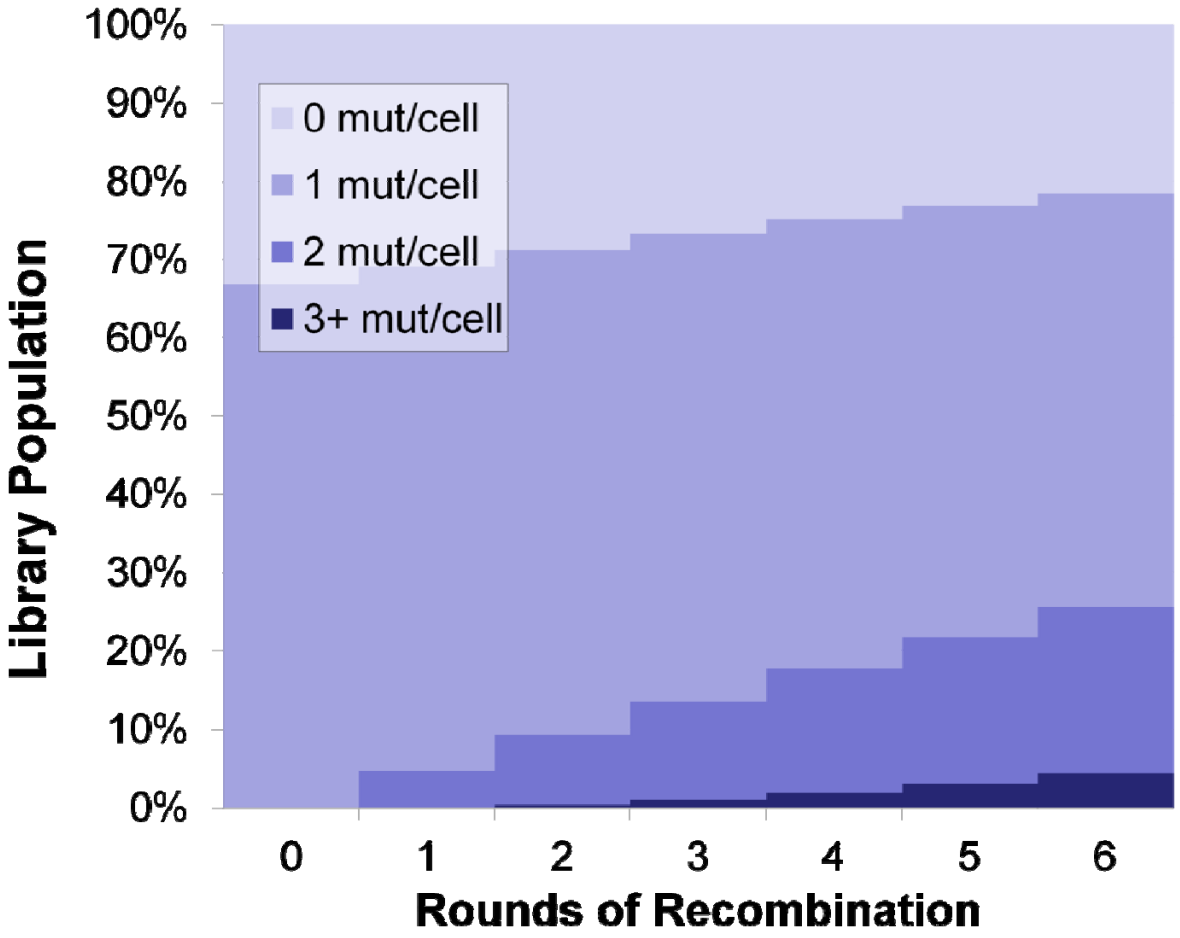
100%
90%
80%
70%
60%
50%
40%
30%
20%
10%
0%
Library Population
0 mut/cell
1 mut/cell
2 mut/cell
3+ mut/cell
0
1
2
3
4
5
6
Rounds of Recombination

b.

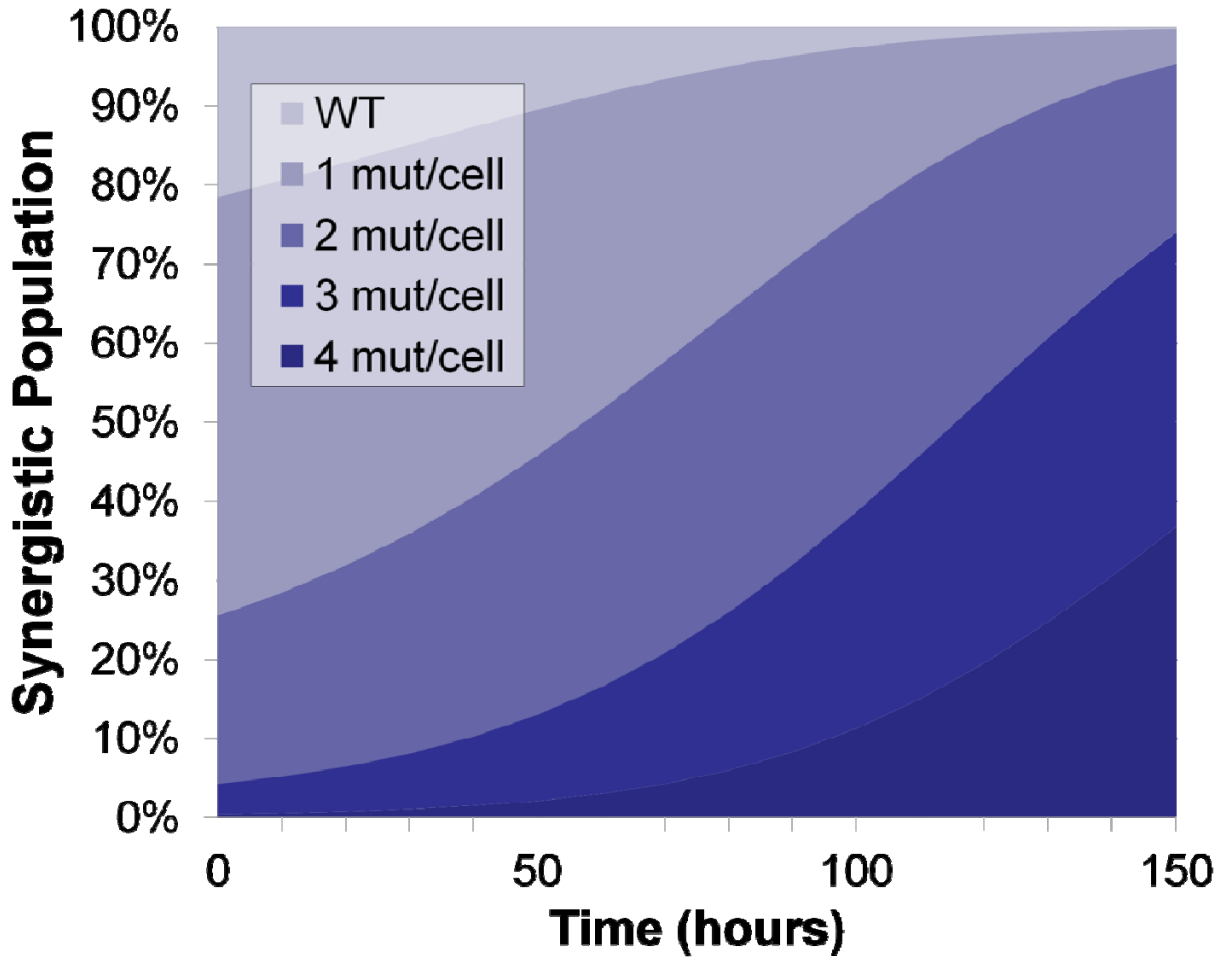
100%
90%
80%
70%
60%
50%
40%
30%
20%
10%
0%
Synergistic Population
WT
1 mut/cell
2 mut/cell
3 mut/cell
4 mut/cell
0
50
100
150
Time (hours)

c.

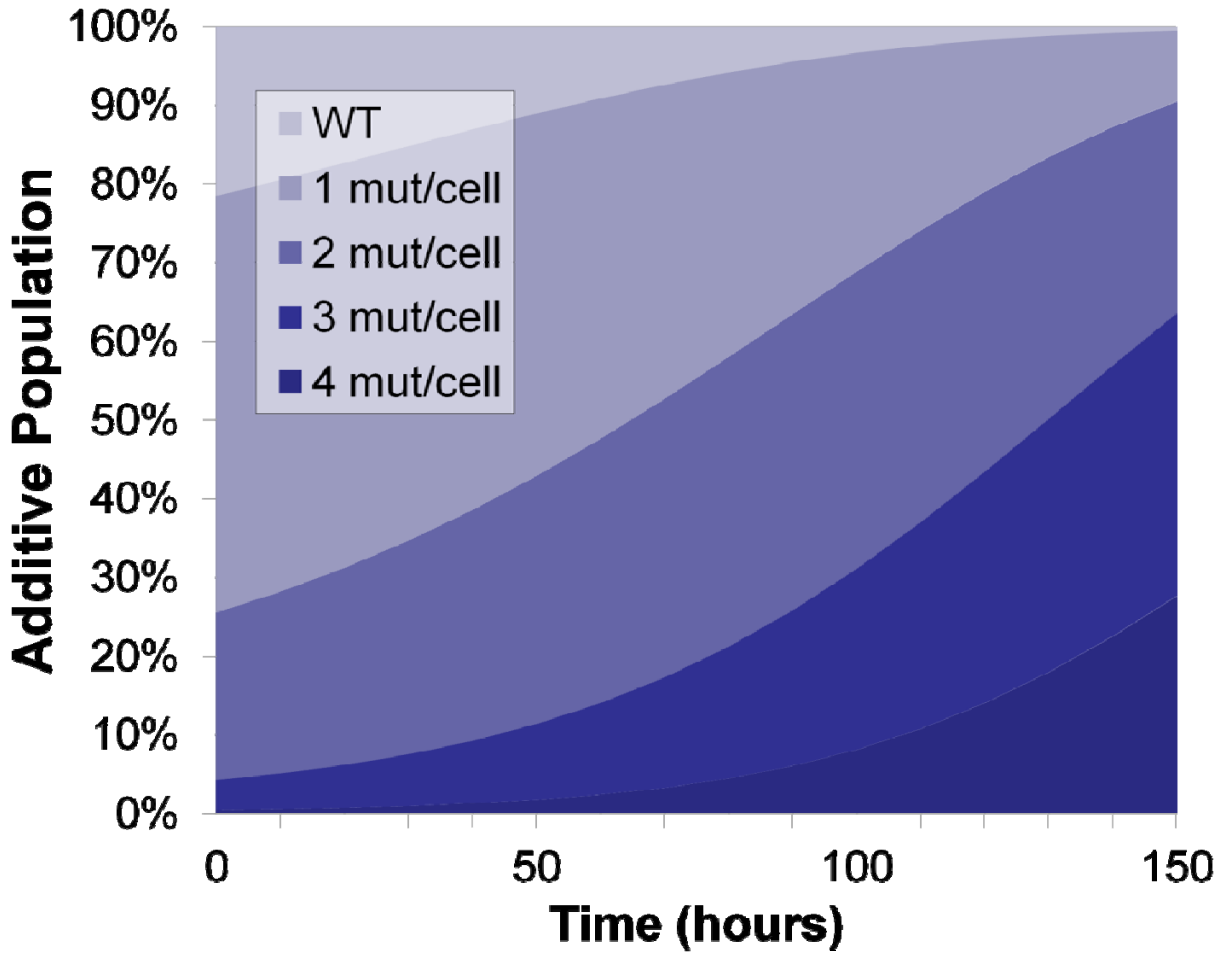
100%
90%
80%
70%
60%
50%
40%
30%
20%
10%
0%
Additive Population
WT
1 mut/cell
2 mut/cell
3 mut/cell
4 mut/cell
0
50
100
150
Time (hours)

d.

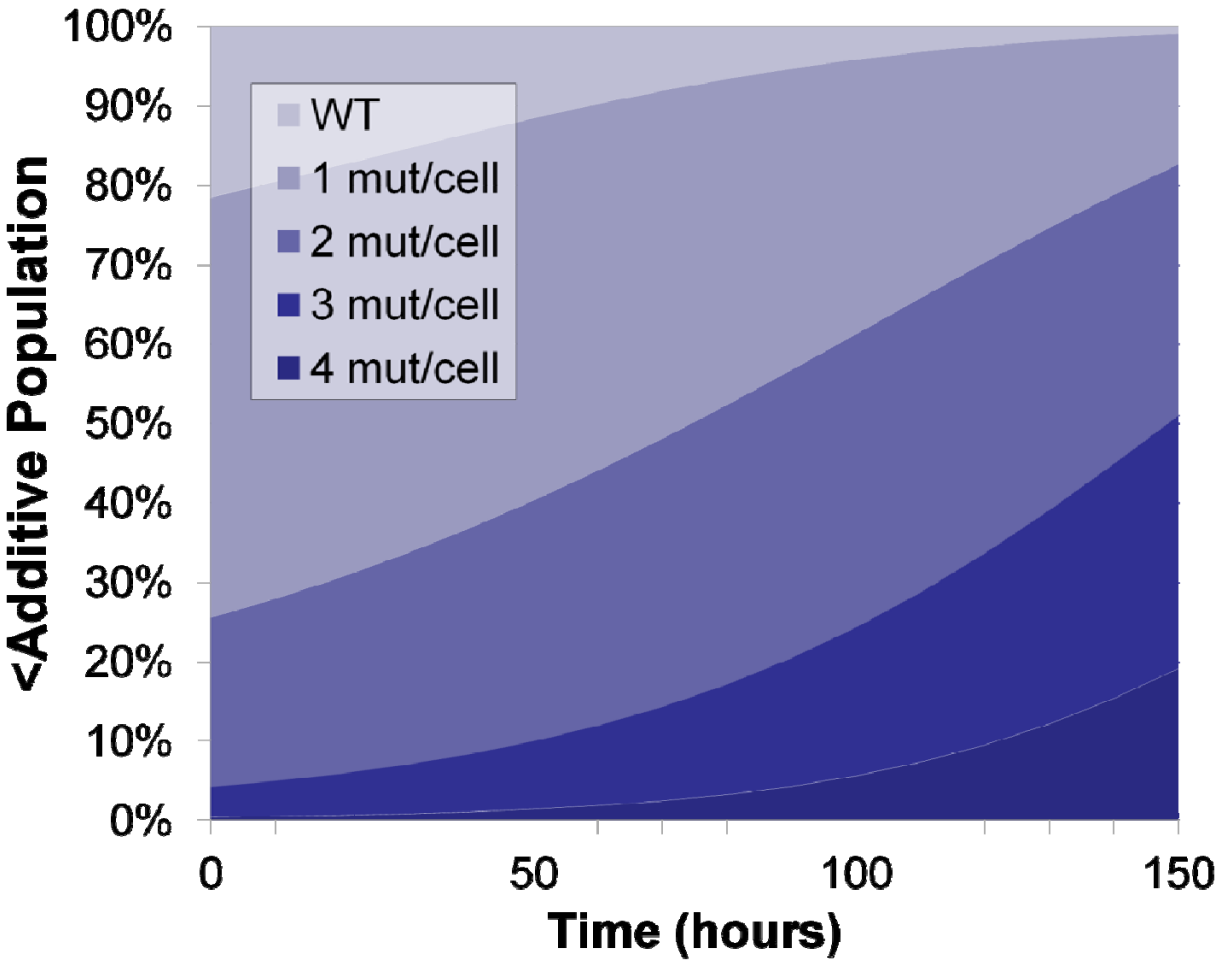
100%
90%
80%
70%
60%
50%
40%
30%
20%
10%
0%
<Additive Population
WT
1 mut/cell
2 mut/cell
3 mut/cell
4 mut/cell
0
50
100
150
Time (hours)

e.

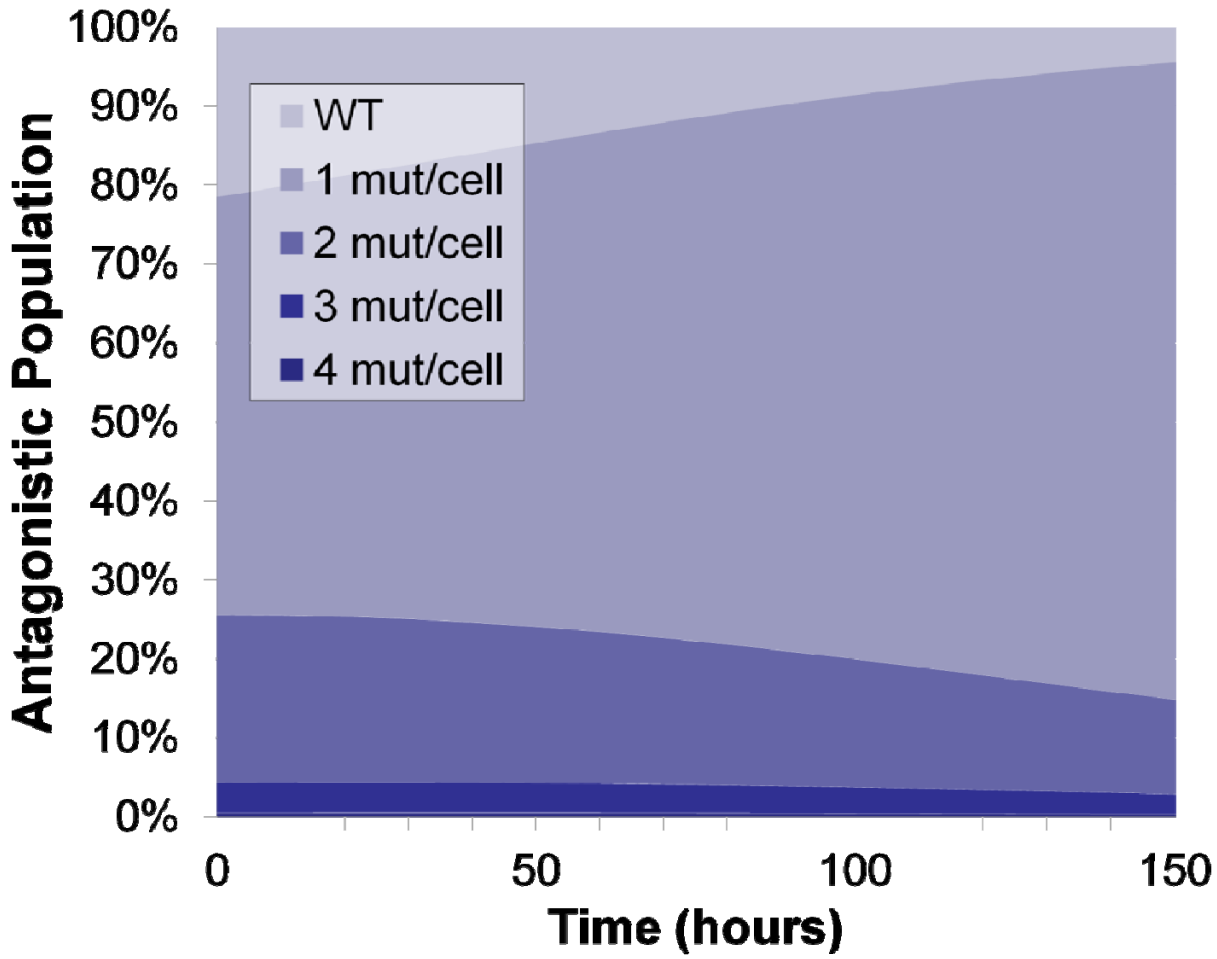

Figure 4.9 – Model Describing Second MAGE Library and Selections

a) Construction of second MAGE library. Shown is the theoretical population distribution of a MAGE library if the recombination efficiency is 7.0%. Each round generates more mutations and the construction of multiple mutations over the 6 rounds. b) Synergistic selection: A theoretical selection where beneficial single mutants are 35% higher in growth rate compared to no mutations and the combinations thereof are synergistic (increase in growth rate is more than additive). c) Additive selection: Same as (b) but combinations are additive. d) Less-than-additive selection: Same as (b) but combinations are less than additive. e) Antagonistic selection: Time for (b) – (3) is 150 hours.

The seconday MAGE library population was subjected to selection in 40% hydrolysate for 95 hours, constituting 22 more generations of growth. The selection was serially transferred three times to avoid stationary phase in the culture. In this selection, no discernable increase in the growth rate was observed. At the end of the selection, samples were taken and plated to isolate individual colonies. Eight colonies were picked for further examination. Because there were only four targets in this selection, it was much easier to sequence many more clones.

All eight colonies had the four target regions sequenced. Four of the eight were identical to the H40 I clone (*i.e.* each had the same *ilvM* RBS mutation), two clones had single mutations which were different from the H40 G or H40 I seed populations (one was in the *tonB* region, the other *ilvM*). Two of the picked clones were double mutants. Both had the H40 I clone's *ilvM* mutation, presumably the parent of the two, and a unique *tonB* mutation as well. The precise nature of these mutations may be seen in Table 4.6 and Figure 4.10. It seems that a mutation in the *ilvM* RBS is confers the most tolerance since seven of eight sequenced clones had either the H40 I mutation or a novel mutation. It is interesting to note that a single point mutation is present in the two H40 I-derived double mutant clones in the *tonB* target region that is not present in the H40 I clone itself. This shows that unintended mutations may be propagated and sustained during this process. The relative strengths of the ribosomal binding sites were again calculated by the RBS Calculator (Figure 4.10) [132]. It does not seem that there is a consistent trend among the RBS scores and tolerance. The H40 P *tonB* RBS score increased, but the *tonB* RBS for H40 Q and H40 T decreased. The H40 U *ilvM* RBS score decreased dramatically.

Clone	*lpcA*	*ilvM*	*tonB*	*lpp*
M2 H40 N	-	H40 I	-	-
M2 H40 O	-	H40 I	-	-
M2 H40 P	-	H40 I	Novel Mutation	-
M2 H40 Q	-	H40 I	Novel Mutation	-
M2 H40 R	-	H40 I	-	-
M2 H40 S	-	H40 I	-	-
M2 H40 T	-	-	Novel Mutation	-
M2 H40 U	-	Novel Mutation	-	-

Table 4.6 – Mutations of Picked Clones from Second Hydrolysate MAGE Library Selection

Each sequenced mutant had at least one mutation. A '-' symbol means that the sequence was native. The 'H40 I' entry means that the mutation found is identical to the *ilvM* mutation found in the original H40 I clone. 'Novel Mutation' means there was a mutation that had not been previously seen.

a.

M2 H40 P – *tonB* up, double mutant

```
H40 P           ACTTAAAGCAGGAGAGCTTCAATG   802.5
                |||  |||   |   |    ||||||||
Wild Type       ACTGAAATGATTATGACTTCAATG   535.2
```

b.

M2 H40 Q – *tonB* up, double mutant

```
H40 Q           ACTTAAAGCTAGGGGACTTCAATG   273.1
                |||  |||         ||||||||||
Wild Type       ACTGAAATGATTATGACTTCAATG   535.2
```

c.

M2 H40 T – *tonB* up, single mutant

```
H40 T           ACTGAAAGCAAGTGAGCTTTAATG   442.0
                |||||||           ||||||||
Wild Type       ACTGAAATGATTATGACTTCAATG   535.2
```

d.

M2 H40 U – *ilvM* up, single mutant

```
H40 U           AGAAATGTGTGGCGGGTTATCATG     4.1
                ||||||||   |      ||||||||
Wild Type       AGAAATGTTGGAGAAATTATCATG   717.7
```

Figure 4.10 – Sequence of mutated RBS

The sequences of the mutated regions in clones H40 P (a), H40 Q (b), H40 T (c), and H40 U (d) are shown highlighted in yellow. The start codon for the targeted gene is in blue text. Only those regions that have novel mutations are shown. The number to the right of each sequence is the score in arbitrary units from the RBS Calculator.

Growth studies of clones selected from the second 40% hydrolysate selection were performed. Figure 4.11 shows these double mutants do not perform better than that of the single mutants from which they derive. It is curious to see that any double mutants were found at all. It would be expected that if they did not confer increased growth, they should not be found at the end of the selection. Based on this observation, it seems that it should not have been expected to select for multiple mutations in this particular situation. While these mutations may have a higher growth rate compared to the wild type strain, this benefit was not enough to overcome the disadvantage of such a small starting population in the first MAGE hydrolysate selection.

It is interesting to note the difficulties of studying growth in hydrolysate. In order to observe an optical density (OD), a sample must be removed from the liquid culture and centrifuged. The supernatant is decanted carefully with a pipette and the cell pellet is subsequently resuspended in water or MOPS minimal media. This process requires that the sample cannot be replaced once the measurement is taken. Since observing many clones at once requires using smaller volumes of culture (because of material and space limitations), very few samples can be taken. Furthermore, the hydrolysate is not a well-defined or consistent substance. Each batch is slightly different in the amount of inhibition of growth is seen with the clones.

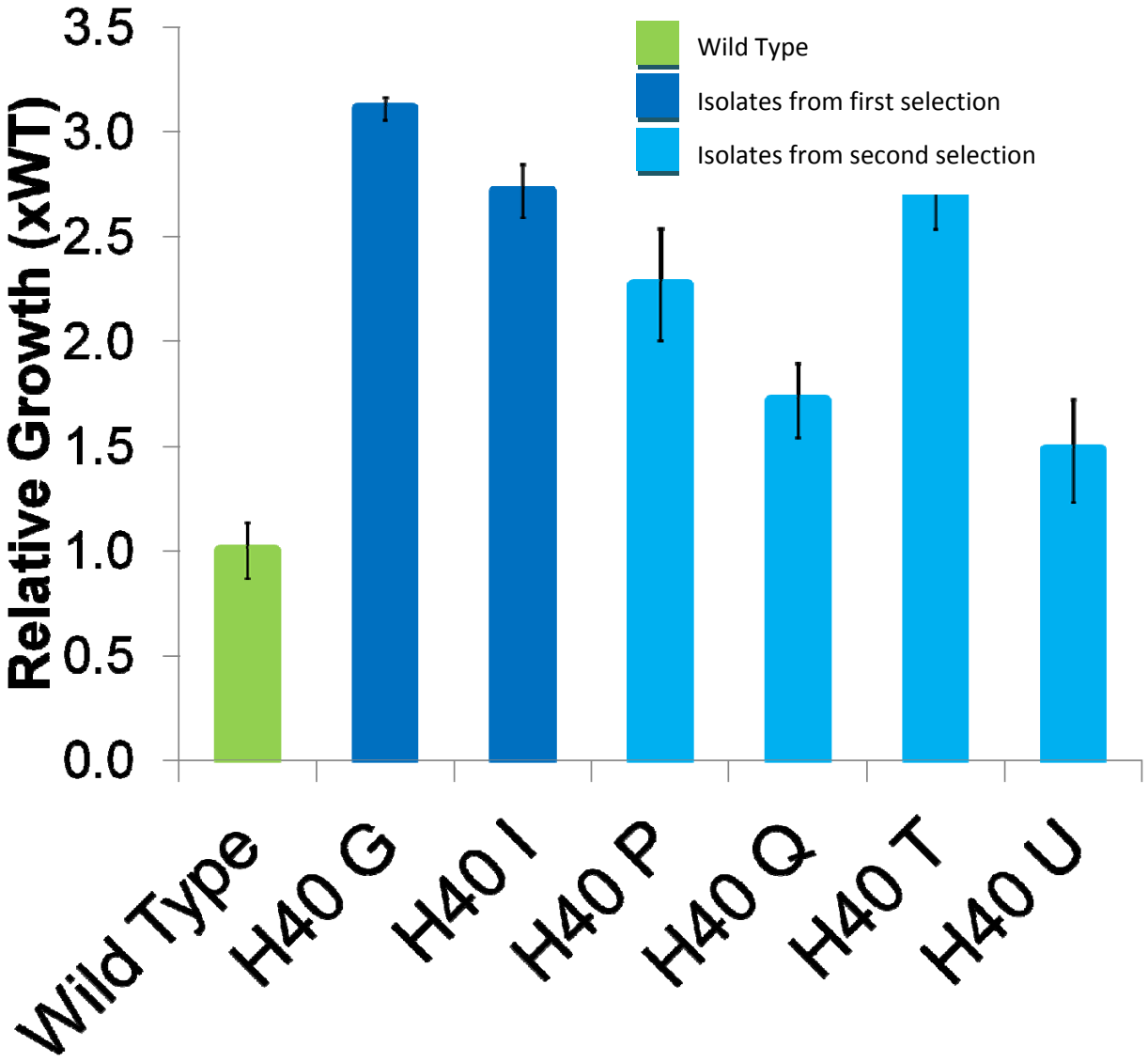

Figure 4.11 - 20 hour growth of post selection isolates in 40% hydrolysate

Growth study of single mutants found in the first MAGE hydrolysate selection (H40 G and H40 I), double mutants found in the second MAGE hydrolysate selection (H40 P and H40 Q), and novel single mutants found in the second MAGE hydrolysate selection (H40 T and H40 U). After 20 hours of growth in 40% hydrolysate, samples were taken from growth cultures and the turbidity was observed after cells had been washed in water. Error bars are 1 standard deviation. n=3. Each isolate has a p-value < 0.05 compared to control.

4.4 Discussion

In order to engineer a strain with a desired trait, various routes of mutation may be employed. Because of the near-infinite ways the *E. coli* genome can be manipulated, it is important to have a coherent strategy to efficiently engineer strains. While nature has the advantage of time, researchers in a lab desire methods that allow such manipulations on the timescale of weeks or even days. A good strategy for engineering a strain for a certain trait would include introducing directed mutations likely to affect fundamental characteristics (in our case, the growth under a desired condition). Ideally, these mutations would be easily identifiable to quickly determine the genotype of the strain.

Here, we have described a two-step process for producing an engineered strain. Generally, a broad search is done to find individual mutants that confer tolerance to the selection conditions. Then, a few of those genes with high-fitness mutants are targeted specifically for an in-depth, narrower search that includes clones with multiple mutations. Specifically, the genome-wide tool TRMR was used to identify genes with a high fitness to lignocellulosic hydrolysate and acetate stress when a mutation, either increasing or decreasing gene expression, was introduced [1]. The microarray-derived fitness data from the TRMR selections informed the decision of which targets to choose when performing a MAGE selection. The ribosomal binding sites of the targeted genes were mutated via multiplex recombination generating a library of mutants, and then a selection was performed [99].

Growth on cellulosic hydrolysate and acetate was chosen because it exemplifies two different selection conditions. The acetate condition involves a metabolite which is connected to various regulatory mechanisms in the cell at very high concentrations. The hydrolysate condition is a complex mixture of various sugars in high amounts and various chemicals that are toxic (both metabolites and substances foreign to *E. coli*). Both of these conditions are relevant to the ongoing effort to engineer biofuel production strains that can be grown on hydrolysate feedstock [96].

4.4.1 Mutations found in TRMR

The goal of the first part of the process, the TRMR selection, is to identify a smaller number of targets. This is desired because we can only use the fittest few mutations when selecting targets for MAGE. This stands in contrast with a previous work. In this work, the SCALES tool was used with the goal of having a low frequency of false-negatives (*i.e.* mutations which may confer tolerance but are not identified as such [130]. In the process discussed in this work, false negatives are not considered as much of a problem as false positives, those mutants which are shown to have a high fitness, but do not confer tolerance. Since we are limited to only a few targets, it is desired that our false positive rate is zero or near zero.

The two TRMR selections used in this work were both successful in producing a limited number of mutants with a high fitness [1]. While these selections greatly reduced the genotypic diversity (which is desired), there was no general theme or motif that emerged from the tolerant clones. This stands in contrast to previous work with acetate using the SCALES technique, where many of the fittest clones involved

metabolic genes involved in the production of amino acids [130]. This reinforces the fact that these two techniques are not searching within the same mutational space. It should not be expected that these two tools' results mirror each other.

To properly confirm that the selections were efficacious, the top fitness mutants of the selection need to be reconstructed. This proved to be problematic in practice, where six of the desired eight clones from the acetate selection were able to be constructed. For this method to be used in the future in the quick and efficient manner that is necessary, this step must be improved. Changing the antibiotic resistance cassette from blasticidin resistance to a more user-friendly one, such as kanamycin or carbenicillin, may speed the process of TRMR clone reconstruction.

Of these six reconstructions, four conferred tolerance to acetate. It seems that the false positive rate in the TRMR selection that yields high-fitness values for non-tolerant clones may be high.

4.4.2 MAGE selections yields mixed results

The second part of the overall scheme is to focus our efforts on a small number of genetic targets that we will mutate repeatedly to generate a library of multiple mutants for subsequent selection. The MAGE process was used here for the purpose of quickly introducing multiple mutations in individual clones.

In practice, the recombination efficiency of single rounds of mutation was relatively low compared to what others have reported [124, 131]. Since each MAGE round takes a minimum of 5 hours (and more often 6-7), performing a dozen rounds requires a few days of constant labor, or a week of standard work. With these same

efficiencies, two dozen rounds of MAGE would only yield one third of the population with two or more mutations per clone. In order to generate a library with a large portion of double or more mutants per clone in a reasonable amount of time, recombination efficiencies must be dramatically increased. One method would be to disable the natural DNA repair mechanisms that combat recombination, but this would also lead to an increase in random mutagenesis that could interfere negatively with the rest of the system.

The number of unique multiple mutants that can exist in a library is dependent on the number of targets that are chosen for mutation. This leads to a natural trade-off of benefits. With more targets, for instance the hydrolysate MAGE library, a larger number of combinations of mutations are in the selection. However, not all combinations may be present or present in a significant number, meaning the selection may be missing out on certain possibilities from the start. Increasing the number of targets increases the number of combinations nearly exponentially. Also, the difficulty of determining which mutations are present in a tolerant clone increases linearly with the number of targets chosen. The more targets that must be sequenced in a single clone, the fewer clones can be sequenced for the same work and cost. Conversely, choosing fewer targets means many more clones can be genotyped. Also, most combinations of mutations can be more thoroughly searched in a selection when there are fewer of them. However, limiting the targets limits the scope of what the selection is able to search. It is entirely possible that a library is so limited in scope that the best solution to the problem lays outside the bounds of the experiment.

Mathematics aside, selection for multiple mutations is not a straight-forward process. Because the desired phenotypes are poorly understood, it is not possible to accurately predict how these individual mutations will interact. From our experiments, it seems that the combination beneficial mutations are less than the sum of their parts. This fact makes finding multiple mutant clones unlikely over the course of a selection on a laboratory time scale.

While finding multiple mutations in a single clone after the initial selection of the MAGE library is ideal, it seems that a step-wise approach might be the most efficient path. Using previously identified tolerant single-mutant clones as the basis for further mutation made finding double mutants much more likely.

It is interesting that no tolerant mutated acetate clone was found from the MAGE process. One possibility to explain this is that where TRMR and SCALES may be able to bypass some transcription-based regulation in changing the gene expression levels, just mutating the ribosomal binding site may not have the same effect. This underscores the fact that the TRMR and MAGE mutations are not the same, and should not be expected to yield tolerant clones right away.

Chapter 5:

Conclusions

In this work, we have explored the engineering *E. coli* to be more tolerant to acetate and to better grow on lignocellulosic hydrolysate for the purpose of the development of better fermentation strains for the production of biofuels.

Chapter two describes the motivation for exploring *E. coli* tolerance to lignocellulosic hydrolysate inhibitory compounds. These cellulosic feedstocks are renewable and are often derived from agricultural waste, a source that is currently underutilized. This process is not already the normative method for producing biofuels because the pretreatment necessary for making the sugars available for fermentation produces not only those sugars, but also various inhibitory compounds. These inhibitions must be overcome for efficient production of biofuels. We not only want to produce a microorganism that is resistant to these toxins, but also to generate knowledge on the mechanisms of toxicity and tolerance. For these goals, various engineering tools and applications are needed.

The choice of which genome engineering tools should be used is of great importance. Before the conclusions derived from the use of these tools can be

discussed, we must first articulate how these tools were chosen. Like the tools in a tool box, the various methods to manipulate, control, or otherwise alter the genetic makeup of bacteria to bestow some trait have strengths and weaknesses. They should be well understood on how to properly use them and the limitations should be known so that the most information and productivity can be gleaned from their use.

To determine the best method to use in our studies, we first describe the ideal tool. We first want the methods we use to be high-throughput and trackable. High-throughput means that a large amount of genetic variety can be tested in a short period of time (*i.e.* a large library that can undergo selection). A method is trackable if the genotype of the populations can be easily ascertained (*e.g.* with DNA microarrays). The method of introducing genetic diversity should be directed. Directed mutations are those that are very likely to effect change within the clone (*e.g.* change in gene expression). The tool's results are best if quantifiable and causal. DNA microarrays yield quantifiable signal data, such that a numerical value can be ascribed to the mutation. Causal results indicate that the change in phenotype is a direct result of the reported mutation, and not merely correlative. Ideally, the method used for genetic engineering would introduce multiple mutations at once to take allow synergistic effects. Finally, the best methods operate well on a lab time scale. While nature may have eons, and the duration of graduate school seemingly just as long, it is best when the entire process can be done in a fortnight or less.

Now that we have described the ideal tools, we examine the tools chosen in this work. SCALES is high-throughput, trackable, causal, quantifiable, and can be done on a lab time scale. TRMR is also high-throughput, trackable, causal, quantifiable,

directed, and can be done on a lab time scale. MAGE is high-throughput, causal, directed, can be done on a lab time scale, and multiple mutations in individual clones can be tested. The choice to use these three methods for these studies has been the most important choice of all. The use of more rudimentary methods could not have generated the amount and type of data seen here. We can now discuss the conclusions of the results of these tools.

In chapter three, SCALES was applied to moderate acetate stress in selection. Key clones were identified that had a high fitness value. Clone fitness values were converted to individual gene fitness data ,such that the data could be analyzed in various ways. When the individual gene data was mapped onto metabolic biochemical pathways, which show which genes encode for enzymes that carry out certain reactions, a pattern emerged. Key regulated steps in pathways that produce certain amino acids and pyrimidine ribonucleotides were catalyzed by the products of high-fitness genes. This led us to correctly hypothesize that supplementation of the products or closely related metabolites would alleviate acetate stress. The discovery of this mechanism of tolerance was not obvious and had not been previously identified in the literature. Supplementation of amino acids previously identified as osmoprotectants and affected by acetate did not confer tolerance. These were tested, but the SCALES data did not predict these to be important.

In chapter four, the combination of two powerful genome engineering tools was discussed. TRMR selections were performed on high levels of acetate stress to elucidate the only the very tolerant clones. While troublesome and not fully successful, six out of eight desired high-fitness mutants were reconstructed. Four of these, *tap* up,

tqsA down, *clcB* down, and *ddpA* up performed statistically significantly better than the control. It was attempted to find a common theme within the high-fitness clones (as in chapter three), but no pattern emerged. In contrast to the SCALES results, few high-fitness genes coded for enzymes that catalyze reactions in the central metabolism.

Using the acetate TRMR selection and a previously reported lignocellulosic hydrolysate TRMR selection, targets were chosen from the top fitness mutants for further study using MAGE. Eight targets from the acetate work were chosen and 27 targets for the hydrolysate work. About a dozen rounds of recombination were performed for the construction of both the acetate and hydrolysate libraries at a replacement efficiency of at or just below 5%. The libraries started with about 50% of the population containing mutations (80-90% of those being single mutants). Selections were performed upon the acetate and hydrolysate libraries. Unfortunately, no resistant clones were identified after the acetate selection. The hydrolysate selection yielded resistant clones, but only single mutants could be found. To determine why this was the case, a second round of MAGE recombination (4 targets, 6 rounds with 7% efficiency) was performed using two of the previously-identified single mutants along with SIMD70 as the basis of the library. After another selection in 40% hydrolysate, clones with multiple mutations were found, but none were more resistant than their single-mutant parents. Seeing this, it was reasonable that multiple mutations in a single clone were not found in the initial selection. Finding clones with multiple mutations that are more resistant to stress than single-mutant clones may be more difficult to find than previously supposed.

The inability to find double or triple mutant clones that are more tolerant to stress than their single mutant counterparts from the MAGE selections was unexpected. However, seen in the light of the antagonistic model of multiple mutation interactions, no multiple mutants should be expected in this situation. This highlights how complex and non-intuitive altering the genome can be. A starting assumption of the MAGE method, as used in this work, was that if two single mutations were good, the combination of those mutations would be better. This, as it turns out, may not be true for our systems. Likely this assumption is true under different circumstances.

A search for purely additive mutations may be better done in a step-wise fashion, much like the second MAGE library described above. However, instead of limiting the scope of the experiment to a few targets, it may be better to sequentially select upon genome-wide libraries with the expectation that a generation of a new library would be required each time an additional mutation was desired. If done with TRMR-like insertions (*i.e.* with DNA barcodes for use with microarray and antibiotic resistance markers), these subsequent libraries may be trackable if the original barcodes from the initial round of selection are removed. Likewise, removal of the original antibiotic resistance cassette may be done to avoid the necessity of simultaneous use of multiple antibiotics.

It would be ideal to search a multiple mutation library for increased tolerance without requiring prior knowledge of what single mutations confer tolerance. To do so, a TRMR-like mutation cassette may be better suited compared to the degenerate MAGE-like approach. To create a library that generated all possible combinations of double TRMR library mutants (both in the ‘up’ and ‘down’ direction), ~64,000,000 unique

mutants would need to be constructed. This number is on the upper limit of what can be achieved on the bench top. Certain practicalities, such as how to identify double mutants on an individual clone and population basis, would have to be addressed, but these issues could be overcome. Such a method would be ideal to identify double mutants requiring a specific combination of two mutations that individually do not confer tolerance. This method has not been attempted yet because the generation of the subsequent TRMR libraries is more difficult and labor intensive compared to the generation of a MAGE library.

In the end, attempting to thoughtfully introduce changes into the near black box of the *E. coli* microorganism is highly complex. Attempting to engineer clones that are tolerant to acetate and lignocellulosic hydrolysate (each adding its own set of complexities) has made this work interesting, to say the least. Acetate is a metabolite connected to various regulatory elements, and it functions as a regulatory molecule as well as carbon source and inhibitor. Lignocellulosic hydrolysate contains such a wide variety of inhibitors and sugars that it is futile to attempt to predict what mutations would make a clone more tolerant.

The use of each of these various methods to do a similar thing recalls the idiom "There are many ways to skin a cat." Here we have seen that some ways are more effective than others, however. The author hopes this work has given the reader some knowledge on the subject that will help you in the reader's future endeavors.

CONSUMMATUM EST

References

1. J.R. Warner, P.J. Reeder, A. Karimpour-Fard, L.B. Woodruff, and R.T. Gill, Rapid profiling of a microbial genome using mixtures of barcoded oligonucleotides. Nat Biotechnol. 28 (2010) 856-862.
2. R.D. Perlack, L.L. Wright, A.F. Turhollow, R.L. Graham, B.J. Stokes, and D.C. Erbach, Department of Agriculture: Biomass as feedstock for a bioenergy and bioproducts industry: The technical feasability of a billion-ton annual supply. Oak Ridge, TN; 2005.
3. European Union: Directive 2003/30/ec of the european parliament and of the counsil, on the promotion of the use of biofuels or other renewable fuels for transport. Brussels, Belgium; 2003.
4. Energy Information Administration: International energy outlook 2000. Washington, DC; 2000.
5. Energy Information Administration: Annual energy outlook 2008: With projections to 2030. Washington, DC; 2008.
6. Energy Information Administration: Short-term energy outlook. Washington, D.C.; 2008.
7. **New energy for america** [http://my.barackobama.com/page/content/newenergy]
8. Department of Energy: Research advances: Cellulosic ethanol. Golden, CO; 2007.
9. T. Searchinger, R. Heimlich, R.A. Houghton, F. Dong, A. Elobeid, J. Fabiosa, S. Tokgoz, D. Hayes, and T.H. Yu, Use of u.S. Croplands for biofuels increases greenhouse gases through emissions from land-use change. Science. 319 (2008) 1238-1240.
10. J. Sanchez and J. Junyang, USDA Foreign Agricultural Service: Gain report: China, peoples republic of, bio-fuels annual report. Beijing; 2008.
11. J. Wilson, USDA Foreign Agricultural Service: Gain report: United kingdom, bio-fuels, biofuels under fire. 2008.
12. K. Sanderson, Us biofuels: A field in ferment. Nature. 444 (2006) 673-676.
13. E. Palmqvist and B. Hahn-Hagerdal, Fermentation of lignocellulosic hydrolysates. I: Inhibition and detoxification. Bioresource Technology. 74 (2000) 17-24.

14. Y. Sun and J. Cheng, Hydrolysis of lignocellulosic materials for ethanol production: A review. Bioresour Technol. 83 (2002) 1-11.
15. N. Mosier, C. Wyman, B. Dale, R. Elander, Y.Y. Lee, M. Holtzapple, and M. Ladisch, Features of promising technologies for pretreatment of lignocellulosic biomass. Bioresour Technol. 96 (2005) 673-686.
16. R. Kumar, S. Singh, and O.V. Singh, Bioconversion of lignocellulosic biomass: Biochemical and molecular perspectives. Journal of Industrial Microbiology & Biotechnology. 35 (2008) 377-391.
17. F. Niehaus, C. Bertoldo, M. Kahler, and G. Antranikian, Extremophiles as a source of novel enzymes for industrial application. Appl Microbiol Biotechnol. 51 (1999) 711-729.
18. L. Olsson and B. HahnHagerdal, Fermentation of lignocellulosic hydrolysates for ethanol production. Enzyme and Microbial Technology. 18 (1996) 312-331.
19. R.J. Ulbricht, S.J. Northup, and J.A. Thomas, A review of 5-hydroxymethylfurfural (hmf) in parenteral solutions. Fundamental and Applied Toxicology. 4 (1984) 843-853.
20. A.P. Dunlop, Furfural formation and behavior. Industrial and Engineering Chemistry. 40 (1948) 204-209.
21. S. Larsson, A. Reimann, N.O. Nilvebrant, and L.J. Jonsson, Comparison of different methods for the detoxification of lignocellulose hydrolyzates of spruce. Applied Biochemistry and Biotechnology. 77-9 (1999) 91-103.
22. B.S. Dien, M.A. Cotta, and T.W. Jeffries, Bacteria engineered for fuel ethanol production: Current status. Appl Microbiol Biotechnol. 63 (2003) 258-266.
23. K. Ohta, D.S. Beall, J.P. Mejia, K.T. Shanmugam, and L.O. Ingram, Genetic-improvement of escherichia-coli for ethanol-production - chromosomal integration of zymomonas-mobilis genes encoding pyruvate decarboxylase and alcohol dehydrogenase-ii. Applied and Environmental Microbiology. 57 (1991) 893-900.
24. J. Zaldivar and L.O. Ingram, Effect of organic acids on the growth and fermentation of ethanologenic escherichia coli ly01. Biotechnol Bioeng. 66 (1999) 203-210.
25. J. Zaldivar, A. Martinez, and L.O. Ingram, Effect of selected aldehydes on the growth and fermentation of ethanologenic escherichia coli. Biotechnol Bioeng. 65 (1999) 24-33.
26. J. Zaldivar, A. Martinez, and L.O. Ingram, Effect of alcohol compounds found in hemicellulose hydrolysate on the growth and fermentation of ethanologenic escherichia coli. Biotechnology and Bioengineering. 68 (2000) 524-530.
27. L.R. Jarboe, T.B. Grabar, L.P. Yomano, K.T. Shanmugan, and L.O. Ingram, Development of ethanologenic bacteria. Biofuels. 108 (2007) 237-261.

28. N. Banerjee, R. Bhatnagar, and L. Viswanathan, Inhibition of glycolysis by furfural in saccharomyces-cerevisiae. European Journal of Applied Microbiology and Biotechnology. 11 (1981) 226-228.
29. S.M. Hadi, Shahabuddin, and A. Rehman, Specificity of the interaction of furfural with DNA. Mutat Res. 225 (1989) 101-106.
30. L.O. Ingram, Adaptation of membrane lipids to alcohols. Journal of Bacteriology. 125 (1976) 670-678.
31. Q.A. Khan, and S.M. Hadi, Effect of furfural on plasmid DNA. Biochemistry and Molecular Biology International. 29 (1993) 1153-1160.
32. Q.A. Khan and S.M. Hadi, Inactivation and repair of bacteriophage lambda by furfural. Biochem Mol Biol Int. 32 (1994) 379-385.
33. Shahabuddin, A. Rahman, and S.M. Hadi, Reaction of furfural and methylfurfural with DNA: Use of single-strand-specific nucleases. Food Chem Toxicol. 29 (1991) 719-721.
34. M.P. Tucker, J.D. Farmer, F.A. Keller, D.J. Schell, and Q.A. Nguyen, Comparison of yellow poplar pretreatment between nrel digester and sunds hydrolyzer. Applied Biochemistry and Biotechnology. 70-2 (1998) 25-35.
35. A. Aden, M. Ruth, K. Ibsen, J. Jechura, K. Neeves, J. Sheehan, B. Wallace, L. Montague, A. Slayton, and J. Lukas, National Renewable Energy Laboratory: Lignocellulosic biomass to ethanol process design and economics utilizing co-current dilute acid prehydrolysis and enzymatic hydrolysis for corn stover. Golden, Colorado; 2002.
36. M.P. Garcia-Aparicio, I. Ballesteros, A. Gonzalez, J.M. Oliva, M. Ballesteros, and M.J. Negro, Effect of inhibitors released during steam-explosion pretreatment of barley straw on enzymatic hydrolysis. Applied Biochemistry and Biotechnology. 129 (2006) 278-288.
37. C. Martin, B. Alriksson, A. Sjode, N.O. Nilvebrant, and L.J. Jonsson, Dilute sulfuric acid pretreatment of agricultural and agro-industrial residues for ethanol production. Applied Biochemistry and Biotechnology. 137 (2007) 339-352.
38. A.S. Schmidt and A.B. Thomsen, Optimization of wet oxidation pretreatment of wheat straw. Bioresource Technology. 64 (1998) 139-151.
39. D.P. Koullas, E. Lois, and E.G. Koukios, Effect of physical pretreatments on the prepyrolytic behavior of lignocellulosics. Biomass & Bioenergy. 1 (1991) 199-206.
40. C. Tengborg, M. Galbe, and G. Zacchi, Reduced inhibition of enzymatic hydrolysis of steam-pretreated softwood. Enzyme and Microbial Technology. 28 (2001) 835-844.
41. J.J. Fenske, A. Hashimoto, and M.H. Penner, Relative fermentability of lignocellulosic dilute-acid prehydrolysates - application of a pichia stipitis-based toxicity assay. Applied Biochemistry and Biotechnology. 73 (1998) 145-157.

42. A.V. Tran and R.P. Chambers, Red oak wood derived inhibitors in the ethanol fermentation of xylose by pichia-stipitis cbs-5776. Biotechnology Letters. 7 (1985) 841-845.
43. A.J. Roe, D. McLaggan, I. Davidson, C. O'Byrne, and I.R. Booth, Perturbation of anion balance during inhibition of growth of escherichia coli by weak acids. J Bacteriol. 180 (1998) 767-772.
44. A.J. Roe, C. O'Byrne, D. McLaggan, and I.R. Booth, Inhibition of escherichia coli growth by acetic acid: A problem with methionine biosynthesis and homocysteine toxicity. Microbiology. 148 (2002) 2215-2222.
45. C.M. Takahashi, D.F. Takahashi, M.L. Carvalhal, and F. Alterthum, Effects of acetate on the growth and fermentation performance of escherichia coli ko11. Appl Biochem Biotechnol. 81 (1999) 193-203.
46. B.T. Koh, U. Nakashimada, M. Pfeiffer, and M.G.S. Yap, Comparison of acetate inhibition on growth of host and recombinant e. Coli k12 strains. Biotechnology Letters. 14 (1992) 1115-1118.
47. G.W. Luli and W.R. Strohl, Comparison of growth, acetate production, and acetate inhibition of escherichia coli strains in batch and fed-batch fermentations. Appl Environ Microbiol. 56 (1990) 1004-1011.
48. K. Nakano, M. Rischke, S. Sato, and H. Markl, Influence of acetic acid on the growth of escherichia coli k12 during high-cell-density cultivation in a dialysis reactor. Appl Microbiol Biotechnol. 48 (1997) 597-601.
49. B.J. Axe D., Transport of lactate and acetate through the energized cytoplasmic membrane of excherichia coli. Biotechnol Bioeng. 47 (1995) 8-19.
50. A. Walter and J. Gutknecht, Monocarboxylic acid permeation through lipid bilayer membranes. J Membr Biol. 77 (1984) 255-264.
51. C.A. Cherrington, M. Hinton, and I. Chopra, Effect of short-chain organic acids on macromolecular synthesis in escherichia coli. J Appl Bacteriol. 68 (1990) 69-74.
52. R.P. Sinha, Toxicity of organic acids for repair-deficient strains of escherichia coli. Applied and Environmental Microbiology. 51 (1986) 1364-1366.
53. C.A. Cherrington, M. Hinton, G.R. Pearson, and I. Chopra, Inhibition of escherichia coli k12 by short-chain organic acids: Lack of evidence for induction of the sos response. J Appl Bacteriol. 70 (1991) 156-160.
54. C.A. Cherrington, M. Hinton, G.R. Pearson, and I. Chopra, Short-chain organic acids at ph 5.0 kill escherichia coli and salmonella spp. Without causing membrane perturbation. J Appl Bacteriol. 70 (1991) 161-165.
55. D. McLaggan, J. Naprstek, E.T. Buurman, and W. Epstein, Interdependence of k+ and glutamate accumulation during osmotic adaptation of escherichia coli. J Biol Chem. 269 (1994) 1911-1917.
56. S.A. Underwood, M.L. Buszko, K.T. Shanmugam, and L.O. Ingram, Lack of protective osmolytes limits final cell density and volumetric productivity of

ethanologenic escherichia coli ko11 during xylose fermentation. Appl Environ Microbiol. 70 (2004) 2734-2740.
57. R.G. Kroll and I.R. Booth, The relationship between intracellular ph, the ph gradient and potassium transport in escherichia coli. Biochem J. 216 (1983) 709-716.
58. M. Goodson and R.J. Rowbury, Habituation to normally lethal acidity by prior growth of escherichia-coli at a sub-lethal acid ph value. Letters in Applied Microbiology. 8 (1989) 77-79.
59. J. Lin, I.S. Lee, J. Frey, J.L. Slonczewski, and J.W. Foster, Comparative analysis of extreme acid survival in salmonella typhimurium, shigella flexneri, and escherichia coli. J Bacteriol. 177 (1995) 4097-4104.
60. P.L. Moreau, The lysine decarboxylase cada protects escherichia coli starved of phosphate against fermentation acids. J Bacteriol. 189 (2007) 2249-2261.
61. R. Iyer, C. Williams, and C. Miller, Arginine-agmatine antiporter in extreme acid resistance in escherichia coli. J Bacteriol. 185 (2003) 6556-6561.
62. H. Richard and J.W. Foster, Escherichia coli glutamate- and arginine-dependent acid resistance systems increase internal ph and reverse transmembrane potential. J Bacteriol. 186 (2004) 6032-6041.
63. M.P. Castanie-Cornet, T.A. Penfound, D. Smith, J.F. Elliott, and J.W. Foster, Control of acid resistance in escherichia coli. J Bacteriol. 181 (1999) 3525-3535.
64. T. Warnecke and R.T. Gill, Organic acid toxicity, tolerance, and production in escherichia coli biorefining applications. Microb Cell Fact. 4 (2005) 25.
65. J. Lin, M.P. Smith, K.C. Chapin, H.S. Baik, G.N. Bennett, and J.W. Foster, Mechanisms of acid resistance in enterohemorrhagic escherichia coli. Appl Environ Microbiol. 62 (1996) 3094-3100.
66. S. Gong, H. Richard, and J.W. Foster, Yjde (adic) is the arginine:Agmatine antiporter essential for arginine-dependent acid resistance in escherichia coli. J Bacteriol. 185 (2003) 4402-4409.
67. L.M. Maurer, E. Yohannes, S.S. Bondurant, M. Radmacher, and J.L. Slonczewski, Ph regulates genes for flagellar motility, catabolism, and oxidative stress in escherichia coli k-12. J Bacteriol. 187 (2005) 304-319.
68. H.E. Schellhorn and V.L. Stones, Regulation of katf and kate in escherichia coli k-12 by weak acids. J Bacteriol. 174 (1992) 4769-4776.
69. C.N. Arnold, J. McElhanon, A. Lee, R. Leonhart, and D.A. Siegele, Global analysis of escherichia coli gene expression during the acetate-induced acid tolerance response. J Bacteriol. 183 (2001) 2178-2186.
70. Z. Ma, S. Gong, H. Richard, D.L. Tucker, T. Conway, and J.W. Foster, Gade (yhie) activates glutamate decarboxylase-dependent acid resistance in escherichia coli k-12. Mol Microbiol. 49 (2003) 1309-1320.

71. Z. Ma, H. Richard, D.L. Tucker, T. Conway, and J.W. Foster, Collaborative regulation of escherichia coli glutamate-dependent acid resistance by two arac-like regulators, gadx and gadw (yhiw). J Bacteriol. 184 (2002) 7001-7012.
72. H. Richard and J.W. Foster, Sodium regulates escherichia coli acid resistance, and influences gadx- and gadw-dependent activation of gade. Microbiology. 153 (2007) 3154-3161.
73. S.H. Choi, D.J. Baumler, and C.W. Kaspar, Contribution of dps to acid stress tolerance and oxidative stress tolerance in escherichia coli o157:H7. Appl Environ Microbiol. 66 (2000) 3911-3916.
74. T.E. Warnecke, M.D. Lynch, A. Karimpour-Fard, N. Sandoval, and R.T. Gill, A genomics approach to improve the analysis and design of strain selections. Metab Eng. (2008).
75. T. Warnecke, A genomics approach to improve the analysis and design of strain selections**.** In Metabolic Engineering VII: Health and Sustainability: September 15 2008; Puerto Vallarta, Mexico.
76. L.P. Yomano, S.W. York, and L.O. Ingram, Isolation and characterization of ethanol-tolerant mutants of escherichia coli ko11 for fuel ethanol production. Journal of Industrial Microbiology & Biotechnology. 20 (1998) 132-138.
77. R. Gonzalez, H. Tao, J.E. Purvis, S.W. York, K.T. Shanmugam, and L.O. Ingram, Gene array-based identification of changes that contribute to ethanol tolerance in ethanologenic escherichia coli: Comparison of ko11 (parent) to ly01 (resistant mutant). Biotechnol Prog. 19 (2003) 612-623.
78. S.H. Yoon, E.G. Lee, A. Das, S.H. Lee, C. Li, H.K. Ryu, M.S. Choi, W.T. Seo, and S.W. Kim, Enhanced vanillin production from recombinant e-coli using ntg mutagenesis and adsorbent resin. Biotechnology Progress. 23 (2007) 1143-1148.
79. J. Bonomo, T. Warnecke, P. Hume, A. Marizcurrena, and R.T. Gill, A comparative study of metabolic engineering anti-metabolite tolerance in escherichia coli. Metabolic Engineering. 8 (2006) 227-239.
80. R.T. Gill, S. Wildt, Y.T. Yang, S. Ziesman, and G. Stephanopoulos, Genome-wide screening for trait conferring genes using DNA microarrays. Proceedings of the National Academy of Sciences of the United States of America. 99 (2002) 7033-7038.
81. M.D. Lynch, T. Warnecke, and R.T. Gill, Scales: Multiscale analysis of library enrichment. Nat Meth. 4 (2007) 87-93.
82. S. Gall, M.D. Lynch, N. Sandoval, and R.T. Gill, Parallel mapping of genotypes to phenotypes contributing to overall biological fitness. Metab Eng. (2008).
83. X. Peng, K. Shindo, K. Kanoh, Y. Inomata, S.K. Choi, and N. Misawa, Characterization of sphingomonas aldehyde dehydrogenase catalyzing the

conversion of various aromatic aldehydes to their carboxylic acids. Applied Microbiology and Biotechnology. 69 (2005) 141-150.
84. H. Alper and G. Stephanopoulos, Global transcription machinery engineering: A new approach for improving cellular phenotype. Metabolic Engineering. 9 (2007) 258-267.
85. H. Alper and G. Stephanopoulos: **Global transcription machinery engineering (application).** U.S. Patent and Trademark Office, Editor. 2005: USA.
86. P. Venkitasubramanian, L. Daniels, and J.P.N. Rosazza, Reduction of carboxylic acids by nocardia aldehyde oxidoreductase requires a phosphopantetheinylated enzyme. Journal of Biological Chemistry. 282 (2007) 478-485.
87. S. van Sint Fiet, J.B. van Beilen, and B. Witholt, Selection of biocatalysts for chemical synthesis. Proc Natl Acad Sci U S A. 103 (2006) 1693-1698.
88. M.J. Lopez, N.N. Nichols, B.S. Dien, J. Moreno, and R.J. Bothast, Isolation of microorganisms for biological detoxification of lignocellulosic hydrolysates. Applied Microbiology and Biotechnology. 64 (2004) 125-131.
89. M.A. Eiteman, S.A. Lee, and E. Altman, A co-fermentation strategy to consume sugar mixtures effectively. J Biol Eng. 2 (2008) 3.
90. M.A. Eiteman, A. Lakshmanaswamy, K.C. Reilly, and E. Altman, Substrate selective uptake to remove acetate and convert sugar mixtures**.** In 30th Symposium on Biotechnology for Fuels and Chemicals: Tuesday, May 6, 2008; New Orleans, LA.
91. W. Coyle, The future of biofuels: A global perspective. Amber Waves. 5 (Nov. 2007) 24-29.
92. Energy Information Administration: Annual energy outlook 2009 with projections to 2030. Washington, D.C.; 2009.
93. D.R. Nielsen, E. Leonard, S.H. Yoon, H.C. Tseng, C. Yuan, and K.L. Prather, Engineering alternative butanol production platforms in heterologous bacteria. Metab Eng. 11 (2009) 262-273.
94. J.R. Borden, S.W. Jones, D. Indurthi, Y. Chen, and E.T. Papoutsakis, A genomic-library based discovery of a novel, possibly synthetic, acid-tolerance mechanism in clostridium acetobutylicum involving non-coding rnas and ribosomal rna processing. Metab Eng. 12 (2010) 268-281.
95. R. Patnaik, Engineering complex phenotypes in industrial strains. Biotechnol Prog. 24 (2008) 38-47.
96. T.Y. Mills, N.R. Sandoval, and R.T. Gill, Cellulosic hydrolysate toxicity and tolerance mechanisms in escherichia coli. Biotechnol Biofuels. 2 (2009) 26.
97. J.D. Bloom and F.H. Arnold, In the light of directed evolution: Pathways of adaptive protein evolution. Proc Natl Acad Sci U S A. 106 Suppl 1 (2009) 9995-10000.

98. S.A. Nicolaou, S.M. Gaida, and E.T. Papoutsakis, A comparative view of metabolite and substrate stress and tolerance in microbial bioprocessing: From biofuels and chemicals, to biocatalysis and bioremediation. Metab Eng. 12 (2010) 307-331.
99. H.H. Wang, F.J. Isaacs, P.A. Carr, Z.Z. Sun, G. Xu, C.R. Forest, and G.M. Church, Programming cells by multiplex genome engineering and accelerated evolution. Nature. 460 (2009) 894-898.
100. J.R. Warner, P.J. Reeder, A. Karimpour-Fard, L.B.A. Woodruff, and R.T. Gill, Rapid profiling of a microbial genome using mixtures of barcoded oligonucleotides. Accepted to Nature Biotechnology. (2010).
101. Y.X. Zhang, K. Perry, V.A. Vinci, K. Powell, W.P. Stemmer, and S.B. del Cardayre, Genome shuffling leads to rapid phenotypic improvement in bacteria. Nature. 415 (2002) 644-646.
102. A. Singh, M.D. Lynch, and R.T. Gill, Genes restoring redox balance in fermentation-deficient e. Coli nzn111. Metab Eng. 11 (2009) 347-354.
103. S. Gall, M.D. Lynch, N.R. Sandoval, and R.T. Gill, Parallel mapping of genotypes to phenotypes contributing to overall biological fitness. Metab Eng. 10 (2008) 382-393.
104. T.E. Warnecke, M.D. Lynch, A. Karimpour-Fard, N.R. Sandoval, and R.T. Gill, A genomics approach to improve the analysis and design of strain selections. Metab Eng. 10 (2008) 154-165.
105. T.E. Warnecke, M.D. Lynch, A. Karimpour-Fard, M.L. Lipscomb, P. Handke, T. Mills, C.J. Ramey, T. Hoang, and R.T. Gill, Rapid dissection of a complex phenotype through genomic-scale mapping of fitness altering genes. Metab Eng. 12 (2010) 241-250.
106. M.D. Lynch and R.T. Gill, Broad host range vectors for stable genomic library construction. Biotechnol Bioeng. 94 (2006) 151-158.
107. F.C. Neidhardt, P.L. Bloch, and D.F. Smith, Culture medium for enterobacteria. J Bacteriol. 119 (1974) 736-747.
108. T. Baba, T. Ara, M. Hasegawa, Y. Takai, Y. Okumura, M. Baba, K.A. Datsenko, M. Tomita, B.L. Wanner, and H. Mori, Construction of escherichia coli k-12 in-frame, single-gene knockout mutants: The keio collection. Mol Syst Biol. 2 (2006) 2006 0008.
109. J. Sambrook and D. Russell: Molecular cloning: A laboratory manual. Cold Spring Harbor, NY: Cold Spring Harbor Laboratory Press; 2001.
110. D. Liger, A. Masson, D. Blanot, J. van Heijenoort, and C. Parquet, Over-production, purification and properties of the uridine-diphosphate-n-acetylmuramate:L-alanine ligase from escherichia coli. Eur J Biochem. 230 (1995) 80-87.

111. H.A. Ernst, A. Pham, H. Hald, J.S. Kastrup, M. Rahman, and O. Mirza, Ligand binding analyses of the putative peptide transporter yjdl from e. Coli display a significant selectivity towards dipeptides. Biochem Biophys Res Commun. 389 (2009) 112-116.
112. K.L. Roland, F.E. Powell, and C.L. Turnbough, Jr., Role of translation and attenuation in the control of pyrbi operon expression in escherichia coli k-12. J Bacteriol. 163 (1985) 991-999.
113. M.A. Eiteman and E. Altman, Overcoming acetate in escherichia coli recombinant protein fermentations. Trends Biotechnol. 24 (2006) 530-536.
114. J.W. Foster, Escherichia coli acid resistance: Tales of an amateur acidophile. Nat Rev Microbiol. 2 (2004) 898-907.
115. T. Polen, D. Rittmann, V.F. Wendisch, and H. Sahm, DNA microarray analyses of the long-term adaptive response of escherichia coli to acetate and propionate. Appl Environ Microbiol. 69 (2003) 1759-1774.
116. C. Kirkpatrick, L.M. Maurer, N.E. Oyelakin, Y.N. Yoncheva, R. Maurer, and J.L. Slonczewski, Acetate and formate stress: Opposite responses in the proteome of escherichia coli. J Bacteriol. 183 (2001) 6466-6477.
117. S.F. Elena and R.E. Lenski, Evolution experiments with microorganisms: The dynamics and genetic bases of adaptation. Nat Rev Genet. 4 (2003) 457-469.
118. R.T. Gill, S. Wildt, Y.T. Yang, S. Ziesman, and G. Stephanopoulos, Genome-wide screening for trait conferring genes using DNA microarrays. Proc Natl Acad Sci U S A. 99 (2002) 7033-7038.
119. H.M. Ellis, D. Yu, T. DiTizio, and D.L. Court, High efficiency mutagenesis, repair, and engineering of chromosomal DNA using single-stranded oligonucleotides. Proc Natl Acad Sci U S A. 98 (2001) 6742-6746.
120. N. Costantino and D.L. Court, Enhanced levels of lambda red-mediated recombinants in mismatch repair mutants. Proc Natl Acad Sci U S A. 100 (2003) 15748-15753.
121. X.T. Li, N. Costantino, L.Y. Lu, D.P. Liu, R.M. Watt, K.S. Cheah, D.L. Court, and J.D. Huang, Identification of factors influencing strand bias in oligonucleotide-mediated recombination in escherichia coli. Nucleic Acids Res. 31 (2003) 6674-6687.
122. S. Datta, N. Costantino, and D.L. Court, A set of recombineering plasmids for gram-negative bacteria. Gene. 379 (2006) 109-115.
123. S.K. Sharan, L.C. Thomason, S.G. Kuznetsov, and D.L. Court, Recombineering: A homologous recombination-based method of genetic engineering. Nat Protoc. 4 (2009) 206-223.
124. J.A. Sawitzke, N. Costantino, X.T. Li, L.C. Thomason, M. Bubunenko, C. Court, and D.L. Court, Probing cellular processes with oligo-mediated recombination

and using the knowledge gained to optimize recombineering. J Mol Biol. 407 (2011) 45-59.
125. K.A. Datsenko and B.L. Wanner, One-step inactivation of chromosomal genes in escherichia coli k-12 using pcr products. Proc Natl Acad Sci U S A. 97 (2000) 6640-6645.
126. S. Datta, N. Costantino, X. Zhou, and D.L. Court, Identification and analysis of recombineering functions from gram-negative and gram-positive bacteria and their phages. Proc Natl Acad Sci U S A. 105 (2008) 1626-1631.
127. T.F. Cooper, D.E. Rozen, and R.E. Lenski, Parallel changes in gene expression after 20,000 generations of evolution in escherichiacoli. Proc Natl Acad Sci U S A. 100 (2003) 1072-1077.
128. M.A. Harper, Z. Chen, T. Toy, I.M. Machado, S.F. Nelson, J.C. Liao, and C.J. Lee, Phenotype sequencing: Identifying the genes that cause a phenotype directly from pooled sequencing of independent mutants. PLoS One. 6 e16517.
129. Q. Zheng and X.J. Wang, Goeast: A web-based software toolkit for gene ontology enrichment analysis. Nucleic Acids Res. 36 (2008) W358-363.
130. N.R. Sandoval, T.Y. Mills, M. Zhang, and R.T. Gill, Elucidating acetate tolerance in e. Coli using a genome-wide approach. Metab Eng. 13 (2010) 214-224.
131. H.H. Wang and G.M. Church, Multiplexed genome engineering and genotyping methods applications for synthetic biology and metabolic engineering. Methods Enzymol. 498 (2011) 409-426.
132. H.M. Salis, E.A. Mirsky, and C.A. Voigt, Automated design of synthetic ribosome binding sites to control protein expression. Nat Biotechnol. 27 (2009) 946-950.